

UNITED STATES
DEPARTMENT OF
COMMERCE
PUBLICATION



NBS TECHNICAL NOTE 813

NBS Reactor: Summary of Activities --- July 1972 to June 1973

QC
00
5753
813
974
2.2

U.S.
DEPARTMENT
OF
COMMERCE
National
Bureau
of
Standards



NATIONAL BUREAU OF STANDARDS

The National Bureau of Standards¹ was established by an act of Congress March 3, 1901. The Bureau's overall goal is to strengthen and advance the Nation's science and technology and facilitate their effective application for public benefit. To this end, the Bureau conducts research and provides: (1) a basis for the Nation's physical measurement system, (2) scientific and technological services for industry and government, (3) a technical basis for equity in trade, and (4) technical services to promote public safety. The Bureau consists of the Institute for Basic Standards, the Institute for Materials Research, the Institute for Applied Technology, the Institute for Computer Sciences and Technology, and the Office for Information Programs.

THE INSTITUTE FOR BASIC STANDARDS provides the central basis within the United States of a complete and consistent system of physical measurement; coordinates that system with measurement systems of other nations; and furnishes essential services leading to accurate and uniform physical measurements throughout the Nation's scientific community, industry, and commerce. The Institute consists of a Center for Radiation Research, an Office of Measurement Services and the following divisions:

Applied Mathematics — Electricity — Mechanics — Heat — Optical Physics — Nuclear Sciences² — Applied Radiation² — Quantum Electronics³ — Electromagnetics³ — Time and Frequency³ — Laboratory Astrophysics³ — Cryogenics³.

THE INSTITUTE FOR MATERIALS RESEARCH conducts materials research leading to improved methods of measurement, standards, and data on the properties of well-characterized materials needed by industry, commerce, educational institutions, and Government; provides advisory and research services to other Government agencies; and develops, produces, and distributes standard reference materials. The Institute consists of the Office of Standard Reference Materials and the following divisions:

Analytical Chemistry — Polymers — Metallurgy — Inorganic Materials — Reactor Radiation — Physical Chemistry.

THE INSTITUTE FOR APPLIED TECHNOLOGY provides technical services to promote the use of available technology and to facilitate technological innovation in industry and Government; cooperates with public and private organizations leading to the development of technological standards (including mandatory safety standards), codes and methods of test; and provides technical advice and services to Government agencies upon request. The Institute consists of a Center for Building Technology and the following divisions and offices:

Engineering and Product Standards — Weights and Measures — Invention and Innovation — Product Evaluation Technology — Electronic Technology — Technical Analysis — Measurement Engineering — Structures, Materials, and Life Safety⁴ — Building Environment⁴ — Technical Evaluation and Application⁴ — Fire Technology.

THE INSTITUTE FOR COMPUTER SCIENCES AND TECHNOLOGY conducts research and provides technical services designed to aid Government agencies in improving cost effectiveness in the conduct of their programs through the selection, acquisition, and effective utilization of automatic data processing equipment; and serves as the principal focus within the executive branch for the development of Federal standards for automatic data processing equipment, techniques, and computer languages. The Institute consists of the following divisions:

Computer Services — Systems and Software — Computer Systems Engineering — Information Technology.

THE OFFICE FOR INFORMATION PROGRAMS promotes optimum dissemination and accessibility of scientific information generated within NBS and other agencies of the Federal Government; promotes the development of the National Standard Reference Data System and a system of information analysis centers dealing with the broader aspects of the National Measurement System; provides appropriate services to ensure that the NBS staff has optimum accessibility to the scientific information of the world. The Office consists of the following organizational units:

Office of Standard Reference Data — Office of Information Activities — Office of Technical Publications — Library — Office of International Relations.

¹ Headquarters and Laboratories at Gaithersburg, Maryland, unless otherwise noted; mailing address Washington, D.C. 20234.

² Part of the Center for Radiation Research.

³ Located at Boulder, Colorado 80302.

⁴ Part of the Center for Building Technology.

NBS Reactor: Summary of Activities July 1972 to June 1973

National Bureau of Standards

APR 29 1974

Robert S. Carter

Reactor Radiation Division
Institute for Materials Research
National Bureau of Standards
Washington, D.C. 20234



U.S. DEPARTMENT OF COMMERCE, Frederick B. Dent, *Secretary*

NATIONAL BUREAU OF STANDARDS, Richard W. Roberts, *Director*

Issued February 1974

National Bureau of Standards Technical Note 813

Nat. Bur. Stand. (U.S.), Tech. Note 813, 135 pages (Feb. 1974)

CODEN: NBTNAE

U.S. GOVERNMENT PRINTING OFFICE
WASHINGTON: 1974

For sale by the Superintendent of Documents, U.S. Government Printing Office, Washington, D.C. 20402
(Order by SD Catalog No. C13.46:813). Price \$1.55.

FOREWORD

The National Bureau of Standards Reactor was built not only to serve the needs of the NBS but also those of the greater Washington Scientific Community and other government agencies. The Reactor Radiation Division was established to operate the reactor and to foster its scientific and technological use. Toward this end, the Division has a small nucleus of scientists experienced in the use of reactors for a wide range of scientific and technical problems. In addition to pursuing their own research and developing sophisticated experimental facilities, they actively seek out and encourage collaboration with other scientists, engaged in challenging programs, whose work can benefit from use of the reactor, but who as yet do not have the reactor experience necessary to take full advantage of the facilities available. The Division also provides irradiation services to a wide variety of users as well as engineering and other technical services.

The reactor operates at 10 MW and is designed to provide a broad spectrum of facilities ranging from intense neutron beams to extensive irradiation facilities, making it one of the most versatile high flux research reactors in the country. Thus it is able to serve a large number of scientists and engineers in a broad range of activities both within and outside the NBS.

This report attempts to summarize all the work done which is dependent on the reactor including a large number of programs outside the Division. The first section summarizes those programs based primarily on Reactor Radiation Division (RRD) initiatives whereas the second and third sections summarized collaborative programs between RRD scientists and other NBS or non-NBS scientists respectively. The fourth section summarizes NBS work originating entirely outside of RRD which requires no collaboration with RRD scientists. The section entitled, "Service Programs" covers those programs originating outside NBS but for which RRD provides irradiation services. The remaining sections are self-explanatory.

ABSTRACT

This report summarizes all those programs which depend on the NBS reactor. It covers the period from July 1972 through June 1973. The programs range from the use of neutron beams to study the structure and dynamics of materials through nuclear physics and neutron standards to sample irradiations for activation analysis, isotope production and radiation effects studies.

Key words: Activation analysis; crystal structure; diffraction; isotopes; molecular dynamics; neutron; nuclear reactor; radiation.

Cover photograph: Reactor Building
National Bureau of Standards
Gaithersburg, Maryland

TABLE OF CONTENTS

	Page
FOREWORD.	iii
ABSTRACT.	iv
A. REACTOR RADIATION DIVISION PROGRAMS	1
Neutron Scattering Studies of Hydrogen in Transition Metals	1
1. Tantalum Hydride	1
2. Palladium Hydride	2
Phase Transitions, Orientational Disorder, and Crystal Dynamics of Ionic and Molecular Solids.	6
1. Alkali Hydrosulfides.	6
2. Ammonium Bromide and Ammonium Iodide.	9
3. Infrared and Raman Band Shape Analysis of Chloroform and Dicyanoacetylene	9
Analyses of the Dynamics of KCN, NaCN, and Related Crystals-- Debye-Waller Factors	15
The Dynamics of Simple Liquids.	16
1. Liquid Rubidium	16
2. Small Wave Vector Excitations.	16
Elementary Excitations in Quantum Liquids	17
1. ^4He , $_{.95}$ - ^3He , $_{.05}$	19
2. Liquid ^3He	19
Rigid Body Thermal Motion in Crystallographic Refinement.	20
Studies on Twinning	21
Thermal Neutron Flux Measurements	25
Intercomparison of Neutron Diffractometers.	26
Direct Tests for Violation of CP Invariance	26
Cold-Neutron Time-Of-Flight Facility.	27
Cold-Neutron Source	28
B. RRD-NBS COLLABORATIVE PROGRAMS.	30
Inelastic Neutron Scattering of α Neon Near the Critical Temper- ature.	30
An Observation of the Deviation from Ornstein-Zernike Theory in the Critical Scattering of Neutrons from Neon.	31

TABLE OF CONTENTS

	Page
The Structure Factor of Neon Near T_c	33
Study of Hindered Rotation in Hydroxylammonium Perchlorate by Constrained Least-Squares Refinement	34
A Bifurcated Hydrogen Bond in $\text{Ca}(\text{H}_2\text{PO}_4)_2 \cdot \text{H}_2\text{O}$	35
The Crystal Structure of $\text{H}_3\text{PO}_4 \cdot 1/2\text{H}_2\text{O}$	37
The Crystal Structure of Lead Deuterium Orthophosphate.	38
Neutron Diffraction Structure Determination of Dichlorotetrapyrazolecopper(II), $\text{Cu}(\text{C}_3\text{H}_4\text{N}_2)_4\text{Cl}_2$	41
Calibration of Detectors for Argon-41	44
C. INTERAGENCY AND UNIVERSITY COLLABORATIVE PROGRAMS	45
Dynamics of Ammonium Ions in NH_4ClO_4 and NH_4NO_3	45
Group Theoretical Analysis of Neutron Scattering in Crystals.	46
Temperature Dependence of the Phonons in HCP Be	47
Magnetization of Rare Earth Compounds by Neutron Diffraction.	49
Excitation Spectra of an Amorphous Ferromagnet	49
Absence of Magnetic Order in $\text{MnO-P}_2\text{O}_5$ Glass	52
Structural Studies of Amorphous Solids.	53
Precision Measurement of Thermal Neutron Scattering Amplitudes.	53
The Structure of $\text{Na}_2\text{ZnCl}_4 \cdot 3\text{H}_2\text{O}$	54
Crystal Structure of NH_4ClO_4 at 300K, 78K and 10K by Neutron Diffraction	55
Refinements of the Crystal Structure of KN_3 and $\beta\text{-NaN}_3$ by Neutron Diffraction	57
Crystal Structure of Dinitro-Pentamethylene-Tetramine	58
Three-Axis Neutron Spectrometer	59
D. NON-RRD NBS PROGRAMS	60
Activation Analysis Section: Summary of Activities	60
1. Research Projects	60
2. Standard Reference Material (SRM) Analyses.	68
3. Cooperative and Service Analyses.	70
4. Facilities	71
5. Conclusion	73
Integral Reaction Rate Measurements for the NBS Neutron Standards Program	74

TABLE OF CONTENTS

	Page
Precision Measurement of the Compton Wavelength of the Electron	76
^{60}Co Gamma Ray Anisotropy Thermometry	77
Emission of Long-Range Alpha-Particles in the Subthermal-, Thermal- and Resonance-Neutron Fission of ^{239}Pu	77
Extreme-Angle Emission of Long-Range Alpha Particles in the Thermal Neutron Fission of ^{235}U	81
Development of Fast-Neutron Beams	85
Proton-Recoil Spectrometer Research	87
Parity Violation in Neutron Capture Gamma-Ray Emission.	93
A Search for Doubly Radiative (N, P) Capture.	97
E. SUMMARY OF REACTOR OPERATIONS	101
F. SERVICE PROGRAMS	103
Activation Analysis Program of the Food and Drug Administration at the NBSR.	103
1. Multi-element Analysis of Foods	103
2. MTELMT: A Computer Language for the Reduction of Neutron Activation Analysis Data	103
3. An Automated Data Acquisition System for Neutron Activation Analysis	106
The Use of Neutron Activation Analysis on Biological Samples by the Veterans Administration Hospital	109
Trace Elements in the Environment and Radioactive Decay Studies	109
The Use of Activation Analysis in Scientific Crime Detection by the Federal Bureau of Investigation	111
U. S. Postal Service Activation Analysis Program.	112
The Use of Neutron Activation Analysis in Scientific Crime Det- ection	113
Activation Analysis Program of the U. S. Geological Survey.	113
Combined Effects of Radiation and Shock Waves in Materials.	115
Neutron Irradiation of LPE Bubble Domain Garnets	116
Chemical Studies on Lunar Materials and Meteorites	116
G. STAFF ROSTER	118
H. PUBLICATIONS	122

A. REACTOR RADIATION DIVISION PROGRAMS

NEUTRON SCATTERING STUDIES OF HYDROGEN IN TRANSITION METALS

We have continued our study in collaboration with H. E. Flotow of Argonne National Laboratory, of the binding and diffusion of hydrogen isotopes in bcc and fcc transition metals, including their relationship to intermetallic forces and hydride phase transitions. A study on the concentration-dependence of hydrogen diffusion in TaH_x was completed and neutron scattering measurements were begun on a single crystal of TaH_{0.02} to provide more precise measurements and analysis of the behavior of hydrogen in this system. It should be noted that the bcc refractory metals and their alloys are prime candidates as first wall materials in nuclear fusion power reactors, so that measurements on the microscopic and macroscopic effects of hydrogen isotopes in these materials are particularly appropriate. Work has also continued in our study of hydrogen isotopes in palladium. Our effort to prepare and examine high concentration (β -phase) crystals of PdD_{>0.7} has been stimulated in part by the discovery of superconducting phase transitions at $\sim 10^\circ\text{K}$ in the hydride.

1. Tantalum Hydride - J. J. Rush, J. M. Rowe and R. C. Livingston

Analysis of our neutron quasielastic and inelastic scattering data for Ta₂H in its α (bcc) and β phases has enabled us to prepare a paper which provides considerable information on the diffusion of hydrogen in this hydride, including the concentration dependence of the diffusion. These results also provide an interesting comparison with our previous results on VH_x (see our 1972 progress report, NBS TN 758). The widths of the quasielastic peaks for α -phase Ta₂H and TaH_{0.15} are shown in Fig. 1 along with theoretical widths predicted for models assuming jumps between octahedral and tetrahedral sites. It can be seen that the tetrahedral-jump model provides the best overall fit to the experimental results, as reported in NBS TN 758, but that in no case is in agreement completely satisfactory. Residence times τ between 2.4 ps (300°C) and 7 ps (153°C)

REACTOR RADIATION DIVISION PROGRAMS

were derived for Ta_2H (compared to previous values between 1.6 (340°C) and 4.0 ps (148°C) for $TaH_{0.15}$). These results indicate a significant concentration dependence of the diffusion rates in $\alpha-TaH_x$ (contrary to suggestions from previous NMR results) with activation energies for diffusion of 10.4 ± 1.2 KJ/mol in $TaH_{0.15}$ and 15 ± 1.2 KJ/mol for Ta_2H . In addition "effective" mean square amplitudes of proton vibration of 0.02 to 0.04\AA^2 were obtained from the momentum-transfer (Q) dependence of the quasi-elastic peak intensities. These are in reasonable agreement with values predicted from our measured vibration frequencies, but they are from 3 to 9 times lower than values obtained previously for $\alpha-VH_x$, which exhibits vibrational frequency distributions very similar to those for $\alpha-TaH_x$, but has a much more rapid diffusion rate ($\tau \sim 0.5$ to 1 ps). This comparison provides additional evidence for our previous suggestion that the apparent Debye-Waller factors derived from neutron data for these and similar hydrides are strongly dependent on the rate of hydrogen diffusion. Our results have been compared in detail with other results on hydrogen-isotope diffusion in refractory metals.

During the past year we have also loaded a large single crystal of tantalum to a concentration of $TaH_{0.02}$, as a continuation of our program to study the diffusion process and effects of interstitial hydrogen isotopes on intermetallic bonding in the bcc refractory metals. The study of single crystal samples should enable us to obtain more detailed information on the hydrogen diffusion mechanism in these metals by allowing measurements in different crystal orientations (rather than measurements averaged over crystallite orientation) and by thus providing a more detailed comparison with theoretical models.

We have very recently measured neutron quasielastic scattering spectra for the $TaH_{0.02}$ single crystal at seven crystal orientations. The data is presently being analyzed and will be discussed in the next annual report.

2. Palladium Hydride - J. M. Rowe and J. J. Rush

In collaboration with H. G. Smith of Oak Ridge National Laboratory, we have measured phonon dispersion curves for a single crystal of $PdH_{0.03}$

in order to examine the possible effect of interstitial hydrogen on the electronic structure (Fermi Surface) of the metal. Our results show that the addition of 3% H to Pd does not significantly alter the lattice dynamics. In particular, the anomaly in the $[110]T_1$ branch (thought to be related to Kohn anomalies) does not change in shape or strength. The measured dispersion curve for the $[110]$ branch of $PdH_{0.03}$ is shown in Fig. 2.

As part of our effort to study the β phase of PdD_x (apparently superconducting at $PdD_{>.75}$) we have, in collaboration with H. E. Flotow and R. Kleb of ANL, designed constructed and tested a high pressure cell for loading deuterium to as high a concentration as possible in a large single crystal of Pd. This rather delicate loading procedure will be attempted in the near future.

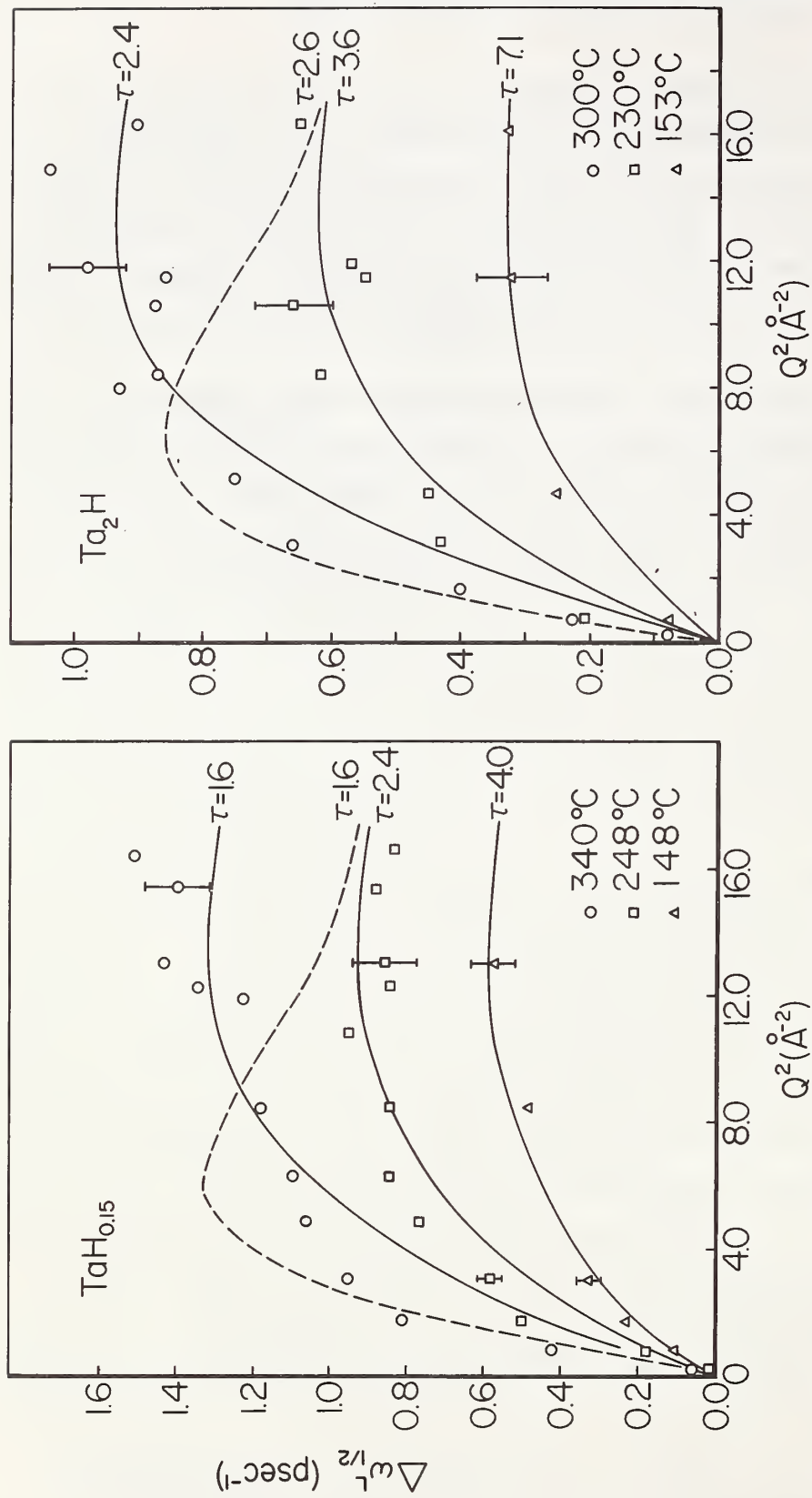


Fig. 1. The full widths at half-maximum ($\Delta\omega_{L}^{1/2}$) of single Lorentzians obtained for TaH_{0.15} and Ta₂H by deconvoluting the experimental quasielastic peaks into a Gaussian (resolution function) and a broadened Lorentzian. The solid and dashed lines are the theoretical widths predicted for instantaneous jumps between the tetrahedral and octahedral models, respectively. The τ values derived from the best fit to the tetrahedral model at various temperatures are also shown.

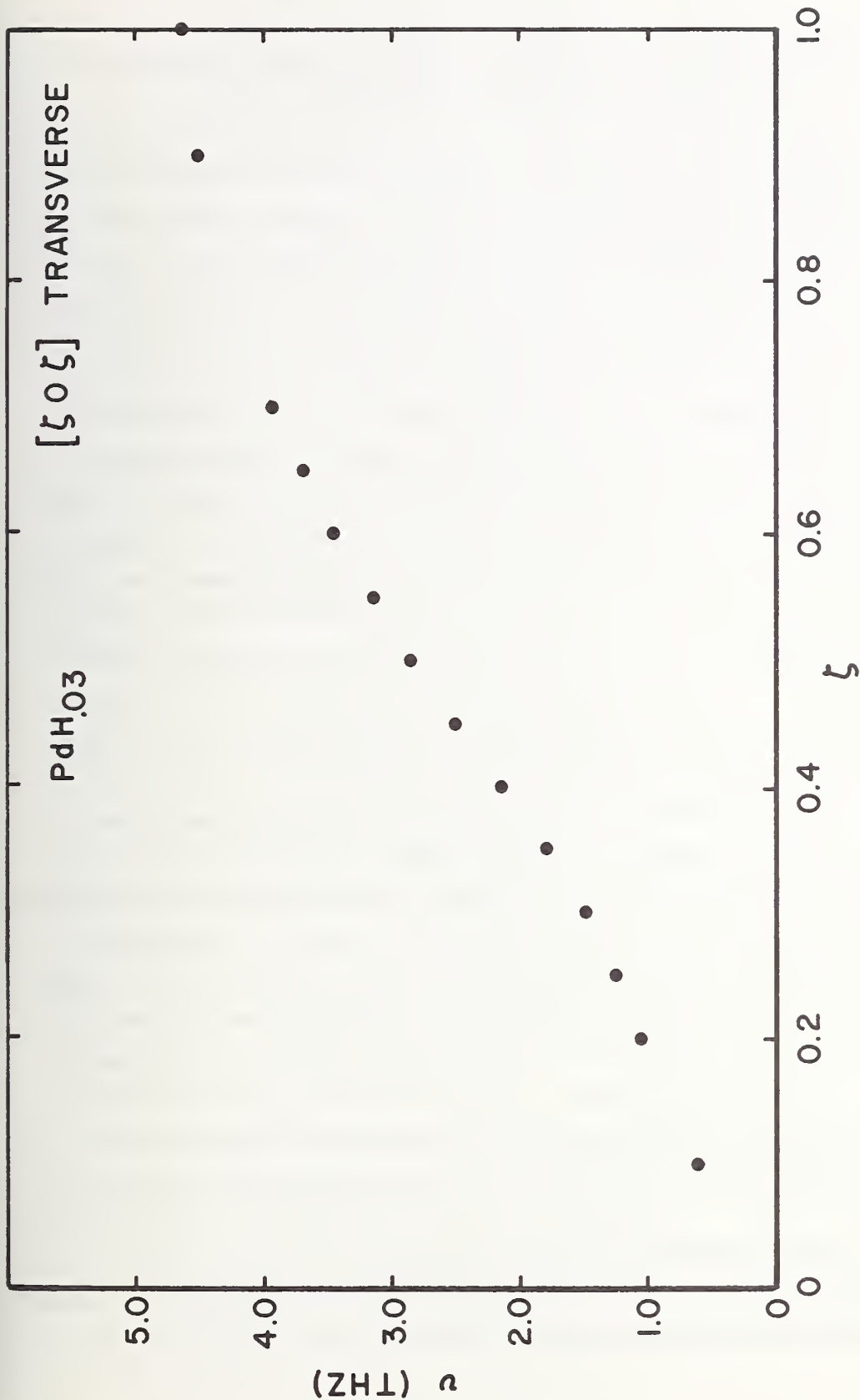


Fig. 2. The frequency vs wave-vector dispersion relation for the PdH_{0.3} transverse (T₁) branch propagating in the [110] direction. The results for pure palladium are not shown, as they would be indistinguishable from the PdH_{0.3} result on this scale.

PHASE TRANSITIONS, ORIENTATIONAL DISORDER, AND CRYSTAL DYNAMICS
OF IONIC AND MOLECULAR SOLIDS

Work has continued on detailed investigations of orientational disorder and order-disorder phase transitions in prototype crystals by neutron scattering techniques and by Raman and infrared spectroscopy. The precise nature of the rotational disorder in the high temperature cubic phases of broad classes of inorganic and organic solids is not generally well understood, nor is the microscopic basis of the changes in physical and thermodynamic properties associated with these order-disorder transitions. During the past year higher resolution quasi-elastic neutron studies and the analysis of an extensive series of Raman scattering measurements on M^+XY^- type crystals (alkali hydrosulfides) have provided new detailed information on the order-disorder phase transformations in these materials. Experiments on ammonium halide single crystals and several globular organic molecules have also been initiated.

1. Alkali Hydrosulfides - J. J. Rush, R. C. Livingston and J. M. Rowe

a. Raman Scattering

Our Raman scattering investigation of the alkali hydrosulfides, NaSH, CsSH and RbSH between 30 and 400°K (in collaboration with G. J. Rosasco of Division 313) has been completed, including most of the analysis and interpretation of the spectroscopic data. Examples of the spectra for NaSH and CsSH are shown in Fig. 1 and 2. These Raman spectra provide clear evidence (in addition to our neutron diffraction measurements mentioned in last year's Report, NBS 758) for the existence of previously unobserved low-temperature phases in each compound. In addition the results show that the order-disorder transitions in these solids are associated with significant changes in the details of their crystal dynamics.

The spectrum at 358°K in the NaCl phase of NaSH (Fig. 1) shows a single broad peak due to SH^- stretching vibrations at 2541 cm^{-1} and a diffuse almost featureless maximum (not shown here) in the region of

the SH librations. In passing through the transition to the trigonal, D_{3d}^5 , phase at $\approx 355^\circ\text{K}$ the stretching peak narrows significantly. The trigonal-phase spectra (Fig. 1) also exhibit broad bands due to SH^- librations ($\approx 450 \text{ cm}^{-1}$) and translational lattice modes (≈ 80 and 160 cm^{-1}) in reasonable agreement with our previous neutron scattering results (see NBS TN 758). All translational lattice modes are Raman "inactive" in the D_{3d}^5 space group, so that the observed peaks are most likely "density of states" maxima attributable to the orientational disorder (probably two fold) in this phase. Finally at $\approx 115^\circ\text{K}$ the character of the spectra in Fig. 1 changes again. The stretching mode band is sharpened considerably and shifted to higher frequency. Simultaneously the lattice mode region shows a dramatic sharpening of the translatory vibration peaks, as well as a splitting of the libration band. These changes in the NaSH spectra clearly indicate a new crystal phase, most likely involving total ordering of the SH^- ions.

The measured spectra for CsSH (Fig. 2) and RbSH, which will not be discussed in detail here, show changes which are analogous to the NaSH results. These include dramatic spectral changes at low temperatures which also give clear evidence of low-temperature "ordered" phases for each of the crystals, with transition temperatures of $\approx 113^\circ\text{K}$ (CsSH) and $\approx 123^\circ\text{K}$ (RbSH). An interesting feature of our results for all these crystals is that the low temperature disorder-order transition appears to occur gradually over a range of temperatures (~ 10 - 20°) in each case. Further details of our neutron diffraction and optical results will be presented in a future report.

b. Neutron Scattering

The orientational disorder of the hydrosulfide ions in CsSH (CsCl phase) and RbSH (NaCl phase) has been investigated by quasielastic neutron scattering with high energy resolution ($\Delta E_{1/2 \text{ max}} = 0.25 \text{ meV}$), using neutron time-of-flight techniques. Examples of the experimental scattering spectra, $S_R(Q, \omega)$ are shown in Fig. 3, plotted vs. frequency in ps^{-1} ($1 \text{ meV} \equiv 1 \text{ ps}^{-1}$). These results have been corrected for multiple scat-

scattering contributions. The results in Fig. 3 represent to our knowledge the clearest demonstration yet observed of the theoretically predicted separation of quasielastic neutron scattering by reorienting ions or molecules into a broadened (Lorentzian) component whose width is dependent on the reorientation rate and an unbroadened component whose intensity vs. momentum transfer, Q , is dependent on the distribution of orientations in the crystal. Theoretical scattering laws for instantaneous jumps between six [100] directions in a cubic lattice are also shown in Fig. 3 for comparison with experimental results. The experimental scattering laws were fitted by least squares to the sum of a Lorentzian component and a delta function broadened by the instrumental resolution. From this fitting procedure the ratio of elastic intensity to total intensity was derived and the results are shown in Fig. 4 for both CsSH and RbSH, again compared to the theoretical ratios predicted for the [100] orientation model.

The results in Fig. 3 and 4 enable us to clearly rule out either a free rotation model for the orientational disorder (which predicts line broadenings an order of magnitude larger than observed) or a small-step rotational diffusion model which predicts a monotonic increase in the width of the broadened component with Q . The model which provides the only satisfactory fit to the experimental results is a model involving instantaneous jumps between a finite number of equilibrium orientations, such as the [100], [110] and [111] crystal directions. Unfortunately all three of these models represent the data reasonably well so that no clear preference for a particular jump geometry can be established from the results.

Residence times, τ , between SH^- ion reorientation have been derived from the theoretical fits to the data, which are about 1 ps for CsSH at 373°K and about 0.4 ps for RbSH at 414°K (the values vary somewhat with jump model). Mean-square proton vibrational amplitudes were also derived from the variation of elastic intensity with Q^2 . It should be noted that the τ values obtained for RbSH (and NaSH) at temperatures 10-20° above their trigonal→cubic transition are only about a factor of

5 higher than the time for a free-rotational jump between equivalent orientations (~ 0.07 ps). Finally our results clearly suggest that in most cases measurements on single crystals will be necessary to establish the details of orientational disorder in solids. As noted below we are extending our measurements to single crystal ammonium halide samples to pursue further the refinement of neutron quasielastic scattering techniques and theoretical analysis procedures toward the detailed measurement of orientational disorder in solids.

2. Ammonium Bromide and Ammonium Iodide - R. C. Livingston, J. M. Rowe and J. J. Rush

Single crystals of ammonium bromide and ammonium iodide (up to 1" x 1" x 1/4") suitable for quasielastic neutron scattering experiments have been grown from an aqueous solution doped with urea by slow evaporation. Preliminary measurements have been obtained in a neutron quasielastic scattering study of ion reorientation in the bcc phase of NH_4Br has been initiated. Equipment has been built with which single crystals can be grown by either slow evaporation or by lowering the temperature of a saturated solution under highly controlled conditions. A project is underway to grow single crystals of deuterated ammonium bromide and ammonium iodide suitable for further neutron inelastic scattering studies.

3. Infrared and Raman Band Shape Analysis of Chloroform and Dicyanoacetylene - R. C. Livingston

As part of a continuing program in the study of molecular plastic crystals and related compounds, we have measured in collaboration with W. G. Rothschild of the Scientific Research Staff at Ford Motor Company, infrared and Raman band shapes for several vibrational modes in the symmetric top molecule chloroform (CHCl_3 and CDCl_3), and in the linear molecule dicyanoacetylene (C_4N_2). The correlation functions obtained by Fourier transforming the band contours yields information about the reorientation rates around specific molecular axes, which are determined by the symmetry of the vibration and the molecular symmetry. Raman data in paral-

lel and perpendicular geometries allow us to separate the intrinsic linewidth from the rotational broadening in both Raman and infrared bands. Although isotopic corrections were applied to the chloroform data, we are now preparing isotopically pure chloroform, ($\text{CH}^{35}\text{Cl}_3$) as a check on our earlier data. The chloroform data will be used to check the M and J rotational diffusion models for a symmetric top as proposed by McClung.

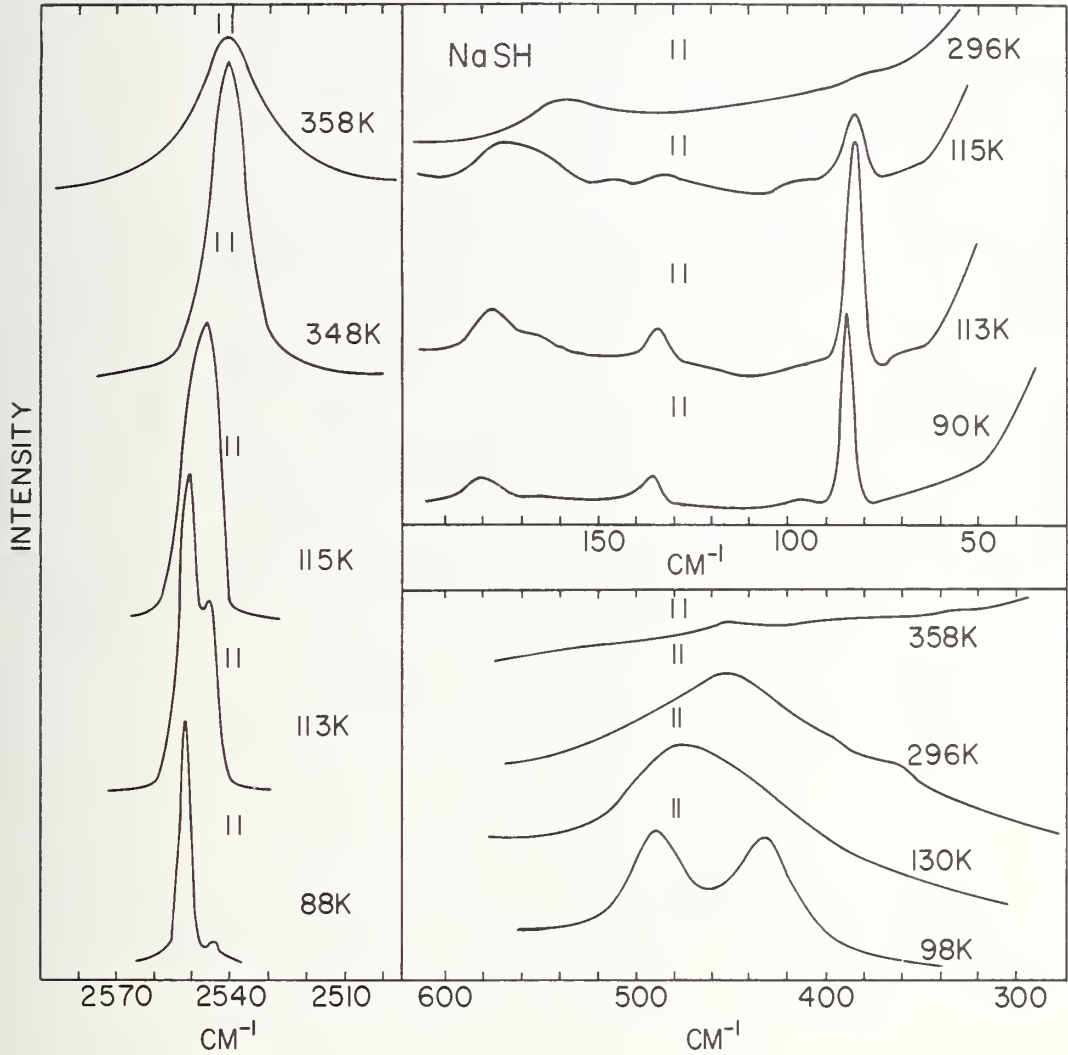


Fig. 1. Smoothed Raman spectra for three crystal phases of NaSH. Spectra slit widths are indicated by vertical bars.

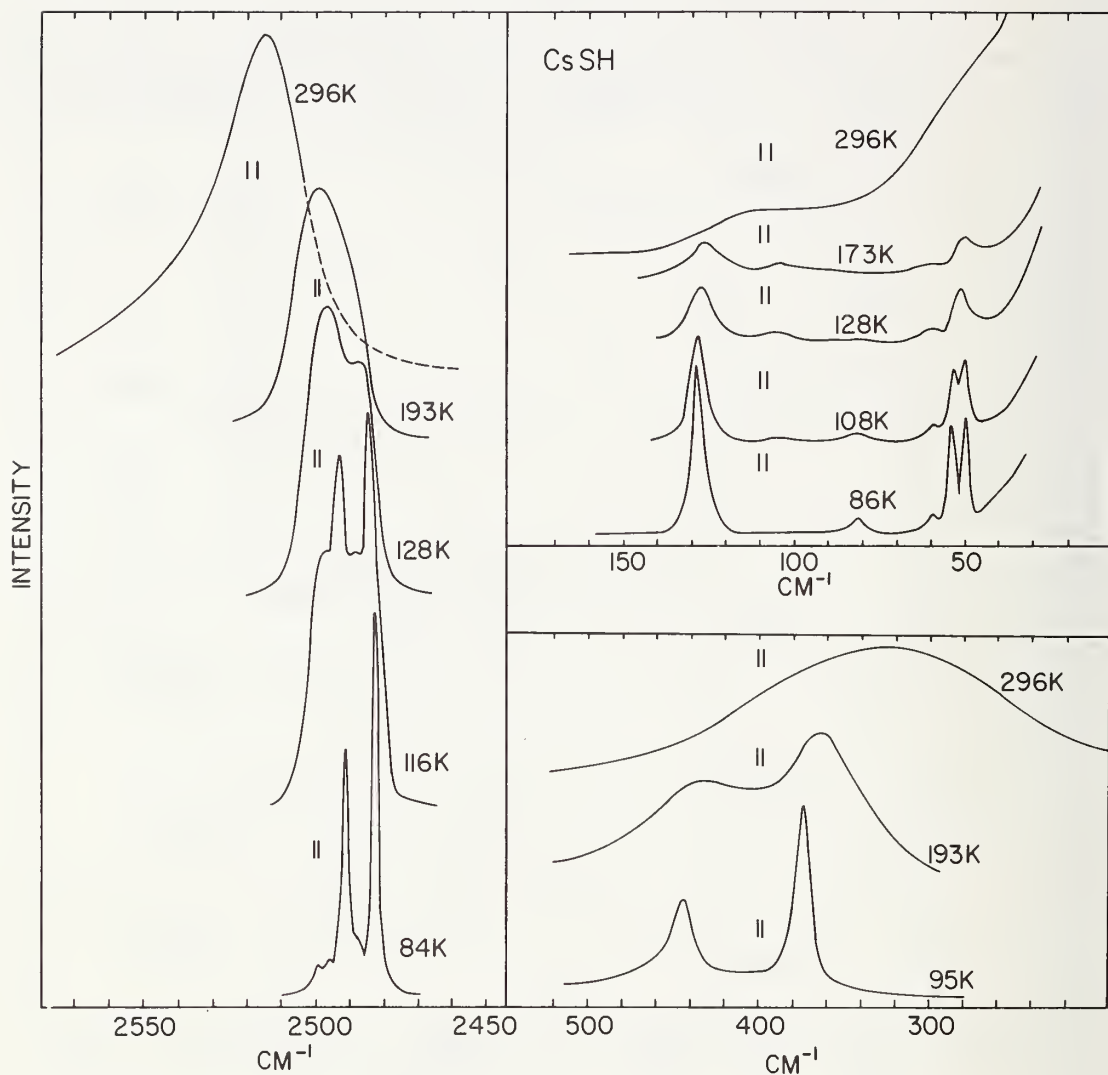


Fig. 2. Smoothed Raman spectra for three crystal phases of CsSH.

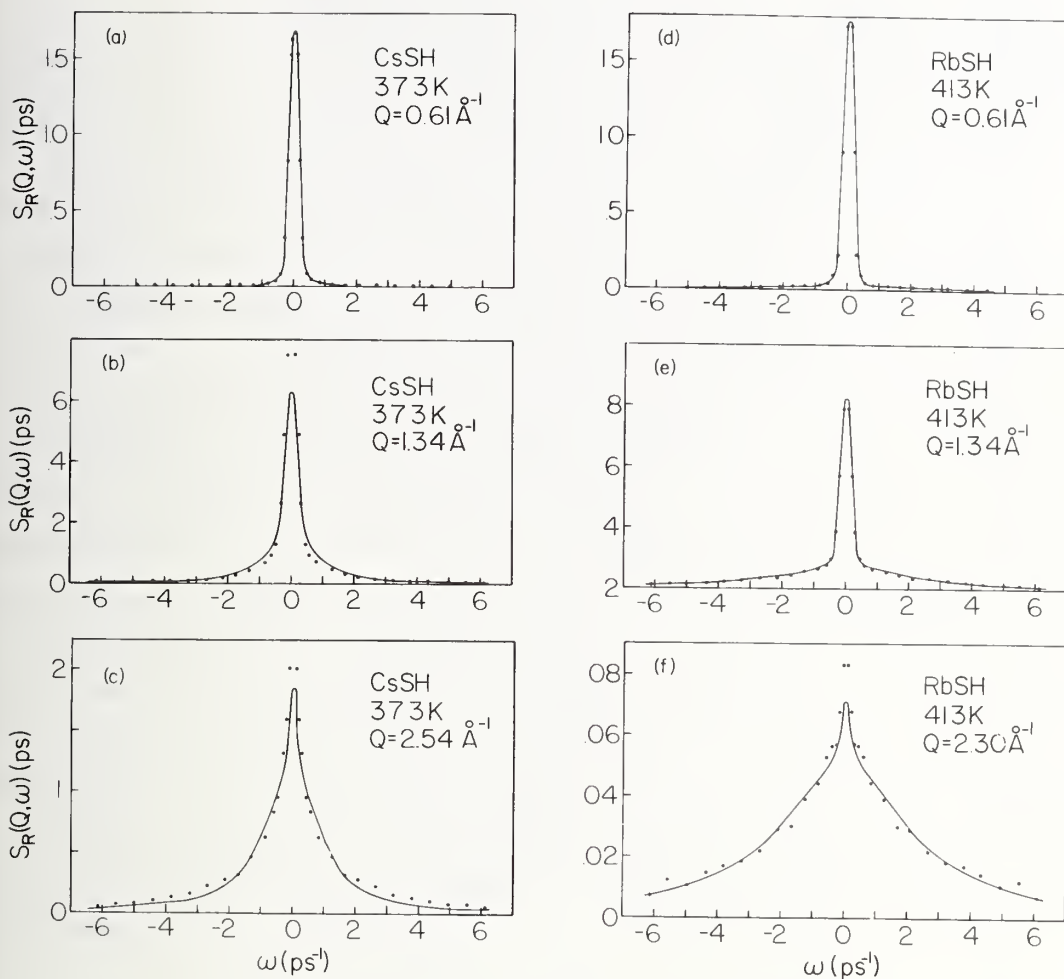


Fig. 3. Examples of quasielastic scattering spectra for CsSH and RbSH at several values of wave-vector transfer Q . Also shown (solid lines) are theoretical scattering laws calculated for the [100] jump reorientation model with $\tau = 1.3$ ps for CsSH and 0.49 ps for RbSH.

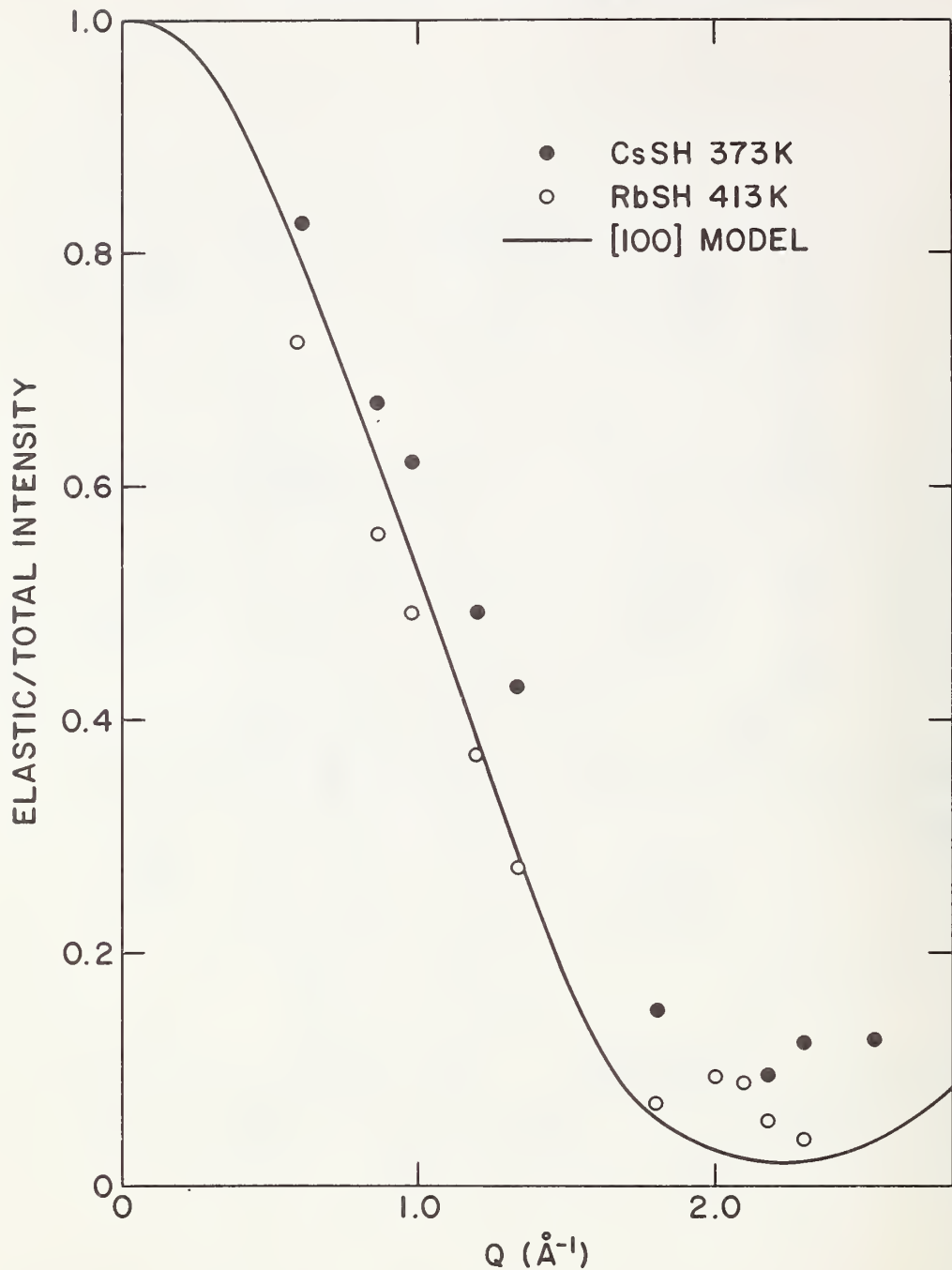


Fig. 4. The ratio of the intensity of the unbroadened component to the total intensity of the quasielastic peak as a function of wave-vector transfer (Q). The solid line is the predicted ratio for an instantaneous jump model assuming the SH^- ion aligns randomly in the 6 [100] directions of the cubic structure.

ANALYSES OF THE DYNAMICS OF KCN, NaCN, AND RELATED CRYSTALS--
DEBYE-WALLER FACTORS

R. C. Casella

Data of J. Rush, M. Rowe, E. Prince and others on both elastic and inelastic neutron scattering in KCN, NaCN, and related compounds indicates anomalous behavior of the Debye-Waller factors in elastic scattering as well as the disappearance of the longitudinal acoustic phonons with increasing energy transfer and complete absence of the optical and librational branches as revealed by inelastic neutron scattering in the high temperature phase. These data present a severe problem in theoretical understanding. The problem is being attacked at two levels. First, based upon the experimentalists insights provided by Rush, Rowe and Prince, phenomenological models such as freely rotating CN^- ions are being constructed. Second, at a fundamental level, an extensive study of the origin and limits of applicability of the Debye-Waller factor in neutron scattering, the degree of reliance on the harmonic approximation, etc. has begun. This work is based upon (and hopefully will clarify and extend) earlier work of Glauber Van Hove, and others. It is hoped that the model-building and fundamental approaches will merge at a later stage and lead to a theoretical understanding of the data. Moreover, potential application to the continuing group-theoretical program, discussed in a separate paragraph, of the fundamental analyses of the Debye-Waller factor is foreseen.

THE DYNAMICS OF SIMPLE LIQUIDS

J. M. Rowe

In contrast to the lattice dynamics of solids, the dynamics of simple liquids are at present poorly understood. The main reason for this is, of course, the lack of long range order in liquids which precludes the use of simplifying assumptions such as the harmonic approximation and one phonon approximation. This in turn means that for liquids, it is essential to measure the shape of the absolute neutron scattering cross-section as a function of wave-vector and energy transfer over the widest possible range for both variables. This information must then be compared with models of the liquid state in order to extract information about the forces acting in the system. Recent results for liquid argon have shown the power of this technique and our present program is to extend such measurements to other simple liquids, particularly to liquid metals.

1. Liquid Rubidium

In collaboration with J. R. D. Copley of Argonne National Laboratory, the coherent scattering function $S(Q, \omega)$, which is proportional to the inelastic neutron scattering cross-section, has been measured at 315°K over a range of wave-vector transfers from $0.8 - 6.5 \text{ \AA}^{-1}$. The data have been corrected for multiple scattering, resolution and others effects, and the corrected results have been used to construct the first two frequency moments. These moments are a sensitive test of absolute accuracy, and are thus very useful in assessing the reliability of the derived scattering function. The final results comprise the most complete and accurate representation of a coherent scattering function yet obtained for a simple liquid metal. Comparison with molecular dynamics calculations and with models for dense liquids will give detailed information about the effective ion-ion potential in the liquid metal.

2. Small Wave Vector Excitations

It is well known that at very small wave vectors (large wavelengths) propagating excitations in the form of sound waves exist for all liquids.

At large wave-vectors no such excitations have been seen for simple classical liquids. The transition region between these two regimes is of fundamental importance to the theory of liquids, but to date it has been little explored experimentally because of intensity and multiple scattering limitations. Utilizing a new code for calculation of multiple scattering, an experiment to study this regime in liquid Rb has been set up in collaboration with J. R. D. Copley of Argonne National Laboratory. Preliminary results show the existence of well-defined propagating modes at wave-vectors extending to 0.8\AA^{-1} . Further experiments to clarify an unexplained zero-frequency peak are presently underway. In conjunction with these experiments, Aneesur Rohman of Argonne National Laboratory has initiated a molecular dynamics computer study of this same system. The combined results of these two programs will be used to establish the physical basis underlying this result for Rb, which contrasts sharply with liquid argon and liquid sodium.

ELEMENTARY EXCITATIONS IN QUANTUM LIQUIDS

J. M. Rowe

In recent years, the techniques of neutron inelastic scattering have been used to establish directly the frequency-wave vector dispersion relation of liquid ^4He as a function of temperature and pressure in both the superfluid and normal phases. These results have led to deeper theoretical understanding of this important quantum fluid. On the other hand, liquid ^3He , which is a Fermi liquid (as opposed to liquid ^4He which is a Bose liquid) has not been studied by neutron scattering because of the very large neutron absorption cross-section of this isotope. Consequently, much less is known about the dynamics of this system in the short wavelength regime. Recent measurements have suggested that ^3He becomes a superfluid at very low temperatures (<8 mK), a result which is certainly intimately related to the dynamics of the fluid. Mixtures of $^3\text{He} - ^4\text{He}$ have important applications in low temperature refrigerators, and measure-

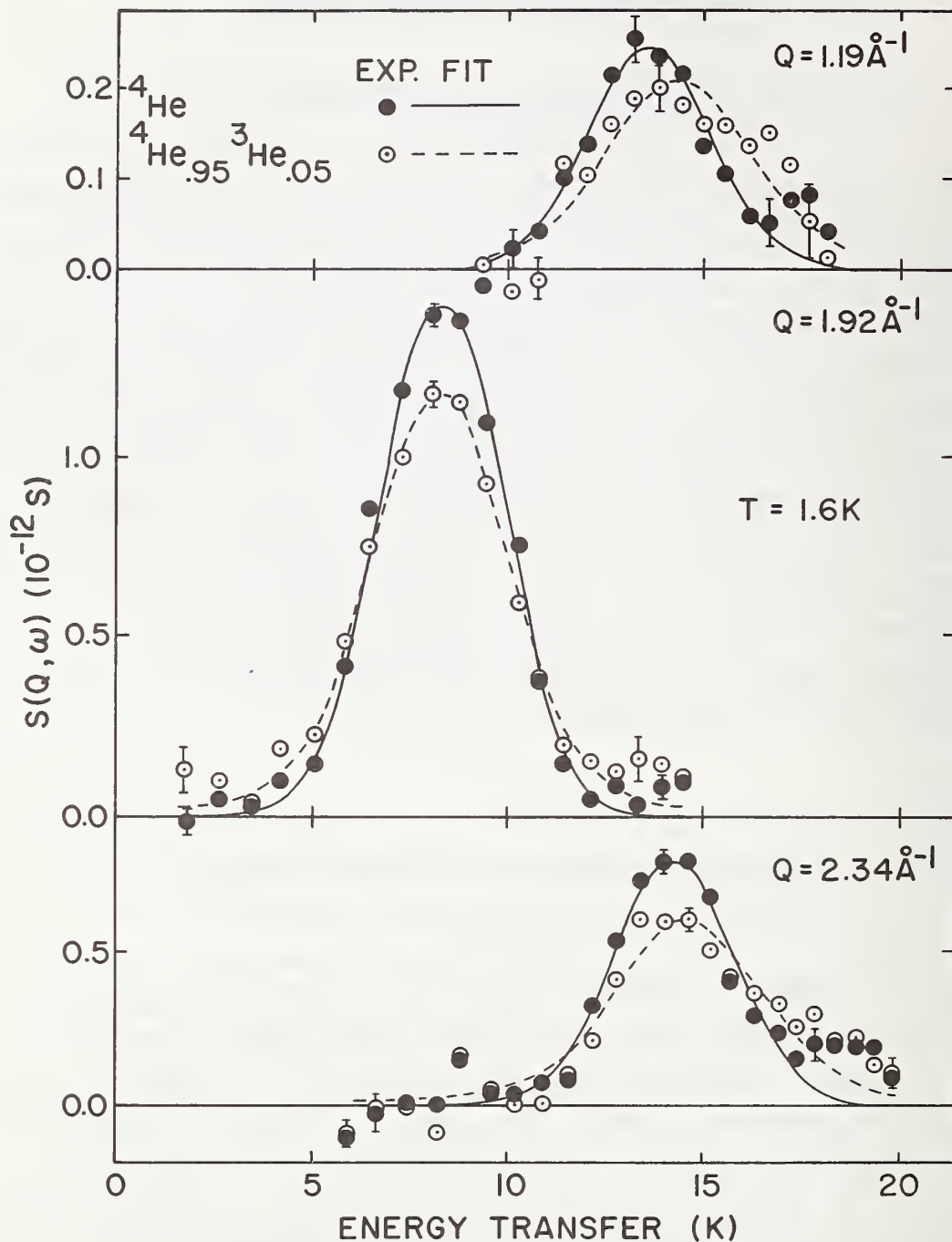


Fig. 1. The experimental scattering law data for ${}^4\text{He}(\bullet)$ and the ${}^4\text{He}_{.95}{}^3\text{He}_{.05}(\circ)$ liquids at three selected angles of scattering for a temperature of 1.6K. The solid and broken lines represent fits to the data which will not be discussed here. The value of wave vector transfer Q shown is determined at the energy corresponding to the peak.

REACTOR RADIATION DIVISION PROGRAMS

ment of the dynamics of these systems has also been hindered by the very high absorption cross-section of ^3He . Recent measurements we describe here on a $^3\text{He}_{.05} - ^4\text{He}_{.95}$ solution have been used to elucidate the basic $^3\text{He} - ^4\text{He}$ interaction and represent the first step in a program to measure the neutron inelastic scattering from ^3He itself.

1. $^4\text{He}_{.95} - ^3\text{He}_{.05}$

In collaboration with D. L. Price and G. E. Ostrowski of Argonne National Laboratory, measurements of the elementary excitations on a $^4\text{He}_{.95} - ^3\text{He}_{.05}$ solution at 1.6°K have been completed. The measurements extended over a wave-vector range of $0.8 - 2.5 \text{ \AA}^{-1}$, and were compared to similar results on pure ^4He . In this experiment, the ratio of neutron scattering to absorption was 1:500, and the relatively new measurement technique of pseudo-statistical chopping for energy analysis was used in order to increase the statistical accuracy of the results. The data were analysed to yield the shift in energy and decrease in lifetime of the excitations compared to pure ^4He . The results of this analysis are in good agreement with recent laser Raman studies of the bound two roton state in such mixtures. Compared to the Raman studies which yield information about only one portion of the elementary excitation spectrum, the neutron results provide information over a wide range of wave-vector transfers, and so give information inaccessible to other techniques. The present results, which give direct information on the excitation spectrum, are in disagreement with earlier conclusions based upon indirect measurements of fourth sound velocities, super fluid fractions and ion mobilities. This in turn shows that the theories used to extract information about the excitations from these previous measurements are seriously in error. Examples of the data taken are shown Fig. 1. The present experiments will be extended to other concentrations and to lower temperature.

2. Liquid ^3He

Planning for measurements on pure ^3He has begun. The essential requirements are for sample holders having good thermal conductivities at

low temperatures (<100 mK) and for the cryogenic equipment to achieve these temperatures. At present, the $^3\text{He} - ^4\text{He}$ dilution refrigerator required is being designed, and delivery is expected late in 1973. The sample holder is also being designed and will arrive before the refrigerator. Experiments are expected to begin early in 1974, in collaboration with D. L. Price, K. Sköld and G. E. Ostowski of Argonne National Laboratory.

RIGID BODY THERMAL MOTION IN CRYSTALLOGRAPHIC REFINEMENT

E. Prince

The formulas for constraining thermal parameters in crystallographic refinement¹ have been extended to include the S tensor of Schomaker and Trueblood². The formulas have been incorporated into a least-squares refinement program and applied to refinement of the heteropoly anion $\text{SiW}_{12}\text{O}_{40}$ (see NBS Technical Note 567) and the ammonium ion in NH_4ClO_4 at various temperatures (described elsewhere in the report).

¹E. Prince and L. W. Finger, *Acta Cryst.* B29, 179 (1973).

²V. Schomaker and K. N. Trueblood, *Acta Cryst.* B24, 63 (1968).

STUDIES ON TWINNING

A. Santoro

1. Preface

The geometrical conditions required for the formation of twins and rules governing the mutual orientation of the individual crystals in a twinned edifice have been analyzed as part of a continuing study of the properties of crystal lattices. Convenient and general procedures for characterizing twinning have been derived. The twinning condition and the description of the twin obliquity obtained as a result of this research, represent significant generalizations of Friedel's classical theory.¹

Some of the results of this work have been applied to the study of the twinning associated with the metal-insulator transition in Cr-doped VO_2 . This application, described in one of the following sections, shows that the procedures developed for determining the geometrical properties of twins are useful for interpreting the complex x-ray and neutron diffraction patterns produced by twinned samples. We will now summarize the work done in this area during the past year.

2. Characterization of Twinning

Let us consider two crystals, not necessarily of the same species, and let us suppose that their lattices are described by the triplets of primitive, non-coplanar, translations \vec{a}'_i and \vec{a}''_i . The two crystals may form a regular aggregate if their lattice dimensions and their mutual orientation are such that they have, exactly or approximately, a superlattice in common. It can be shown that these two conditions are met if the equation

$$\sum_k \sum_{\ell} B_{ij} B_{j\ell} A'_{\ell k} - A''_{ij} = 0 \quad (k, \ell, i, j = 1, 2, 3) \quad (1)$$

is satisfied with rational coefficients B_{ij} . The elements A'_{ij} and A''_{ij} in the above expression are the scalar products

$$A'_{ih} = \vec{a}'_i \cdot \vec{a}'_h, \quad A''_{ij} = \vec{a}''_i \cdot \vec{a}''_j.$$

¹Friedel, G. (1926). *Lecons de cristallographie*. Paris: Berger-Lerrault. Reprinted (1964), Paris: Blanchard.

Equation (1) expresses the geometrical conditions necessary for the formation of regular aggregates such as syntaxic and epitaxial growths and twins. The rational elements B_{ij} define the mutual orientation of the individuals in the aggregate.

Twins are regular aggregates constituted by individual crystals of the same species. The twinning condition, therefore, is expressed by equation (1) in which it is $\tilde{A}' = \tilde{A}''$. It is possible to show that equation (1) is more general than Friedel's conditions of twinning. The use of this equation permits one to predict not only the possible twin laws associated with a crystalline material, but also the well known regular associations of crystals mutually oriented according to non-crystallographic rotations. Equation (1) also permits one to give a very general description of the "twin obliquity".

Work on this subject has been completed and a paper has been submitted for publication in Acta Crystallographica.

3. Twinning in Cr-Doped VO_2 - M. Marezio and P. D. Dernier (Bell Laboratories) and A. Santoro

Cr-doped VO_2 undergoes a metal-insulator transition in which the high-temperature phase, with a rutile-type structure, is slightly distorted into a monoclinic structure. As the distortion results in a final phase having symmetry lower than that of the initial phase, the transition is usually associated with twin formation.

Table I shows the crystal data relative to the samples of Cr-doped VO_2 analyzed in the present study. In Table II are shown the twin laws predicted by the theory. Each of the samples studied was twinned on more than one law and, with the exception of $[010]_{90^\circ}$, all the predicted twin laws were observed at least once.

The appearance of the diffraction patterns depends on the particular twin laws operating in each sample. Thus, the laws (100) and (001) can be easily detected as they produce doubling of the diffraction spots. The laws (201) and $(20\bar{1})$, however, are characterized by a small value of the obliquity and individuals twinned with these laws give reflections almost exactly superposed. In fact, a spot with film coordinates h, k, l

is formed by the superposition of three reflections, one from each individual of the twin, having indices

$$(hkl)_I, (2l \ k \ h/2)_{II}, (2\bar{l} \ k \ \bar{h}/2)_{III}.$$

It follows that spots with h and k both odd are produced only by individual I, while spots with k odd and inconsistent with the lattice parameters are produced only by individuals II and III. This observation on the geometrical characteristics of the diffraction patterns makes it possible to determine the volume of the sample belonging to each individual and to obtain the structure from the intensities measured from twinned samples. The structure of $V_{0.976}Cr_{0.024}O_2$ was in fact determined, and refined to an R factor of 2.9%, once the twinning problem was solved.²

It is possible to show that, if twinning takes place with the laws (201) and $(20\bar{1})$, the diffraction patterns simulate a lattice having a cell related to the true one by the axes transformation $10\bar{2}/010/002$ and a space group Cc or C2/c. This is another case in which twinning, if not detected, can lead to erroneous parameters and space groups.

Work on this subject has been completed and a paper is in press in *Acta Crystallographica*.

4. Possible Applications

Other possible applications of the results of our study on twinning are the following:

(i) As the method proposed for deriving the possible twin laws associated with a crystalline material can be easily adapted to automatic computations, it is feasible to systematically check whether the known twins abide by the rules of Friedel without exceptions and to clarify, where the structure is known, the relationship between the geometrical and the structural theories of twinning. Such extensive critical evaluation of published crystal data would result in a more complete and reliable characterization of crystalline materials.

²M. Marezio, D. B. McWhan, J. P. Remeika and P. D. Dernier, *Phys. Rev. B5*, 2541-2551 (1972).

Work in this area, in collaboration with A. D. Mighell (Inorganic Materials Division, IMR), is contemplated.

(ii) Epitaxial relationships among the crystalline species constituting urinary and biliary calculi have been suggested, but are far from being exhaustively investigated.^{3,4} Since the necessary geometrical conditions for the formation of epitaxial and syntaxial growths can be found with relative ease by using the results of the present work, it becomes possible to carry out an extensive study of the geometrical and structural properties of the calculi's components.

Experimental and theoretical work in this area, in collaboration with Dr. A. D. Mighell (Inorganic Materials Division, IMR) is planned.

TABLE I

Crystal data for Cr-doped VO₂ at room temperature

	VO ₂ +0.5 at.%Cr	VO ₂ +2.5 at.%Cr
a	9.081(1) Å	9.0664(7)Å
b	5.781(1)	5.7970(5)
c	4.516(1)	4.5255(4)
β	90.91°(1)	91.88°(1)
Space group	C2/m	C2/m

TABLE II

Possible twin laws for Cr-doped VO₂. Twin axes and planes are referred to the monoclinic cells whose parameters are given in Table I.

		VO ₂ +0.5 at.%Cr	VO ₂ +a.5 at.%Cr
[010] _{90°}	2		
(20 $\bar{1}$) \equiv [102] _{180°}	2	0.3°	0.1°
(201) \equiv [10 $\bar{2}$] _{180°}	2	0.3	0.1°
(100) \equiv [001] _{180°}	1	0.9°	1.88°
(001) \equiv [100] _{180°}	1	0.9°	1.88°

³K. Lonsdale, *Nature* 217, 56-58 (1968).

⁴K. Lonsdale, and D. J. Sutor, *Soviet Physics-Crystallography (Transl.)*, 16, 1060-1068 (1972).

THERMAL NEUTRON FLUX MEASUREMENTS

V. W. Myers and M. Ganoczy

A manganese sulfate bath has been used at a beamport for determining the absolute thermal neutron intensity of the beam. Boron loaded cobalt glass beads were activated in the known thermal flux. The beads were then used for calibrating a NaI well detector. The data from this experiment is being analyzed. An unknown thermal flux could be measured by activating a cobalt glass bead in the flux and then counting it in the calibrated well detector.

INTERCOMPARISON OF NEUTRON DIFFRACTOMETERS

V. W. Myers

Collaboration is continuing in a program of the International Union of Crystallography for the comparison of neutron flux at various neutron spectrometers. Gold foils are activated in the diffracted beam. Foils were counted at NBS for irradiation at the Oak Ridge HFIR. In addition, foils will be irradiated at NBSR, Georgia Technical Research Reactor, and possibly other facilities and counted at NBS. This study should be completed by June 1974.

DIRECT TESTS FOR VIOLATION OF CP INVARIANCE

R. C. Casella

In 1968-69 it was first demonstrated independently of the CPT theorem that time reversal symmetry (T) is violated in the CP-violating pionic decays of the neutral kaon.¹ (Previously the result had been deduced from the CPT theorem coupled with the data of Fitch, Cronin, and collaborators.) This more general demonstration of T violation was subsequently verified by Kabir, Steinberger, and others. Because of the importance of the violation in Nature of the fundamental CP and T ($\sim 10^{-3}$) effect, it is essential to base the conclusions on as few theoretical assumptions as possible. One assumption which, in one form or another, has entered into the deductions of symmetry breaking by Christenson et al., Lee, Oehme, and Yang, Wu and Yang, Casella, Kabir, and others is the well-known Weisskopf-Wigner approximation for decaying states. Recently, in collaboration with B. Robertson, we have devised tests, one of which, when applied to preliminary data of Steinberger and collaborators at CERN, indicates that the CP violation can be established independently of the validity of the Weisskopf-Wigner approximation. Experiments of Banner

et al. independently corroborate this conclusion. A paper reporting on our work will appear. The fundamental origin of the CP and T violations remains an intriguing mystery.

¹R. C. Casella, *Phys. Rev. Lett.* 21, 1128 (1968); 22, 554 (1969).

COLD-NEUTRON TIME-OF-FLIGHT FACILITY

R. S. Carter, A. A. Cinquepalma, D. H. Fravel,
and J. B. Sturrock

The cold neutron time-of-flight facility is designed for inelastic neutron scattering studies of solids and liquids. A neutron beam from the reactor is filtered through polycrystalline beryllium to eliminate neutrons with wavelengths shorter than 3.92\AA . The beam then passes through a four rotor phased chopper system which chops the beam into short bursts of neutrons of selected energy. The sample to be studied is placed immediately after the choppers and the scattered neutrons are detected in a large bank of detectors arranged along the arc of a circle with a 2.4 meter radius. The detectors are located in a shielding room. The detector information is fed into a multi-channel analyzer and the neutron energy determined from the flight time of the neutrons from the sample to the detectors.

The facility has been completed and a study of the background counting rates was initiated. The results to date showed that many of the detectors appeared to have an unusually large sensitivity to γ -rays resulting in excessive back ground counting rates. This problem is undergoing further study. The shielding from sources other than the facility beam itself appears to be adequate (~ 2 c/m per detector) for those detectors which do not have an abnormal gamma-ray sensitivity. The beam from the facility itself, however, introduced a neutron background of as much as 15 counts per minute per detector for those detectors nearest the beam. The addition of 6" of Be in the beam was necessary to reduce the fast neutron background from the beam to manageable proportions ($\sim 2-3$ counts per min-

ute per detector from fast neutron scattering and ~ 2 counts per minute room background). Methods to minimize the scattering of thermal neutrons are being investigated.

COLD-NEUTRON SOURCE

R. S. Carter, E. M. Guglielmo, and F. J. Shorten

The NBS reactor includes a special port, 22" in diameter, which penetrates the reflector up to the edge of the fuel elements. This large opening was designed to provide space for the insertion of a cold neutron source close to the core. By inserting a large, low temperature moderator it is possible to significantly increase the available intensity of very low energy neutrons ($\lambda > 4\text{\AA}$) which are very useful for many types of molecular dynamic studies.

The moderator will be a cylinder of D_2O ice 14" in diameter by 12" long. A small amount of H_2O may be added to optimize the moderating property of the source. The source will have a reentrant hole 4" deep by 8" in diameter for beam extraction. The hole will be filled with beryllium which has the property of reflecting the higher energy neutrons back into the moderator while passing the lower energy neutrons. The moderator will be maintained at 25 K by cold helium gas passing through tubing in the moderator. The vacuum cryostat containing the moderator will be constructed of thin-walled aluminum to minimize heating by capture gamma rays. The cryostat will be mounted on a shielding plug and the whole assembly will roll inside a second plug and shield assembly which itself will roll into the special port of the NBSR. The shield mounted on the second plug surrounds the cryostat and consists of about 4" of lead and bismuth which greatly reduces the gamma ray heating of the moderator. Two 6" and two 2" diameter beams can be extracted from the cold source through the reactor shield. One of the 6" beams will be used for the cold neutron time-of-flight facility while the others await future development.

REACTOR RADIATION DIVISION PROGRAMS

The helium for cooling is provided by an all helium refrigerator using a turbine expansion engine developed by the NBS cryogenic laboratory in Boulder. It has a one kilowatt capacity at 25 K which is sufficient to handle the heat generated in the moderator at twice the current reactor power.

The bismuth tip and cryostat are the only items which remain to be installed. The cryostat has undergone extensive testing during the past year and meets all necessary requirements. The bismuth tip which had to be completely refabricated is still not completed. Many of the components have been made but final assembly and the pouring of the bismuth and lead have yet to be done.

B. RRD-NBS COLLABORATIVE PROGRAMS

INELASTIC NEUTRON SCATTERING OF α NEON NEAR THE CRITICAL TEMPERATURE

B. Mozer
(Inorganic Materials Division)

Inelastic neutron scattering experiments on neon within 10 milli-Kelvin of the critical temperature have been carried out using the high resolution Fermi chopper time-of-flight system. Small angle scattering data was obtained for a number of angles from 3.5 to 12.5° using 2.8\AA neutrons and 1.4\AA neutrons from the second order transmitted by a filter. The angular range covers a kappa region for elastic and quasi-elastic scattering of 0.144 to 0.490 \AA^{-1} for the first order beam and double that for the $\lambda/2$ beam. The scattering from each wavelength is distinct and allows additional information to be collected during the experiment. The kappa values used overlap the intense scattering associated with critical phenomena as observed in the diffraction experiments. The wavelength and energy resolution of the system for the first order neutrons are 1.95% and 3.90% respectively. The latter corresponds to an energy resolution of about 0.4 meV. Incoming beam energy resolution is about 0.25 meV. Energy resolution would be almost doubled for $\lambda/2$ detected neutrons.

Preliminary data analysis shows some quasielastic broadening for the smaller angles. This small broadening does not seem capable of being resolved into two components associated with Brillouin scattering from a liquid at the critical point. At a larger angle, the line shape changes into a spectrum of two barely resolvable peaks. This splitting of the spectrum could be interpreted as a splitting associated with a propagating phonon mode in the liquid. At larger angles the spectra is considerably broadened and the signal almost lost. Analysis of the scattering from the $\lambda/2$ neutrons has just begun and can be used for checking the consistency of the interpretation of the scattering from the first order neutron within the decreased energy resolution. Scattering of the higher energy neutrons by neon is observed to produce a well defined signal showing broadening at the larger momentum transfers.

AN OBSERVATION OF THE DEVIATION FROM ORNSTEIN-ZERNIKE THEORY
IN THE CRITICAL SCATTERING OF NEUTRONS FROM NEON

V. P. Warkulwiz and M. S. Green
(Temple University, Philadelphia, Pa.)

and

B. Mozer
(Inorganic Materials Division)

One-component fluids near their critical point have long been known to display a striking phenomenon called critical opalescence in which incident radiation is strongly scattered. L. S. Ornstein and F. Zernike¹ in 1914 proposed a theory to describe the scattering of radiation by a fluid near its critical point. They obtained the following result which is good for small values of the momentum transfer Q :

$$I(Q) \propto [Q^2 + (1/\xi)^2]^{-1};$$

where

$Q = (4\pi/\lambda)\sin \theta/2$; λ is the wavelength of the incident radiation; θ is the scattering angle;

$I(Q)$ is the intensity of the scattered radiation;

ξ is the range of density fluctuation correlations in the fluid.

Ornstein-Zernike theory has long been accepted as providing a reasonably good explanation of critical opalescence. It has also been extended to describe critical scattering in two-component and magnetic systems with a fair degree of success. However, certain theoretical and experimental results suggested that Ornstein-Zernike theory might not be exact and led M. E. Fisher² to propose the following modification of the Ornstein-Zernike formula:

$$I(Q) \propto [Q^2 + (1/\xi)^2]^{-1+\eta/2}.$$

The critical exponent η is a measure of the deviation from Ornstein-Zernike theory. Other forms for $I(Q)$ have also been proposed,³ but for $(Q\xi)^2$ large and η small they all reduce to $I(Q) \propto (Q^2)^{-1+\eta/2}$.

We have performed an experiment which was designed specifically to look for a departure from Ornstein-Zernike theory in the critical scattering of neutrons from neon in the region $(Q\xi)^2$ large. This was

done on a diffractometer set up at the thermal column where a thermal neutron beam with a high cadmium ratio and sufficient intensity was provided. In order to obtain sufficiently small values of Q without going to very small scattering angles, it was necessary to produce an incident beam with wavelengths in the range 4 to 9 angstroms. This was accomplished by using a monochromator composed of a liquid nitrogen cooled beryllium filter followed by a mechanical velocity selector. The monochromator produced a spectrum with wavelengths between 4 and 7 angstroms peaked at 5 angstroms. Such a broad spectrum could be used because neither the width of the spectrum nor its shape was required in the analysis of the data. The diffractometer was controlled by the NBS reactor time-shared diffractometer control system. Data was taken over the angular range -3° to 10° with a statistical precision of about 0.5%. The critical point was determined from our own measurements of the coexistence curve of neon using a sample cell with a built-in capacitor.

A preliminary analysis of the data indicated the critical exponent η to be greater than 0.10 and less than 0.18.

¹L. S. Ornstein and F. Zernike, *Proc. Roy. Acad. Sci. Amsterdam* 17, 793 (1914).

²M. E. Fisher, *J. Math. Phys.* 5, 944 (1964).

³H. L. Swinney and B. E. A. Saleh, *Phys. Rev.* A7, 747 (1973).

THE STRUCTURE FACTOR OF NEON NEAR T_C B. Mozer
(Inorganic Materials Division)

and

V. W. Warkulwiz
(Temple University, Philadelphia, Pa.)

The structure factor of neon near the critical temperature, T_C , has been determined from neutron diffraction experiments. One experiment was performed on neon at a thermodynamic state within 8 to 10 multi-Kelvin of T_C . The measurements were divided into three parts. The first measurement consisted of a scattering experiment for small momentum transfers, $\kappa = 4\pi \sin\theta/\lambda$, which were performed at the thermal column as described by Warkulwiz, Green and Mozer. The next two parts of the measurements were performed at the BT-2 spectrometer where a 2.4\AA beam of neutrons was used to provide data for a momentum transfer region of 0.2 to 3.5\AA^{-1} which overlapped with the small angle, small κ data. The last part of the experiment was performed with a 1\AA beam of neutrons to obtain the structure factor from 2.5 to 9\AA^{-1} and to provide overlap with the 2.4\AA data. The second experiment was performed on Neon about 2.0 Kelvin above T_C .

The scattering data for the two thermodynamic points are essentially identical except in the forward direction where the critical scattering is pronounced. Structure is observed for momentum transfers as large as 9\AA^{-1} associated with the hard core of the interatomic potential. The overall structure except in the forward direction, is similar to that of liquid neon reported by de Graaf and Mozer¹ in the liquid state. Further data analysis is in progress.

¹L. A. de Graaf and B. Mozer, *J. Chem. Phys.* 55, 4967 (1971).

STUDY OF HINDERED ROTATION IN HYDROXYLAMMONIUM
PERCHLORATE BY CONSTRAINED LEAST-SQUARES REFINEMENT

E. Prince and J. Rush

and

B. Dickens
(Polymers Division)

Hydroxylammonium perchlorate, $\text{NH}_3\text{OHClO}_4$, (referred to hereafter as HAP) crystallizes in the orthorhombic space group $P2_1cn$, with cell dimensions $\underline{a}=7.52\text{\AA}$, $\underline{b}=7.14\text{\AA}$, $\underline{c} = 15.99\text{\AA}$. There are two crystallographically independent formula units in the unit cell, which contains a total of eight formula units.

Several years ago a preliminary set of neutron diffraction data was collected from a crystal of HAP because neutron cross-section measurements gave an indication of large amplitude thermal motions of hydrogen atoms in this compound. Consideration of the crystal structure of this compound made it seem likely that this large amplitude motion was a torsional oscillation, or hindered rotation, of the NH_3 end of the NH_3OH ion about the NO bond. At the time of the preliminary experiment no attempt was made to refine the structure because the available programs for least-squares refinement could treat curvilinear thermal motion only by introducing a much larger number of parameters than could possibly have physical significance. Because the techniques developed to treat the motions of the methyl groups in durene^{1,2} seemed to be applicable to this problem a new, more extensive data set was collected. For least-squares refinement a model was constructed in which conventional, anisotropic temperature factors were assigned to the atoms in the perchlorate groups and to the OH hydrogen atoms, but the ONH_3 portions of the hydroxylammonium ions were treated as rigid bodies. Isotropic translation and libration parameters were assigned to the groups and in addition the hydrogen atoms bound to the nitrogen were considered to be in torsional oscillation about the NO bond. Preliminary refinement with anisotropic temperature factors for the atoms of the perchlorate groups and the hydroxyl hydrogen atoms but

with isotropic temperature factors for the ONH_3 groups give a weighted R index of .081. The special model, which actually has fewer adjustable parameters, refined to a weighted R .051, a highly significant improvement. Figure 1 is a stereoscopic pair showing one half of the unit cell. The apparent r.m.s. amplitude of torsional oscillation of the NH_3 groups is about 26° , which would correspond to a peak displacement for a harmonic oscillator of 37° from the equilibrium position. Because the potential maximum would correspond to a displacement of 60° , this is consistent with frequent reorientation or hindered rotation.

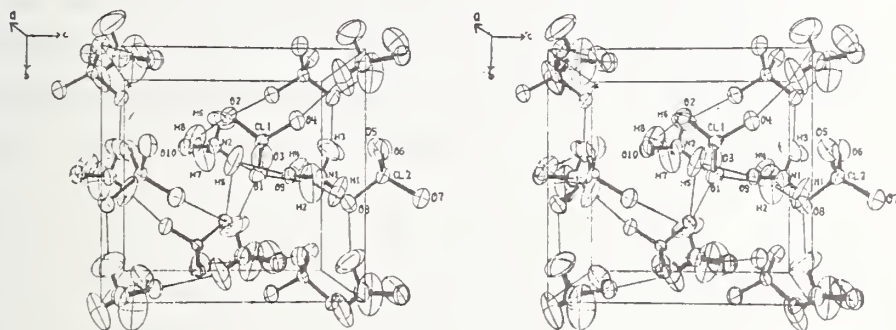


Fig. 1. The crystal structure of $\text{NH}_3\text{OHC1O}_4$. Half the unit cell is shown viewed along a. The thin lines indicate hydrogen bonds.

¹E. Prince and L. W. Finger, *Acta Cryst.* B29, 179 (1973).

²E. Prince, L. W. Schroeder, and J. J. Rush, *Acta Cryst.* B29, 184 (1973).

A BIFURCATED HYDROGEN BOND IN $\text{Ca}(\text{H}_2\text{PO}_4)_2\text{H}_2\text{O}$

L. W. Schroeder
(Polymers Division)

and

E. Prince

On the basis of a redetermination of the structure of $\text{Ca}(\text{H}_2\text{PO}_4)_2\text{H}_2\text{O}$ from x-ray data, Dickens and Bowen (1971) proposed a bifurcated hydrogen bond involving the water molecule. A study of the infrared spectrum of

this material by Berry (1968) led to the suggestion that the protons may be distributed over several sites.

A set of neutron diffraction data, 1228 reflections observed within the limiting sphere of 100 deg. 2θ angle, was collected on a fairly large crystal of dimensions 3 mm x 5 mm x .37 mm. All the hydrogen atoms were located from a Fourier synthesis calculated with signs based on the previous structural model. Refinements including isotropic extinction led to an R index of .06 and a weighted R of .09. A comparison of F_o and F_c showed that many reflections with $F_c < 1.0$ ($\times 10^{-12}$ cm) had F_o values as much as 5 times greater than F_c . These reflections (about 60) were suspected of suffering effects of simultaneous diffraction and were eliminated from subsequent refinements which led to R and weighted R indexes of .055 and .068. Positional parameters did not change significantly, but some thermal parameters changed by 3-4 times their standard deviations.

The differences between our model and the previous one based on x-ray data are insignificant in terms of bond distances and angles between all atoms except hydrogen. No evidence of disordered protons in the structure was found and the previously proposed bifurcated hydrogen bond was located. Our results imply that the extra features of the infrared spectrum observed by Berry result from coupling of various proton motions rather than crystal disorder.

B. Dickens and J. S. Bowen, *Acta Cryst.* B27, 2247 (1971).

E. E. Berry, *Spectrochimica Acta* 24A, 1727 (1968).

THE CRYSTAL STRUCTURE OF $\text{H}_3\text{PO}_4 \cdot 1/2\text{H}_2\text{O}$ B. Dickens, L. W. Schroeder
(Polymers Division)

and

E. Prince

Although the coarse details of the crystal structure of $\text{H}_3\text{PO}_4 \cdot 1/2\text{H}_2\text{O}$ were known from an earlier x-ray investigation using photographic data, there was ambiguity in the suggested hydrogen bonding scheme. The structure was therefore refined using neutron diffraction data.

$\text{H}_3\text{PO}_4 \cdot 1/2\text{H}_2\text{O}$ is very hygroscopic and melts at 29.3°C. After several failures to glue a crystal onto a rod in a nitrogen atmosphere, a suitable crystal was grown by successive remelting of several smaller crystals in a quartz tube sealed by epoxy cement. Because of the method of crystal growth, the crystal adhered poorly to the tube wall and had to be re-oriented frequently under computer control. However, secondary extinction exerted much less effect on the data than is normal for solution grown crystals, and extinction corrections, normally a problem in neutron diffraction, presented no difficulty. The hydrogen atoms were found and the structure refined with anisotropic temperature factors to

$$R_w = [\sum \omega (|F_o| - |F_c|)^2 / \sum \omega |F_o|^2]^{1/2} = 0.022 \text{ using 1208 observed reflections.}$$

The structure is shown in figure 1. Both crystallographically discrete H_3PO_4 molecules have similar environments, being extensively hydrogen bonded to each other and the water molecule. The water molecule forms hydrogen bonds of normal strength to the H_3PO_4 molecules. These hydrogen bonds are appreciably non-linear because of repulsion between the water hydrogens and the hydrogens accepted by the water oxygen in hydrogen bonds for the H_3PO_4 molecules. Four close H...H distances, in the range 2.161(3) to 2.290(3)Å, imply H...H van der Waals interactions, similar to the case in $\text{Ca}(\text{OH})_2$.

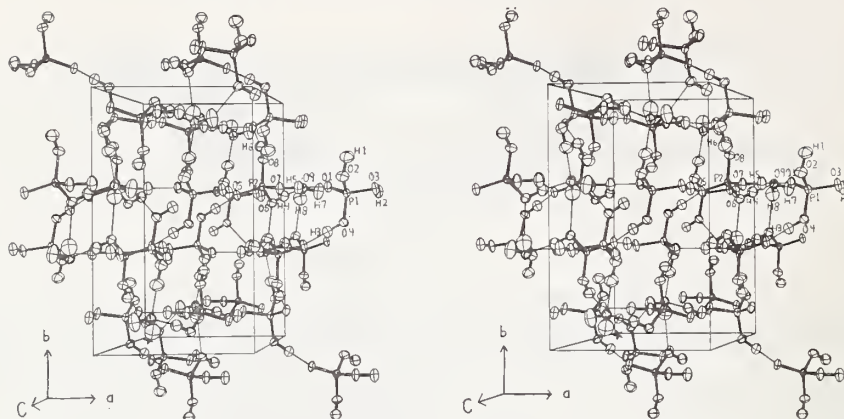


Fig. 1. Stereographic illustration of the crystal structure of $\text{H}_3\text{PO}_4 \cdot \frac{1}{2}\text{H}_2\text{O}$. The water molecule oxygen and the P of one of the two crystallographically discrete H_3PO_4 molecules are both shaded.

THE CRYSTAL STRUCTURE OF LEAD DEUTERIUM ORTHOPHOSPHATE

C. S. Brickenkamp
(Inorganic Materials Division)

and

E. Prince

Except for the hydrogen atom position, the x-ray crystal structure of PbHPO_4 essentially has the space-group symmetry $P2/c$. Consideration of the most probably hydrogen position, however, favored the noncentrosymmetric space group Pc , subgroup of $P2/c$, and this was confirmed by subsequent piezoelectric and pyroelectric measurements.

The neutron diffraction study of the deuterium-substituted lead phosphate, PbDPO_4 was undertaken: (1) to obtain more accurate values for all atomic positions (the crystal used for x-ray data was later found to be a split crystal); (2) to determine the position of the deuterium atom in order to explain the direction of the polar axis found in the pyroelectric tests and to contribute to our ultimate goal of discovering the mechanism involved in the thermal decomposition of PbHPO_4 to $\text{Pb}_2\text{P}_2\text{O}_7$; and (3) to attempt to resolve, if necessary, any full-matrix-least-squares refinement difficulties due to the close proximity of the deuterium

position or positions to the pseudo-center of symmetry. Table I gives crystal data and atomic positions for PbHPO_4 as determined with x-rays and for PbDPO_4 as far as refinement has proceeded with the neutron diffraction study.

Table 1. Crystal data and atomic parameters for PbHPO_4 and PbDPO_4 .

<u>PbHPO_4</u>	<u>PbDPO_4</u>
$a = 4.688(4)\text{\AA}$	$a = 4.6855(5)\text{\AA}$
$b = 6.649(5)\text{\AA}$	$b = 6.6911(7)\text{\AA}$
$c = 5.781(5)\text{\AA}$	$c = 5.7867(8)\text{\AA}$
$\beta = 97.11(2)^\circ$	$\beta = 97.10(1)^\circ$
space group: Pc	space group: Pc
$z = 2$	$z = 2$
$D_m = 5.661 \text{ g/cm}^3$	
$D_x = 5.631 \text{ g/cm}^3$	
$\lambda = .7107 \text{ (MoK}\alpha)$	$\lambda = 1.232$
525 unique reflections	361 unique reflections
$R = 0.11$	$R = .10 \text{ (2nd cycle)}$

The temperature factor expression used is: $\exp[-(\beta_{11}h^2 + \beta_{22}k^2 + \beta_{33}l^2 + 2\beta_{12}hk + 2\beta_{13}hl + 2\beta_{23}kl)]$.
 Numbers in parenthesis are estimated standard deviations.

PbHPO₄ (refined in space group P2/c)

	x	y	z	β_{11}	β_{22}	β_{33}	β_{12}	β_{13}	β_{23}
Pb	0.0	0.1999(2)	0.25	0.0133(8)	0.0115(4)	0.0128(5)	0.0	0.0036(4)	0.0
P	0.5	-0.2069(14)	0.25	0.012(4)	0.009(2)	0.021(4)	0.0	0.005(3)	0.0
0(1)	0.376(6)	0.339(4)	-0.070(6)	0.033(10)	0.019(4)	0.042(10)	-0.000(6)	0.018(8)	-0.005(5)
0(2)	0.260(5)	0.074(4)	-0.371(4)	0.030(8)	0.029(6)	0.201(5)	-0.008(6)	0.000(5)	0.000(5)

PbDPO₄ (refined in Pc)

Pb	.0029	.1991(6)	.2498	.023(2)	.008(1)	.022(2)	-.003(2)	-0.003(1)	.003(2)
P	.497(4)	-.207(1)	.236(2)	.020(4)	.008(2)	.011(2)	.009(3)	-.001(2)	.007(2)
0(1)	.385(2)	.336(1)	-.074(2)	.012(3)	.008(2)	.000(1)	.009(2)	.003(2)	.002(2)
0(2)	.260(3)	.072(2)	-.376(2)	.015(4)	.017(3)	.005(2)	-.002(3)	-.009(2)	-.004(2)
0(3)	-.367(4)	-.342(3)	.060(4)	.04(1)	.017(4)	.057(7)	-.013(5)	.025(7)	-.016(4)
0(4)	-.251(3)	-.080(2)	.378(2)	.026(6)	.006(2)	.015(3)	-.002(3)	.007(3)	.002(2)
C(1)	.494(4)	.522(3)	.482(3)	.035(4)	.024(4)	.037(4)	-.010(4)	.013(3)	-.020(3)

NEUTRON DIFFRACTION STRUCTURE DETERMINATION OF
 DICHLOROTETRAPYRAZOLECOPPER(II), $\text{Cu}(\text{C}_3\text{H}_4\text{N}_2)_4\text{Cl}_2$

A. Mighell and C. Reimann
 (Inorganic Materials Division)

and

A. Santoro and E. Prince

As part of a study of compounds with complex cations, the structure of dichlorotetrapyrazole(II), $\text{Cu}(\text{C}_3\text{H}_4\text{N}_2)_4\text{Cl}_2$ has been determined using neutron diffraction. The purpose of this neutron investigation was to obtain accurate hydrogen parameters, to verify that internal hydrogen bonding occurs, to distinguish the ring carbon and nitrogen atoms, and to compare the geometry of the $\text{Cu}(\text{C}_3\text{H}_4\text{N}_2)_4\text{Cl}_2$ with that of $\text{Ni}(\text{C}_3\text{H}_4\text{N}_2)_4\text{Cl}_2$ ¹ and $\text{Ni}(\text{C}_3\text{H}_4\text{N}_2)_4\text{Br}_2$.²

Dichlorotetrapyrazolecopper(II) crystallizes in the monoclinic space group C2/c with Z=4 and lattice parameters $a=13.657$, $b=9.20$, $c=14.90\text{A}$ and $\beta=118.045^\circ$. Single crystal neutron intensities were collected and the structure was refined by full matrix least squares to an R value of 4.5%. Considerable difficulty was encountered in the refinement because of extinction in many of the intense reflections. For this reason, further refinement to correct for extinction is planned.

The complex is centrosymmetric with the copper atom located at a center of symmetry. All other atoms are in general positions. There are two pyrazole ligands and one chlorine atom in the structure that are crystallographically independent. The figure shows the $\text{Cu}(\text{Pz})_4\text{Cl}_2$ complex. A comparison of the bond distances of this structure with those of the related $\text{Ni}(\text{Pz})_4\text{Cl}_2$ complex are given in the Table. The bond distances in $\text{Cu}(\text{Pz})_4\text{Cl}_2$, compared to the related nickel complex are similar in the pyrazole ligands but differ significantly in the coordination distances. The Cu-Cl distance is 2.84A compared to the Ni-Cl distance of 2.51A. Likewise the average Cu-N coordination distance is 2.02A compared to 2.09A in the nickel complex

This neutron study makes it possible to distinguish unambiguously

Table 1. Comparison of bond distances in $\text{Cu}(\text{Pz})_4\text{Cl}_2$ and $\text{Ni}(\text{Pz})_4\text{Cl}_2$.

Bond	$\text{Cu}(\text{Pz})_4\text{Cl}_2^*$	$\text{Ni}(\text{Pz})_4\text{Cl}_2^{**}$
Me-Cl	2.840(2)	2.507(1)
Me-N(1)	2.015(1)	2.097(2)
Me-N(3)	2.010(2)	2.087(2)
Ring 1		
N(1)-N(2)	1.346(3)	1.345(4)
N(2)-C(1)	1.347(3)	1.357(4)
C(1)-C(2)	1.391(5)	1.371(7)
C(2)-C(3)	1.399(3)	1.393(5)
C(3)-N(1)	1.332(3)	1.329(4)
C(1)-H(1)	1.069(7)	---
C(2)-H(2)	1.065(7)	---
C(3)-H(3)	1.072(8)	---
N(2)-H(7)	1.006(8)	---
Ring 2		
N(3)-N(4)	1.337(4)	1.342(6)
N(4)-C(4)	1.337(4)	1.333(6)
C(4)-C(5)	1.373(5)	1.356(6)
C(5)-C(6)	1.396(5)	1.389(6)
C(6)-N(3)	1.320(3)	1.321(4)
C(4)-H(4)	1.088(7)	---
C(5)-H(5)	1.092(7)	---
C(6)-H(6)	1.084(11)	---
N(4)-H(8)	1.024(7)	---

*Neutron diffraction data

**X-ray diffraction data

the ring carbon and nitrogen atoms and thus establish that the ring is coordinated to the transition metal via the nitrogen atom. Also it is possible to accurately determine the hydrogen atom positions. In the two independent pyrazole rings there are 6(C-H) distances and 2 (N-H) distances. The average N-H distance of 1.03A is significantly shorter than the average C-H distance of 1.08A. In the complex, $\text{Co}(\text{C}_3\text{H}_4\text{N}_2)_6(\text{NO}_3)_2$, also studied by neutron diffraction³ a similar difference in N-H and C-H bond lengths is observed.

The accurate location of the hydrogen atoms established that there is internal hydrogen bonding in the complex. These bonds are presumed to be responsible for the fact that the planes of the pyrazole rings are vertical to the plane defined by the coordinating pyrazole nitrogen atoms N(1) N(1') N(3) N(3'). The N-H...Cl hydrogen bonds are stronger than the C-H...Cl bonds because the hydrogen atoms attached to the nitrogen atoms N(2) and N(4) are closer to the chlorine atoms than the hydrogen atoms attached to C(3) and C(6). The distances for these four possible internal hydrogen bonds are: in ring one, N(2)-H(7)...Cl is 2.40A and C(3)-H(3)...Cl is 2.66A. In ring two, N(4)-H(8)...Cl is 2.28A and C(6)-H(6)...Cl is 2.73A. As the N-H...Cl bonds are stronger than the C-H...Cl bonds, the rings are tipped slightly toward the chlorine atoms as shown by the following angles:



Both the ring tipping and the shorter hydrogen bond distance involving H(8), show that ring 2 is more strongly hydrogen bonded than ring 1.

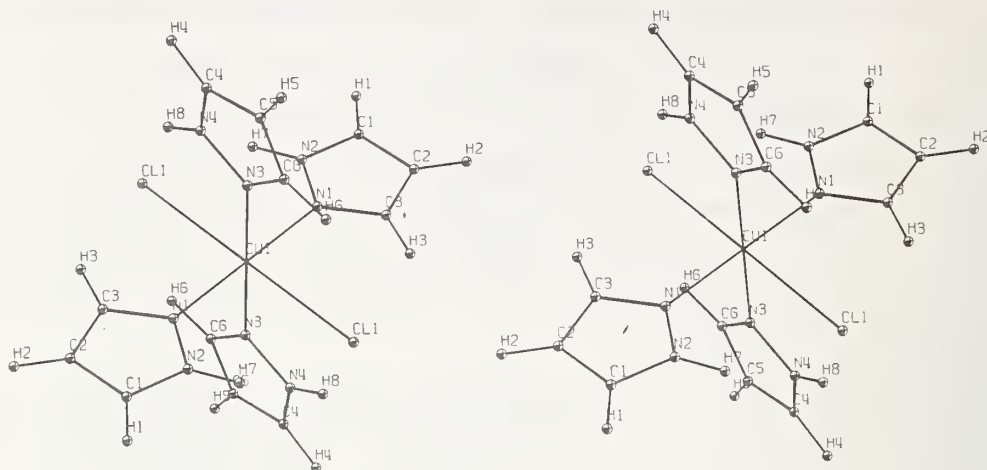


Fig. 1. Stereo view of the $\text{Cu}(\text{Pyrazole})_4\text{Cl}_2$ complex. The copper atom is located at a center of symmetry of the space group. Bond distances and angles are indicated in the accompanying table.

¹Reimann, Mighell and Mauer, *Acta Cryst.* 23, 135 (1967).

²Mighell, Reimann and Santoro, *Acta Cryst.* B25, 595 (1969).

³Prince, Mighell, Reimann and Santoro *Cryst. Struct. Comm.* 1, 247 (1972).

CALIBRATION OF DETECTORS FOR ARGON-41

H. E. DeSpain
(Center for Radiation Research)

A technique for calibrating detectors for argon-41 is being developed. The NBSR is used to produce a sample of argon-41, which is consequently assayed and injected into a detector. Efforts thus far have been concentrated in perfecting a method for reproducible counting and gas transfer.

C. INTERAGENCY AND UNIVERSITY PROGRAMS

DYNAMICS OF AMMONIUM IONS IN NH_4ClO_4 AND NH_4NO_3

H. Prask and S. Trevino
(Picatinny Arsenal, Dover, N.J.)

and

J. J. Rush

Quasielastic neutron scattering studies have been made for polycrystalline samples of NH_4NO_3 and NH_4ClO_4 as a function of temperature. These studies were performed using the PA-NBS three-axis spectrometer with an energy resolution of 0.56 meV.

In the case of NH_4NO_3 , numerous measurements have shown that the occurrence of structural phase transitions is dependent upon the presence of water in the samples. In view of this the present work was aimed at elucidating the interrelation of water content and NH_4^+ dynamics. The NH_4NO_3 samples were studied "wet" ($\lesssim 1\%$ H_2O by weight) at temperatures of 23°C (Phase IV), 45°C (III), 95°C (II), 120°C (II) and 132°C (I). After drying at 132°C , the samples were studied at 95°C (II), 60°C (II), 45°C (IV) and 23°C (IV).

The present results confirm that dried samples of NH_4NO_3 do not exhibit the Phase III structure, but transform $\text{IV} \rightarrow \text{II}$ directly. The quasielastic neutron data, obtained for a range of momentum transfers ($0.6 - 4.2 \text{ \AA}^{-1}$) at each temperature, are consistent with a jump-rotational reorientation for all phases. Furthermore, the broadening of the quasielastic peaks for Phase II (95°C) with and without water are significantly different, suggesting that "surface" water affects NH_4^+ binding throughout the bulk of the crystal.

Ammonium perchlorate was studied by means of quasielastic neutron scattering at temperatures of 55, 66, 78, 105, 130 and 150°K . Over this range of temperatures, the maximum widths of the neutron spectra range from the instrumental resolution width to $\approx 1 \text{ meV}$. This represents a significant change in NH_4^+ dynamics, although it is now well-established that no structural phase change occurs over this temperature interval.

Quantitative analysis of both NH_4NO_3 and NH_4ClO_4 quasielastic neutron scattering data is in progress.

GROUP THEORETICAL ANALYSIS OF NEUTRON SCATTERING IN CRYSTALS

S. Trevino and H. Prask
(Picatinny Arsenal, Dover, N.J.)

and

R. Casella

Work on the continuing program of application of symmetries to classify the phonon spectra of materials via inelastic neutron scattering has advanced. The general methodology of treating harmonically vibrating and librating rigid molecules, developed during the period of the previous progress report, has undergone continued application and comparison with experiment. In addition to our fundamental paper on the subject now published, two further papers, one on the aforementioned applications and one, a general theoretical paper oriented towards chemists, are presently in preparation or contemplated. The selection rules have been calculated for the crystal NaNO_3 . Table 1 gives the results for a few significant reciprocal lattice points at the zone center. Examination of the table reveals the power of the selection rules. For example, the identification of the E_g translational phonon obtained using the (0,4,-1) point and the rotational phonon observed at the (0,2,13) point is accomplished unambiguously. In addition, it was found that the two A_{2g} phonons were not pure modes but mixed translation-rotation phonons by combining the observations at the (0,0,15) and (0,2,1) reciprocal lattice points. Most of the modes at the Γ point have been observed and classified by this procedure. Finally, a more complete discussion of the Debye-Waller factor in the context of the group theoretical analysis is contemplated.

TEMPERATURE DEPENDENCE OF THE PHONONS IN HCP Be

H. Alperin, S. Pickart, and J. Rhyne
(Naval Ordnance Laboratory, White Oak, Md.)

An inelastic neutron scattering experiment is in progress to determine if there is a correlation between an anomalous increase in ductility in polycrystalline Be at $\sim 700\text{K}$ and the fundamental force constants. Last year's progress report described our room temperature results for the phonon dispersion curves in the $[0001]$ and $[11\bar{2}0]$ propagation directions, and selected phonons in these groups have now been redetermined at 695°K .

Phonon energy vs. wavevector relations for the c-axis direction are shown in Figure 1 for room temperature and 695°K . It can be seen that there is an overall softening of the modes at the high temperature as a function of increasing wavevector. Similar results were observed for the $[11\bar{2}0]$ propagation direction, amounting to a percentage shift of $\sim 2.9\%$.

To determine whether this behavior is anomalous, one has to remember that phonon-phonon interactions, arising from anharmonic effects, normally broaden the energy width and decrease the phonon energy as the temperature increases. The theoretical behavior of anharmonicity is insufficiently known to make definite predictions as to the magnitude of this effect, but we may relate our observations to some previous measurements.¹ These previous results, when scaled to the same temperature interval relative to the melting temperature as in our case, showed a percentage shift of 3.7% , so we conclude that the effects we observe are most probably due to normal temperature effects and are not anomalous.

These results do not disprove the presence of an anomaly, which may occur at a higher temperature or a section of the Brillouin zone not yet explored. The measurements are being extended to higher temperatures and other propagation vectors to examine these possibilities.

¹K. E. Larson, S. Holmryd and N. Dahlborg, Inelastic Scattering of Neutrons in Solids and Liquids, p. 587 (IAEA, 1961).

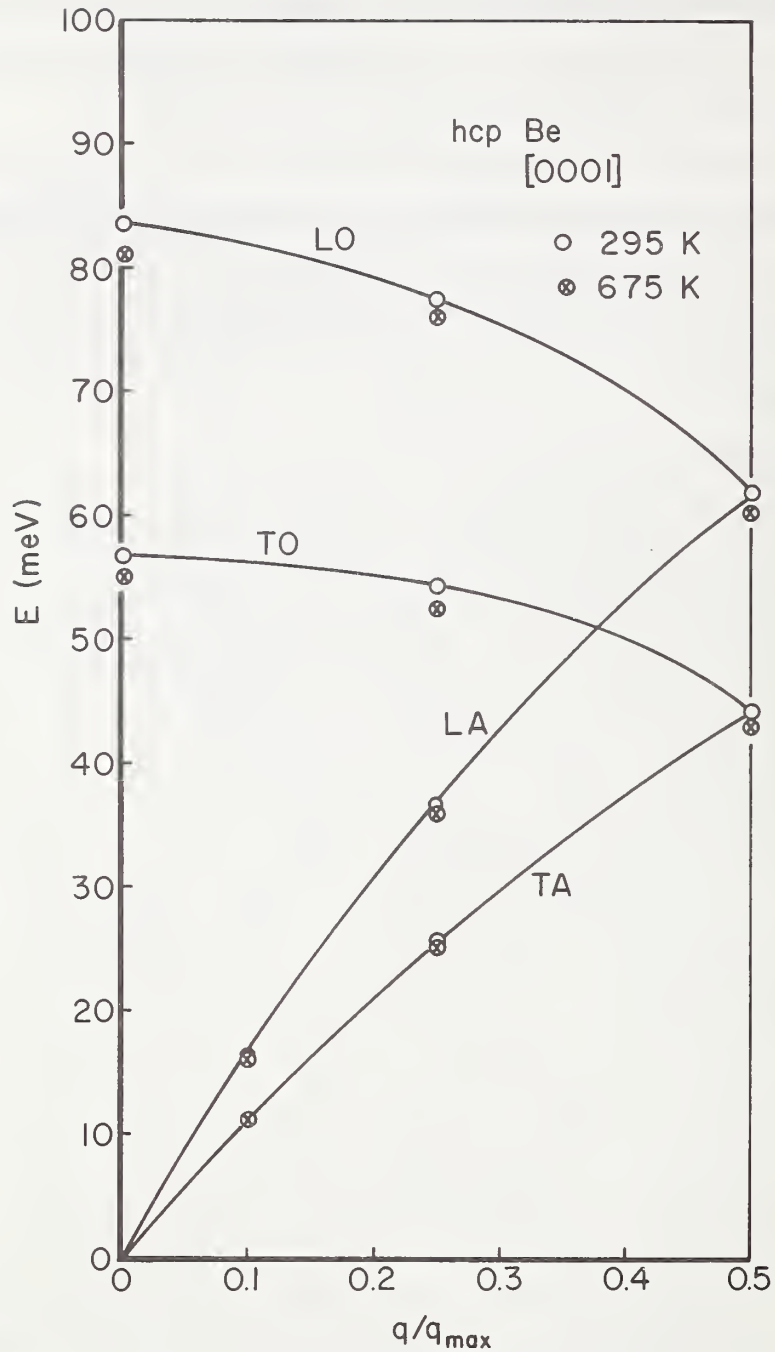


Fig. 1. Dispersion curves (energy transfer vs. wavevector) in hcp Be at room temperature and 695K for transverse and longitudinal branches (acoustic and optic).

MAGNETIZATION OF RARE EARTH COMPOUNDS BY NEUTRON DIFFRACTION

J. Rhyne and S. Pickart
(Naval Ordnance Laboratory, White Oak, Md.)

The determination of the sublattice magnetization is of critical importance in studying the magnetism of compounds. In the case of the Laves phase rare earth compounds (e.g., $TbFe_2$) which have a ferrimagnetic arrangement of rare earth and transition metal spins, individual sublattice magnetizations can not be determined by conventional magnetometer experiments. The only direct method of obtaining the magnetization is by neutron diffraction in which the rare earth and transition metal magnetizations may be determined individually by analyzing the magnetic scattering contribution to the total neutron Bragg intensity.

We have applied the method to a series of the Laves phase compounds including $TbFe_2$, $ErFe_2$, $TmFe_2$ and $DyFe_2$ and have obtained the magnetizations as a function of temperature from 4 K to the Curie Temperature (typically 700 K). The rare earth spins which are largely polarized by the strong Fe-Fe exchange field show an essentially conventional temperature dependence of the magnetization, while the iron magnetization remains essentially constant from low temperature up to near the critical temperature where it rather abruptly decreases to zero. Models for this magnetic behavior and its effect on the magnetostrictive properties are being developed.

EXCITATION SPECTRA OF AN AMORPHOUS FERROMAGNET

H. Alperin, J. Rhyne and S. Pickart
(Naval Ordnance Laboratory, White Oak, Md.)

A new class of magnetic materials has emerged from the discovery that sputtered rare earth-iron alloys are magnetically and crystallographically amorphous.¹ These materials are different from previously reported² amorphous magnets in that they contain no glass former atoms (P, C, Si or B), can be prepared in bulk form and contain 100% of

magnetic atoms, thus possessing relatively strong magnetization. Selected compositions of these materials, which can readily be formed with varying rare earth-iron ratios, are presently being developed for application as permanent magnet, thin film memory elements, and magnetostrictive transducers.

In order to fully exploit such applications, basic knowledge concerning the nature of the magnetic state in a spatially disordered system of atoms must be obtained. The magnetic excitations, or spin waves, which can be measured by neutron scattering, reflect the dynamics of such a system and are thus essential to adequately test theoretical models of the fundamental spin interactions.

Inelastic magnetic time-of-flight spectra have been obtained at various temperatures from amorphous TbFe_2 , and show significant differences from the crystalline state. These spectra are shown in Fig. 1 for the two phases at room temperature and indicate that, compared to the crystalline phase, the amorphous material has a broadened spectrum that is shifted to lower energies. This effect has been predicted by various theoretical treatments², and results both from a depletion of high-frequency modes caused by the break-up of short wavelength correlations, which shifts the peak in the density of states to lower energy, and from the increased lifetime of the spin waves which smears out discrete modes.

At temperatures above T_c of the amorphous phase (433K) the frequency spectrum is similar to that of a typical paramagnet, i.e. peaked at energy transfer of zero, but preliminary measurements through the Curie transition has failed to show any vestige of critical scattering, which is expected on general thermodynamic grounds at any second-order phase transition. It is planned to repeat these measurements with improved resolution to explore the possibility that the critical fluctuations are confined to a wavevector smaller than used in the experiment (0.04\AA^{-1}) or in a smaller temperature interval [$(T-T_c)/T_c < .01$].

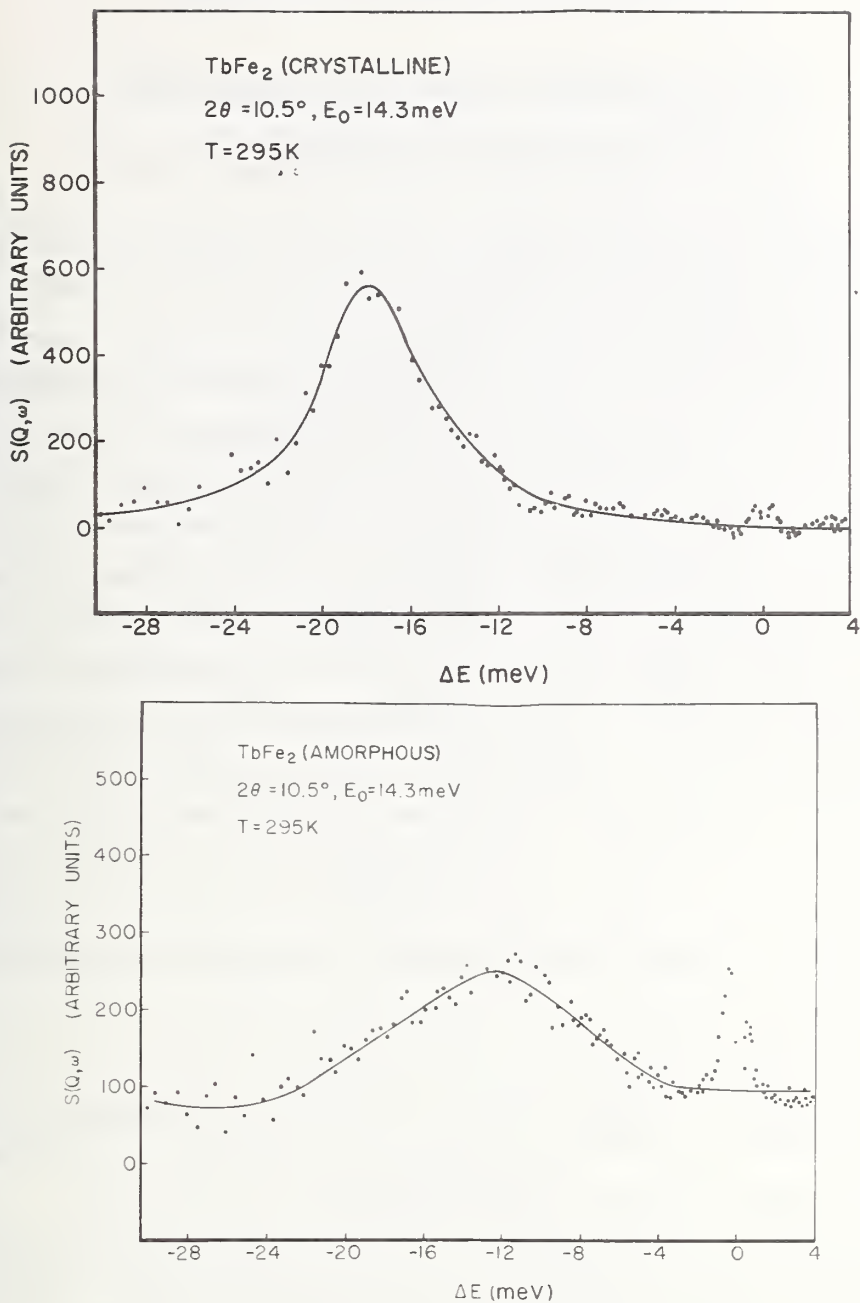


Fig. 1. Corrected time-of-flight spectra for polycrystalline (a) and amorphous (b) $TbFe_2$ at room temperature.

¹J. Rhyne, S. Pickart and H. Alperin, *Phys. Rev. Lett.* 29, 1562 (1972).

²See references cited in *Amorphous Magnetism* (Hooper and de Graaf, Eds.) Plenum Press, N.Y. (1973).

ABSENCE OF MAGNETIC ORDER IN $\text{MnO-P}_2\text{O}_5$ GLASS

J. Rhyne and H. Alperin
(Naval Ordnance Laboratory, White Oak, Md.)

The question of antiferromagnetic ordering in glasses loaded with transition metal atoms has been widely discussed¹ in the literature, and its answer would be of considerable importance to amorphous magnetism. Magnetic susceptibility data on a 50 mole per cent $\text{MnO-P}_2\text{O}_5$ glass by J. Friebele² indicated a paramagnetic-antiferromagnetic transition temperature of 90 K, below which the Mn spin groups supposedly order antiferromagnetically. The technique of neutron scattering provides a sensitive test of magnetic order, particularly antiferromagnetic order in which a doubled magnetic periodicity generates additional scattered intensity at angular positions not observed in the paramagnetic phase.

We examined a sample of the 50 mole per cent $\text{MnO-P}_2\text{O}_5$ glass by neutron scattering over the temperature range from 300 K to 2 K and found it to be a structurally homogeneous amorphous material, but without any evidence of long range antiferromagnetic order, in contrast to the inference from the susceptibility results, but in agreement with previous results¹ on cobalt-loaded glasses. These results indicate that if antiferromagnetic interactions exist between the Mn and Co spins, they are of such a short range nature that no measurable spin-spin correlation (as seen in the case of TbFe_2) exists. The neutron study gave no evidence of ordered clustering of the Mn atoms within the glassy matrix such as has plagued some other amorphous magnetic glass work.¹

Further work is planned on these and other analogous "magnetic" glass systems to further investigate the general question of magnetic interactions in amorphous materials.

¹Review papers by Egami, Sacli, Simpson, Terry and Wedgewood, *Proc. Intl. Symposium on Amorphous Magnetism*, Plenum Press (1973).

²J. Friebele, Thesis, Vanderbilt University.

STRUCTURAL STUDIES OF AMORPHOUS SOLIDS

J. H. Konnert, J. Karle and G. A. Ferguson
(Naval Research Laboratory, Washington, D.C.)

The atomic arrangement in vitreous solids is the subject of an increasing number of current investigations. This renewed interest is stimulated, in part, by recent technological advances made possible by use of materials existing in the glassy state. Such advances include semiconductors, fiber communication and laser devices.

Basic structural studies of simple glasses using the diffraction technique have been reported.¹ New data reduction procedures were developed, and employed in the analysis of these simple systems, to reveal structural detail which had not been previously observed. The present experimental program is designed to obtain high precision diffraction data on selected samples of semiconducting materials. These materials include As_2Se_3 , AsTe and As_2S_3 . Data reduction, employing the methods mentioned above, will be applied to study temperature dependent structural details of these systems.

¹J. H. Konnert, J. Karle and G. A. Ferguson, *Science* 179, 177-179 (1973).

PRECISION MEASUREMENT OF THERMAL NEUTRON SCATTERING AMPLITUDES

C. Schneider
(U.S. Naval Academy, Annapolis, Md.)

Prism refraction measurements have yielded a value of 4.147(2) fm for the scattering amplitude of the silicon nuclear potential. Refraction profiles are analyzed by computer with automatic corrections for higher order contamination wavelengths. The extension of the prism technique to materials of several barns per atom attenuation cross-section has been accomplished by calculating the small correction due to preferential attenuation across the prism for a standard slit arrangement. Reversal of the prism will be used to confirm this correction. Preliminary mea-

surements on a Ge prism yielded $b = 8.28(8)$ fm for the nuclear scattering amplitude in good agreement with other determinations.

A small variation of the torsion goniometer calibration with torque applied to the mounting plate has been studied and found useful in simplifying the calibration. A very slow (<10 msec/hour) angular drifting of the double crystal spectrometer due to small temperature gradients between the crystals has been observed to cycle on a daily basis with a maximum amplitude of 0.1 secs. arc. The double crystal spectrometer has been studied as a tool in the measurement of thin film inhomogeneities by mirror reflection.

Use of the double crystal geometry to observe the small angle scattering of neutrons from critical fluctuations, polymers, defects and magnetic inhomogeneities is under consideration. For most experiments, the angular range of interest is from several seconds to several degrees arc so that the instrument would benefit from interchangeable crystal pairs of various matched mosaics.

THE STRUCTURE OF $\text{Na}_2\text{ZnCl}_4 \cdot 3\text{H}_2\text{O}$

R. J. Khanna
(University of Maryland)

and

E. Prince

Sodium zinc chloride trihydrate, $\text{Na}_2\text{ZnCl}_4 \cdot 3\text{H}_2\text{O}$, crystallizes in the trigonal space group $P31m$, with $a=6.876\text{\AA}$, $c=5.955\text{\AA}$, and 1 formula unit per unit cell. A data set was collected on this compound in order to determine the configuration of the water molecule and the arrangement of hydrogen bonds. The data are being analyzed at the University of Maryland.

CRYSTAL STRUCTURE OF NH_4ClO_4 AT 300K, 78K AND
10K BY NEUTRON DIFFRACTIONC. S. Choi and H. J. Prask
(Picatinny Arsenal)

and

E. Prince

Earlier studies of NH_4ClO_4 structure by several investigators suggested that the ammonium group in the crystal is undergoing essentially free rotation at room temperature. No low temperature structural studies had been performed. To investigate the orientation and the thermal motion of the ammonium group in the crystal, a single crystal neutron diffraction study was undertaken for three different crystal temperatures, 300K, 78K and 10°K.

The NH_4ClO_4 crystal has an orthorhombic unit cell, Pmna, with the cell dimensions $a = 9.20$, $b = 5.82$, $c = 7.45$ for 300±K, $a = 9.02$, $b = 5.85$, $c = 7.39$ for 78°K and $a = 8.94$, $b = 5.89$, $c = 7.30$ for 10°K. Initial positions for H atoms were obtained from the room temperature data by the difference Fourier synthesis for which the F_c was obtained from the heavy atoms only. Hydrogen peaks (negative) were observed in the map with sufficient clarity to indicate that the NH_4^+ are not undergoing completely free rotation even at room temperature.

Since the amplitudes of thermal motions of the H atoms in the ammonium group are so large, they cannot be represented satisfactorily by the conventional thermal ellipsoid. Hence the structure was refined by the rigid body refinement method developed by Prince and Finger. The refinement converged rapidly for the structure at 10°K and at 78°K but it failed to converge for the room temperature data. The thermal motions of the ammonium groups at room temperature are still too large to be handled by the rigid body refinement method, which is based on the normal distribution function simplified to third cumulant.

The librations of the ammonium group at low temperatures (10°K and 78°K) are very large only about one principle axis. The root mean square angular displacement about the "unique" axis was 26° for the

structure at 10°K and 36° for that at 78°K but the orientations of the principle axes remained essentially the same. The oscillation amplitudes about the other two principle axes were approximately the same at each temperature, about 9° at 10°K and 16° at 78°K. Each ammonium group is surrounded by ten oxygen atoms with short N...O distances ranging from 2.9Å to 3.2Å. This almost isotropic environment leads to a very low barrier for reorientation, as has been proposed from other work. Among these ten oxygens, four appear to be hydrogen bonded to the four H atoms of the ammonium group.

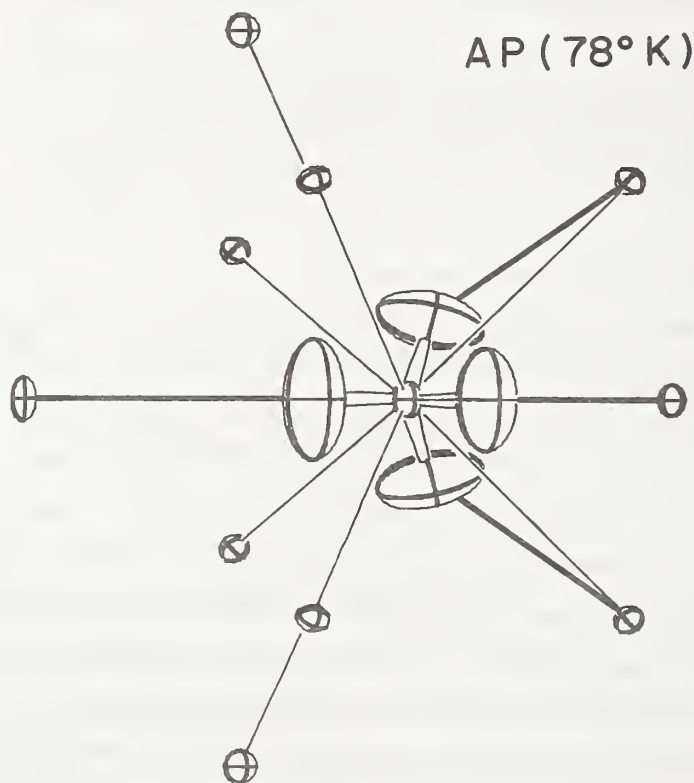


Fig. 1. The ammonium group and its oxygen neighbours (78°K) viewed along the axis of the largest libration motion. The thermal ellipsoids are sealed to include 20% probability.

REFINEMENTS OF THE CRYSTAL STRUCTURE OF KN_3 AND
 $\beta\text{-NaN}_3$ BY NEUTRON DIFFRACTIONC. S. Choi
(Picatinny Arsenal, Dover, N.J.)

The crystal structures of KN_3 and $\beta\text{-NaN}_3$ are well known since the pioneering work by Hendricks and Pauling in 1925. The potassium azide and sodium azide form typical ionic type crystal structures with linear and symmetric N_3 anions. The N-N distances of the N_3 anions reported by earlier x-ray investigators are not precise and range from 1.145\AA to 1.17\AA with large standard deviations. This study is aimed to obtain accurate N-N distance of the azide anions by using neutron diffraction techniques. These alkali metal azides are meta-stable and suffer severe radiation damages by x-rays but not by the thermal neutrons.

KN_3 crystallizes in tetragonal $I4/mcm$ with the unit cell dimensions $a = 6.304(1)$ and $c = 7.540(2)\text{\AA}$. The reflection intensities of 161 out of 195 independent reflections were measured with 0.983\AA wavelength neutrons. The structure was refined by full matrix least squares methods to yield R-index of $R_w = 0.022$ and $R = 0.024$. The N-N distance was $1.174(1)\text{\AA}$ without correction and 1.184\AA after correction with the riding model.

The crystal structure of $\beta\text{-NaN}_3$ is being refined.

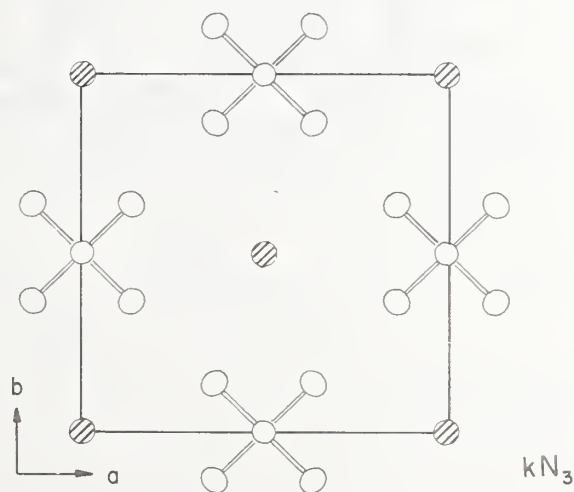


Fig. 1. Crystal structure of KN_3 projected along c-axis.

CRYSTAL STRUCTURE OF DINITRO-PENTAMETHYLENE-TETRAMINE

C. S. Choi and S. Bulusu
(Picatinny Arsenal, Dover, N.J.)

and

F. Mauer
(Inorganic Materials Division)

The title compound, $C_5H_{10}N_6O_4$, code named as DPT is one of the several derivatives of HMX (cyclo-tetramethylene-tetranitramine). The crystal structure of DPT was studied by x-ray diffraction with $MoK\alpha$ radiation. Preliminary investigations by precession photographs revealed

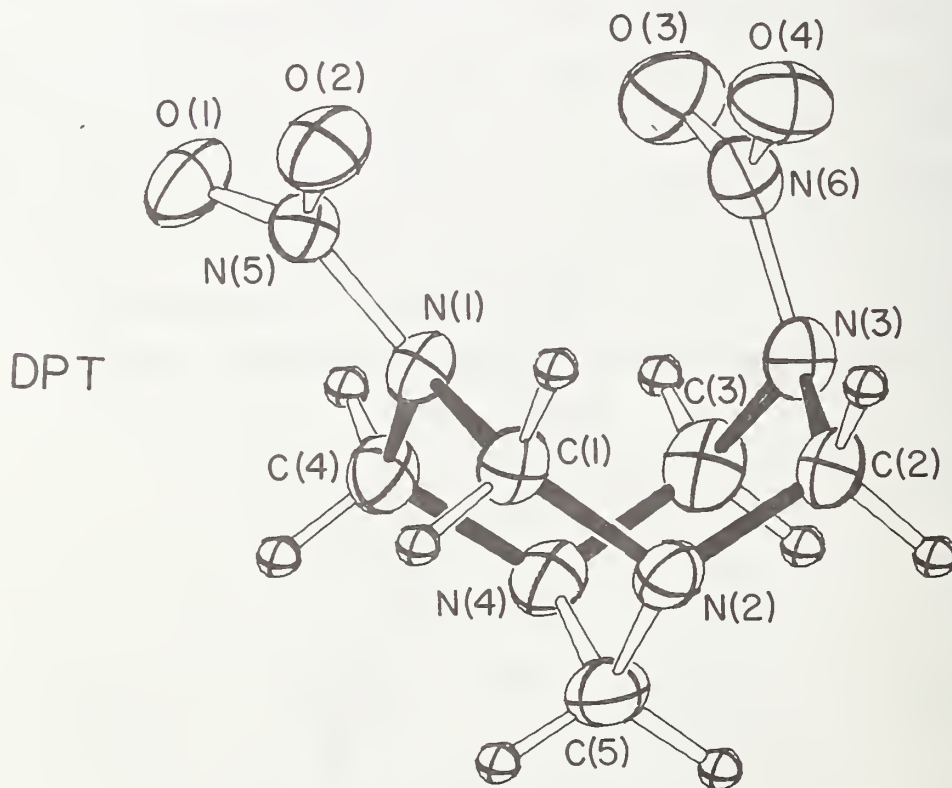


Fig. 1.

the space group to be monoclinic $P2_1/C$. The unit cell dimensions are $a = 9.345(5)$, $b = 8.284(5)$, $c = 11.566(5)$ and $\beta = 105.6(1)^\circ$, and contains four molecules per unit cell. A total of 1420 independent reflection intensities were observed by an automated three circle diffractometer

equipped with a solid state detector. The crystal structure was solved by the symbolic addition procedure and was refined by the full matrix least squares method to the final R-index $R = 0.035$ and $R_w = 0.037$.

The DPT molecule consists of an eight-membered C-N ring with an additional methylene group bridging between the two valley points of the ring, and two planar nitro groups attached to the C-N ring, as shown in the Fig. 1. The DPT molecule possesses a pseudo mirror symmetry about the plane passing through the N-N axes of both nitro groups and C atom of the methylene bridge. The bond lengths and angles of the molecule generally agree with those of HMX and RDX. The DPT molecule has rather tight intramolecular packing and exhibits several short intramolecular interatomic distances.

THREE-AXIS NEUTRON SPECTROMETER

H. Prask and S. Trevino
(Picatinny Arsenal, Dover, N.J.)

and

R. Carter, J. Rowe, J. Rush and A. Cinquepalma

A high-efficiency, high-versatility three-axis neutron spectrometer has been designed for use at the NBSR. The new instrument will incorporate an automatic shutter system in the monochromator shield so that variable E_{in} scans are possible, combined with the variable E_{fin} scans used with present instruments. The angular range for monochromator ($2\theta_m$) and sample (ϕ) will be increased significantly over present instruments: $-10^\circ \leq 2\theta_m \leq 100^\circ$, $-120^\circ \leq \phi \leq 120^\circ$. Two complete analyzer systems will be employed, increasing the rate of data collection by as much as a factor of two.

Fabrication of the new instrument is nearing completion.

D. NON-RRD NBS PROGRAMS

ACTIVATION ANALYSIS SECTION: SUMMARY OF ACTIVITIES

P. D. LaFleur and D. A. Becker
(Analytical Chemistry Division)

The Activation Analysis Section of the Analytical Chemistry Division is physically located in the NBS Reactor Building. It has at present fifteen members, and has programs in a variety of areas related to trace element analysis. These programs include both research projects, and analytical programs on a wide variety of real sample matrices. Summaries of the work in these areas are included below.

1. Research Projects

a. Sampling and Analysis of Chesapeake Bay Organisms and Sediments for Trace Metal Profile Determinations.

Determination of water quality involves a comprehensive study of an aquatic system, rather than analysis of water only. Food chain organisms, sediments, and water all must be included in such a study. A project has been initiated in the Activation Analysis Section for the determination of trace metals in Chesapeake Bay organisms and sediments, as well as water. Sampling and analytical methodology is under development for this study. Also included is a fresh water tributary to the Bay, the Patuxent River, as described in the following project.

Members of the Activation Analysis Section went into the Bay on the Chesapeake Bay Institute Research Vessel, H. Ridgley Warfield to experience and participate in the aquatic sampling techniques. Samples taken include oysters, plankton, sediment, annelids living in the sediment, and water samples. Improved sampling techniques for organisms and sediments are in the process of being developed, which will reduce the possibility of trace element contamination during sampling and storage. Analysis of the various types of samples to determine their trace element profile has begun. It is expected that variations in these profiles will be observed, depending on sediment depth, sampling area, time of year, and other factors.

The results of this project will also allow correlation with mercury biotransformation studies taking place in the NBS Inorganic Materials and Metallurgy Divisions.

b. Trace Elements in Water.

A cooperative research program between the NBS Activation Analysis Section and the University of Maryland is concerned with trace element analysis in natural waters. One of the primary objectives of this program at the present time is the development of adequate sampling and sample handling techniques for water analysis. At present, natural water samples are being taken using a teflon sampling device developed in this program. The samples are then filtered directly into a specially prepared 1 mil polyethylene film container, and frozen immediately (while still in the sampling area) in liquid nitrogen.

In order to irradiate samples for long periods of time, and as a pre-irradiation concentration step, a freeze-drying technique was used to remove the water without melting, allowing the impurities to remain behind on the polyethylene film. Radioactive tracers were used to study the retention yields of this freeze-drying procedure. It was found that the elements quantitatively retained on the film when freeze-drying a 100 ml river water sample (pH adjusted to 1.5) include: Na, Sc, V, Cr, Fe, Co, Zn, As, Se, Br, Rb, Sr, Cd, Sb, Cs, Ba, Ce and Tb. Work has begun on the determination of trace element profiles from the 100 ml samples of Patuxent River water using these techniques.

c. Forensic Activation Analysis.

In cooperation with the NBS Law Enforcement Standards Laboratory (LESL), the Activation Analysis Section has this past year had a program in the examination and evaluation of the neutron activation analysis technique for the determination of gunshot residues. This program in general covered the areas of sampling methodology, radiochemical separation procedures, stability of residues on the hand as a function of time firing, and the evaluation of background levels of barium and antimony to

be found in the general population. This is an on-going program, and will continue during the next year.

d. The Application of a Mass Separator to Activation Analysis.

The mass separator research program of the Activation Analysis Section is concerned with the development of practical analytical procedures for the application of electromagnetic isotope separation techniques to activation analysis.

As the need to determine trace elements of interest in biological and environmental samples at lower and lower concentrations increases, interference from other elements in the sample also increases, and ultimately is the limiting factor in the application of nuclear activation analysis techniques. An isotope separator has been used, along with radiochemical separations, to provide a single radionuclide in a form suitable for counting. By evaluation of the parameters of isotope separator operation, and determining the fraction of a given nuclide which is actually deposited on a catcher foil, it is possible in some cases to determine a given trace element without interference from any other trace element. The ultimate sensitivity for a given trace element would then be dependent only upon the nuclear parameters for production of suitable radionuclides and the mass separator yields.

Over the past year, the operating characteristics of the mass separator have been studied and procedures were developed for the determination of lead and cadmium in environmental samples. This work will continue with particular emphasis on the determination of iodine in biological and environmental samples and upon the determination of cerium in samples of the Trace Elements in Glass SRM's.

e. Activation Analysis Using an Isotopic Californium-252 Source.

At the 1968 International Conference on Modern Trends in Activation Analysis, a significant paper recommended ^{252}Cf as a neutron source for activation analysis. They pointed out the advantages in cost, half-life, volume, and gamma and heat emission of ^{252}Cf relative to other isotope

sources and the advantages of ^{252}Cf over accelerator sources such as largely eliminating maintenance, the dependable, continuous and stable neutron emission, and a lessening in shielding requirements. Since that time about seventy journal articles and conference proceedings have appeared in the literature describing ^{252}Cf activation analysis. These have dealt with determinations varying from the in vivo determination of sodium to field exploration for minerals. An evaluation of the utility of ^{252}Cf activation analysis must include estimates of sensitivities.

These are at least 200 sensitivity tables for thermal neutron activation analysis in the literature. From any of these and the determination of the yields of one or two thermal neutron reactions with a specific ^{252}Cf source, a sensitivity table can be estimated for that specific source. This is not the case, however, for fast neutron activation analysis with the isotope source. As has been noted, the ^{252}Cf fission neutron spectrum is sufficiently different from that of ^{235}U , that serious error may be introduced if any of the average cross section data readily found in the literature for the ^{235}U fission neutron spectrum, are used in calculations related to ^{252}Cf experiments. These yields of reactions of analytical interest have been made and reported elsewhere.

The NBS ^{252}Cf facility consists of 8 sources of 50 μg each at the time of these experiments. They are arranged in an octagonal array around the irradiation position. Samples are packaged in a polyethylene snap-cap vial of 1 cm diameter and 2.5 cm length. This is wrapped with 1 mm thick cadmium foil and placed in a larger polyethylene vial with spacers to assure that the sample is in the position of maximum neutron flux. A compressed air pneumatic transfer system sends the vials to the irradiation position and return.

The (n,n') reactions were of particular interest in this study. In addition some (n,p), (n, α) and (n,2n) yields were measured. The conditions for analysis were one gram of the element irradiated with a source strength of one milligram of ^{252}Cf , with the flux being 3.5% of the total neutron output. The determination of lead in paint using this system has also been made.

Since large amounts of lead in the paint on walls in dwellings are potentially hazardous to children, especially in certain susceptible age groups who may ingest it, a rapid and quantitative analytical technique for lead would be most useful. Most analytical methods for screening suspect homes require lengthy dissolution times or other chemical procedures. Activation analysis with unmoderated neutrons from a ^{252}Cf source inducing the nuclear reaction $^{204}\text{Pb}(n,n')^{204\text{m}}\text{Pb}$ and/or $^{207}\text{Pb}(n,n')^{207\text{m}}\text{Pb}$ followed by gamma spectrometry with Ge(Li) or NaI(Tl) detectors respectively is shown to be a reliable and potentially rapid nondestructive method for this determination. The lower limit of determination in a 1.5 gram sample of paint with a 600 μg source of ^{252}Cf is of the order of one percent. Larger sources would increase the sensitivity or permit more rapid analyses. The potential exists for partially automating the determination.

f. High Sensitivity Activation Analysis.

Nuclear activation analysis is widely recognized as a sensitive method of trace analysis with the possibility of producing results with excellent accuracy and precision, when carefully done. The technique is widely applied in the analysis of environmental, biomedical, oceanographic, and industrial samples for their trace element content. With the judicious application of neutron and high energy photon irradiations, most of the elements in the periodic table may be determined. Although there is much discussion in the literature of the very high sensitivity and the capacity for excellent accuracy using these techniques, neither property is fully realized in practical analysis because of such factors as lack of knowledge of neutron or photon flux distributions and/or energy spectra and possible contamination during pre-irradiation processing, or occasionally, from the irradiation container itself. Since improvement of measurement science is an integral part of the NBS mission, it was felt important for NBS to play a leadership role in defining problem areas and pursuing solutions to these problems.

To this end, considerable effort has been expanded over the last

several years in the characterization of the NBS reactor and LINAC irradiation facilities, in terms of flux distribution and density. Work in the past year has been focused on the characterization of neutron spectra in the NBS reactor to assess possible effects of resonance absorption and interfering nuclear reactions. These studies will also be continued. In addition, analytical procedures have been developed for the determination of chromium, zinc, hafnium, and other elements using activation analysis with radiochemical separations. These methods have been applied to biological samples, such as the NBS Standard Reference Materials (SRM) orchard leaves and bovine liver, in the Trace Elements in Glass SRM's, and in pure materials analysis.

g. The NBS Measurement System for Natural ^{37}Ar .

A project to determine the cosmic-ray production rate and the natural levels of 35-day ^{37}Ar in the atmosphere has been underway at the National Bureau of Standards for the past year. The prime objective of this project is to determine the (absolute) spatial dependence of ^{37}Ar production in the atmosphere, on the one hand, and the spatial distribution of the naturally-produced ^{37}Ar (observed concentrations) on the other. This information will then be used, through cooperation with L. Machta (N.O.A.A.), to derive information about atmospheric mixing.

As the lowest ^{37}Ar concentrations of interest are but 10^{-3} dpm/l-Ar, very high sensitivity measurement techniques are required. Among the techniques which we have adopted are: quantitative separation of the noble gases from about 1 m^3 of air, using a CaC_2 reactor; gas chromatographic separation of the argon fraction; isotopic enrichment (by a factor of ~ 70) of purified argon; use of specially selected low-level gas proportional counters together with massive shielding and anticoincidence mesion cancellation; and the application of pulse discrimination based upon both amplitude (energy) and rise time. On-line computer techniques are being applied for data acquisition and system control.

Using this system, we have completed the first measurements of cosmic ray produced ^{37}Ar from the southern hemisphere. By means of thermal

diffusion the very low natural specific activity of ^{37}Ar was enriched by about a factor of 70 to 100 in a period (6-10 days) significantly less than the half-life (35.1 days) of ^{37}Ar . Results of southern hemispheric samples confirmed that the time scale for interhemispheric (north-south) atmospheric mixing is significantly longer than the half-life of ^{37}Ar .

h. Quantitative Applications of ^{17}O Tracer Using the Nuclear Track Technique

Many nuclides emit charged particles (p, d, t, α and fission fragments) after capturing a thermal neutron. However, some of these isotopes are unacceptable for quantitative applications of the Nuclear Track Technique because they either have low thermal neutron cross-sections or low isotopic abundances or both. Such is the case with ^{17}O , which has a very low isotopic abundance (0.04%) and a moderately low thermal neutron cross-section (0.235b); however, since oxygen compounds highly enriched in ^{17}O are available, the analytical application of the $^{17}\text{O}(n,\alpha)^{14}\text{C}$ reaction may be feasible.

In collaboration with the Weizmann Institute of Science, Rehovot, Israel, a study was undertaken at the National Bureau of Standards to determine the feasibility of using this isotope as a tracer in biological systems. The group at the Weizmann Institute supplied two oxygen-17 enriched compounds, Al_2O_3 with 20% ^{17}O and citric acid with 7% ^{17}O . These compounds were pressed into pellets in a KBr pellet die using a hydraulic press. The pellets were then sandwiched between two pieces of cellulose acetate (CA) and vacuum sealed in a polyethylene bag. The combination was then irradiated in a highly thermal neutron environment in the NBS RT-4 pneumatic tube facility.

After a 2 sec irradiation in a thermal neutron flux of $1.33 \times 10^{13} \text{ n} \cdot \text{cm}^{-2} \text{ sec}^{-1}$, the combination was separated and the detectors were etched in a solution of 7 parts 6.5N NaOH and 5 parts 12% NaClO_3 for 30 minutes at 40°C . The etched detectors were then rinsed, dried and the track density counted with the aid of an image analyzing microscope.

Consideration must be given to the interfering elements such as

boron and lithium as both of these will produce alpha tracks when they capture a neutron. A concentration of ~ 10 ppm of boron will interfere with oxygen determination, while the lithium concentration must be at least 100 ppm before it interferes seriously. In this study there was no interference problem. Application of this technique for oxygen determination and particularly oxygen distribution in biological tissue appears practical and a study of this possibility is in progress.

i. A Method for the Determination of Rare Earths Using Neutron Activation Analysis and Reversed-Phase Chromatography.

Recently, the interest in the quantitative determination of rare earth elements has grown considerably, especially in space programs. There has also been a need for quantitative methods for rare earth element determinations in different matrices at the National Bureau of Standards. We have therefore applied some of our earlier qualitative investigations with di(2-ethylhexyl) orthophosphoric acid (HDEHP) to separations of these elements for their subsequent quantitative determination.

The chemical separation was made using a column (11 cm x 40 cm) of "Corvic" powder (poly(vinyl chloride-vinyl acetate)) loaded with HDEHP and operated at a constant temperature. Since our earlier solvent extraction studies with HDEHP had shown perchloric acid to be the most favorable of three acids (HCl , HNO_3 , HClO_4) for rare earth separation, the optimum operating conditions (time, flow, acid concentration, etc.) were established using this acid.

The rare earth elements in NBS Standard Reference Material 480, Trace Elements in Glass, a sodium glass to which 61 trace elements, (including the thirteen naturally occurring rare earths), were added, have determined by neutron activation analysis. The samples were irradiated in RT-4, chemically separated using the above procedure, and then counted on a Ge(Li) detector. A total of 11 different rare earths were determined at the 500 ppm and 50 ppm levels in the glass, with good precision and accuracy.

2. Standard Reference Material (SRM) Analyses

Much of the section's efforts during the past year have been directed towards the development of high precision and accuracy in neutron activation analysis, with a primary aim being the analysis and certification of NBS Standard Reference Materials.

In total, the section during the past year has analyzed 163 SRM samples while determining 251 elemental concentrations. These analyses encompassed a variety of materials, including coal, fly ash, fuel oil, molybdenum concentrate, glasses, urine, tuna fish, orchard leaves, bovine liver, and several metals.

For a number of the above mentioned SRM's the Activation Analysis Section was responsible for a large fraction of the total effort applied towards their production and certification. These materials are discussed further below.

a. Biological SRM's

The biological SRM's already issued include the Orchard Leaves (SRM 1571) and the Bovine Liver (SRM 1577). At present SRM 1571 has 19 elements certified and information values for 10 additional elements. Of these 29 elements, over half were determined by neutron activation or the nuclear track technique. SRM 1577 presently has 11 elements certified, with information values on 11 additional elements. Again, over half of these elements were determined by nuclear techniques. Several additional biological materials are under development at present, including a Tuna Fish Standard (SRM 1578), which should be issued soon with a number of toxic elements certified for trace content.

b. Fossil Fuel SRM's

Trace element characterization of fossil fuels has gained a considerable amount of importance because of the need to identify and quantify the emission of certain toxic elements and/or compounds into the atmosphere. The literature on the analysis of fossil fuels and their by-products contains much analytical data; however, emphasis in many cases is placed on

the extreme sensitivity of the method used rather than the accuracy obtained. There was felt to be a need for fossil fuel standards so that pollution monitoring devices can be calibrated, and the data obtained can be more meaningful in terms of accuracy and precision. In a joint program with the Environmental Protection Agency, the National Bureau of Standards is in the process of certifying coal, fly ash, fuel oil, and gasoline as Standard Reference Materials.

To determine the homogeneity of the fossil fuels both macro and trace elements were analyzed using non-destructive neutron activation analysis. Elements such as vanadium, manganese and aluminum were readily detected and measured with a precision of 1-2%. Replicate analysis gave a good indication that the fossil fuels were homogeneous within these limits. For the determination of As, Cd, Hg, Se, and Zn the most sensitive and useful (n, γ) reactions involve short-lived nuclides. To obtain good sensitivities for these elements, they must be chemically separated from the activated matrix. The method used was a modified combustion technique, which simultaneously determined As, Cd, Hg, Se, and Zn. The radiochemical separation involves the combustion of the sample followed by reduction with carbon monoxide and subsequent volatilization of the metals. The results obtained by this method were in good agreement with other analytical techniques. In most cases, the accuracy and precision of analysis was from 2 - 5%.

In addition to the homogeneity testing, activation analysis was used to analyze for 9 elements in these materials. At present, the fossil fuel SRM's are undergoing additional analyses by a number of different analytical techniques, including activation analysis, and at least three of them (coal, fly ash, and fuel oil) should be issued in the next year.

c. Calibrated Glasses as SRM Neutron Monitors for Fission Track Studies.

Four glasses of different uranium concentrations, SRM 961 (461 ppm), SRM 962 (37.4 ppm), SRM 963 (0.823 ppm) and SRM 964 (0.0721 ppm), were prepared for use as neutron monitors to aid fission track studies. These

glass wafers were irradiated in the NBS reactor and the neutron flux was monitored using copper and gold foils.

The glasses were polished, polycarbonate and mica detectors were affixed to either side of each glass, and this configuration was sealed in polyethylene. Each package was placed in an individual irradiation container; included in every tenth container were a gold and copper neutron monitor.

In order to allow the user selection of thermal to fast neutron ratios, two glasses which were irradiated in separate reactor locations are provided. Glasses were irradiated in reactor facility RT-3 which has a Cd ratio for Au and Cu of 10.2 and 65, respectively, and RT-4 which has a Cd ratio for Au and Cu of 87 and 536, respectively.

These Fission Track Glass SRM's will aid fission track laboratories in the interlaboratory comparison of data and in monitoring neutron flux levels in their irradiation facilities.

3. Cooperative and Service Analyses

In addition to the analyses on SRM's, a large number of additional analyses were made on non-SRM materials. These include cooperative analyses, where the analysis is made on samples of mutual interest to NBS and some other organization, and also service analyses, where the technical expertise of the section is needed by an NBS or other governmental agency.

During the past year, the Activation Analysis Section has completed cooperative and service analyses to the extent of 131 samples, for 347 elemental determinations. These samples were obtained from five other NBS laboratories, and such other agencies as the Frederick Cancer Institute, the U. S. Army (Fort Belvoir), and the National Institutes of Health. The determinations included over 30 different elements, in matrices ranging from high purity silicon, glasses and coal, to drugs and organic polymers. In particular, two extended programs of analyses were undertaken in cooperation with other NBS laboratories, which are described below.

a. Clay and Clay-Based Papers Study

A cooperative analytical program was initiated with the Fibrous Systems Section of the Product Evaluation Technology Division here at NBS. This laboratory is concerned with the trace element profiles of a variety of clays and clay-based papers.

The analyses were performed for both short-lived and long-lived radionuclides. The short-lived elements (Al, V, Ti, Mn, Cl and Mg) were determined after irradiation in RT-5, the thermal column pneumatic tube facility. The longer-lived radionuclides were determined after irradiation in RT-3, and included over twenty (20) elements in the initial survey analyses. Work on this project is continuing during the coming year.

b. Determination of Gold in High Purity Silicon

Another cooperative program which took place in the past year was with the Semiconductor Characterization Section of the Electronic Technology Division of NBS. This laboratory required the accurate, non-destructive analysis for low concentrations of gold in a highly purified elemental silicon matrix. This gold had been added during manufacture as a dopant, in order to modify the silicon's electronic characteristics. The analyses were required to be accurate because the data were needed for "cause and effect" relationships between the analyzed gold content and the electronic characteristics as found by measurements on the same samples. This program has been of considerable assistance to their project, and will be continued in the future.

4. Facilities

During the past year, there were two particular facilities projects in the Activation Analysis Section which may be of interest and which are included here. The first concerns our irradiation capabilities, namely, the approval and manufacture of RT-6. The second concerns our detection capabilities, namely the calibration of all four Ge(li) detectors for their total absolute photopeak efficiency at a variety of geometries and gamma-

ray energies.

a. Pneumatic Tube Facility RT-6

Significant progress has been made in the past year in cooperation with the Reactor Radiation Division on the preparation of pneumatic tube facility RT-6. This facility is to be located in the vertical tube location VT-3 in the reactor reflector area. It will use a small size polyethylene rabbit as the irradiation container, and should have characteristics somewhere between RT-3 and RT-4. The prime advantage for this facility will be the location of the send-receive terminals, which are located in two of the B-wing hot laboratories. These locations will allow the use of RT-6 for very short-lived radionuclides, with counting on the Ge(L9) detector systems also located in the B-wing. This system should be available early next year.

b. Calibration of Ge(Li) Detector Systems

In the past, two of our Ge(Li) and one 7.5 cm x 7.5 cm NaI(Tl) detector systems had been partially calibrated for their total absolute photopeak efficiencies. These measurements were made at a few different geometries using several NBS SRM γ -ray Point Source Standards. Now, however, a recently issued NBS SRM Mixed Radionuclide Point Source Standard (SRM 4215) has made additional calibrations much easier. This source contains 9 radionuclides, with a total of 11 calibrated γ -ray peaks, all at approximately the same relative intensity. These peaks, ranging from 0.0877 MeV (^{109}Cd) to 1.836 MeV (^{88}Y), are calibrated in γ /s with total uncertainties of 3% or less. Using this source, all of our Ge(Li) detector systems were calibrated for this γ -ray energy range at distances of 0-30 cm. These efficiencies have been found to be extremely useful in the estimation of sensitivities for activation analysis, in calculating estimates of elemental concentrations when no standards are available, and in the evaluation of various detector systems.

5. Conclusion

The Activation Analysis Section of the Analytical Chemistry Division has been active in a number of significant research areas. They have also analyzed a wide variety of sample types for many different elements. Work is continuing in most of these areas, as well as in several additional projects recently initiated.

INTEGRAL REACTION RATE MEASUREMENTS
FOR THE NBS NEUTRON STANDARDS PROGRAM

J. A. Grundl and I. G. Schröder
(Nuclear Sciences Division)

Neutron standards activities at the reactor this year have centered around the reactor thermal column facility where the extracted thermal beam has been employed in support of integral cross section measurements and an extensive program of absolute fission rate calibrations for AEC's Interlaboratory LMFBR Reaction Rate Program (ILRR). Two elements of this support work prominent during the period covered by this report are outlined below:

1. Performance Maximization and Operational Checks of the NBS Double

Fission Chambers. The NBS Double Fission Chamber is a high-resolution double ionization chamber of minimized volume and mass designed to measure absolute fission rates in a wide variety of neutron environments. The performance characteristics and the absolute efficiency of the chamber have been investigated in the reactor thermal column beam ($n_{\text{v}} \approx 6 \times 10^6$, gold cadmium ratio $>10^4$). Some results of these investigations are as follows:

- establishment of a triple-scaler method for obtaining and verifying the fission pulse rates from the double chamber. This method, simple and convenient, provides a redundant readout of the primary pulse rate, a continuous monitor of the extrapolation-to-zero of the fission pulse height distribution, and a sensitive check of gain stability.
- determination of the linearity of dead time corrections for random pulse rates of up to 10^4 per second.
- measurement of the absolute efficiency of the chamber for detecting fission fragment. The observed efficiency, between 0.998 and 0.985, appears to vary linearly with the thickness of the fissionable deposits.

The NBS fission chambers may be assembled with any of a number of fissionable deposits (e.g. ^{239}Pu , enriched or normal uranium,

and ^{237}Np), and has been operated successfully in a half-dozen different neutron fields important for fast neutron standardization:

- core center of the CFRMF Reactor at Idaho Falls, Idaho (purpose: fission activation detector calibrations for the ILRR Program mentioned above).
- $\Sigma\Sigma$ standard neutron facility at the CEN-SCK Laboratories in Mol, Belgium (purpose: international comparison of absolute fission detectors, and spectrum characterization).
- thermal neutron beam (purpose: calibration of a triple-axis neutron spectrometer at the NBS Research Reactor).
- ^{252}Cf spontaneous fission neutron source at the NBS Van de Graaff low-scatter room (purpose: absolute fission cross section measurements).
- NBS thermal column beam (purpose: intercalibration of the NBS fission chamber and ANL fission track recorders).
- Van de Graaff neutron facility at the Univ. of Toronto (purpose: investigation of proposed BIPM intercomparison of Van de Graaff facilities).

Each of these neutron environments presented unique operational requirements for the fission chamber, and each of these requirements was met by means of beam measurements at the NBS reactor thermal column.

2. Preliminary Mass Assay of Fissionable Deposits. Fission rate ratios obtained with pairs of fissionable deposits placed back-to-back in the double fission chamber and then exposed to the thermal column beam is part of the effort to establish the masses of principle isotopes for the NBS set of fissionable deposits. Comparing fissile deposits of similar isotopic composition is a simple type of measurement now underway which will provide an inventory of deposits of various thicknesses and known relative masses. The significance of these rather routine ratio measurements may be realized when it is noted that the fission rate measurements undertaken in the neutron fields listed under item 1 above covered a neutron flux range of nearly four orders of magnitude, and required the operation of three individual double fission chambers containing six fissionable deposits.

Comparing fissionable deposits of different isotopic composition is only beginning. An example of this work is the mass ratio between a ^{235}U and a normal uranium deposit which has been obtained based upon fission counting and the isotopic composition of normal uranium. The latter is established to $\pm 0.1\%$ by the NBS Mass Spectrometry Section. An independent mass ratio for the same pair of deposits based on absolute alpha counting by the NBS Radioactivity Section agrees with the fission counting method to better than 0.5%.

PRECISION MEASUREMENT OF THE COMPTON WAVELENGTH OF THE ELECTRON

W. C. Sauder, E. G. Kessler and R. D. Deslattes
Optical Physics Division

We intend to measure the Compton wavelength of the electron by means of precision crystal diffraction spectroscopy of the radiation emitted in two-photon annihilation of positronium. This will yield a non-quantum electrodynamic determination of the fine structure constant at the one ppm level. The measurement will be carried out with a two-axis, Laue case transmission crystal diffraction spectrometer that was designed and constructed at NBS. This instrument is capable of determining Bragg angles of 2.5 degrees or less with an angular sensitivity of better than 10^{-4} arc second.

In addition to performing the annihilation measurements employing a high activity (20 kilocurie) ^{64}Cu source, we will determine the wavelengths (and therefore energies) of several nuclear gamma lines in the region 80-1000 keV.

During the current year we have completed the installation and testing of the experimental apparatus, including the source cryostat that will provide a 7°K helium moderator in a 0.2 T magnetic field for the annihilating positronium. At the present time we are beginning the angular calibration of the spectrometer.

^{60}Co GAMMA RAY ANISOTROPY THERMOMETRY

H. Marshak, R. J. Soulen and D. B. Utton
(Heat Division)

A new stabilized counting system will enable us to improve the precision of the comparison measurements between a ^{60}Co γ -ray anisotropy thermometer and a Josephson junction noise thermometer. In addition, a new "bottom" for our dilution refrigerator will enable us to extend our measurements from 20 mK to 12 mK or lower. This will also help to improve the precision of our measurements since the anisotropy increases by a factor of two.

A NMR/ON experiment was performed on a 15 microns thick sample and no effect was seen. X-ray analysis of the sample indicated it was no longer a single crystal. A new sample is being prepared and x-ray analysis is being carried out along each step in its production; e.g. both before and after irradiation.

Some work was also done on studying the thermal contact problem of our ^{60}Co thermometer in the temperature region of 20 to 40 mK.

EMISSION OF LONG-RANGE ALPHA-PARTICLES IN THE
SUBTHERMAL-, THERMAL- AND RESONANCE-NEUTRON FISSION OF ^{239}Pu

I. G. Schröder
(Nuclear Sciences Division)

An analysis of the slow neutron fission resonances in ^{235}U and ^{239}Pu has led not only to a classification of the fission widths into two groups for each spin value but also to a separation of these resonances into two groups according to the degree of mass asymmetry of the fragments. All these measurements though firmly establishing the existence of two resonance groups disagree on the detailed assignment of individual resonances to each group. Prompted by these ideas many investigators, in recent years, have looked for a correlation between the emission of long-range alpha particles (LRA) in fission and some of the observed characteristics

of the fission process in the slow-neutron resonance region. The many results obtained do not agree even qualitatively. No detailed measurements exist in the case of ^{239}Pu , in spite of the fact that this isotope shows the greatest variation in the degree of mass asymmetry of any known isotope in the low-neutron energy region, i.e. the mass distribution peak-to-valley ratio for the 0.297 eV resonance is twice as large as the ratio for thermal fission. The purpose of the present experiment was therefore to study the possible dependence on neutron energy of the binary-to-ternary ratio and of the energy distribution of LRA emitted in the low-energy neutron fission of ^{239}Pu .

To study the characteristics of LRA emission in the subthermal- and thermal-neutron regions respectively, a beryllium and a quartz filter (both at liquid nitrogen temperature) were used in conjunction with a mechanical monochromator; this monochromator was employed to select only a given portion of the filtered neutron distribution. Lastly a samarium filter was used to isolate the 0.297 eV resonance in ^{239}Pu . Solid state detectors were used to detect both alpha-particles and fission fragments.

The relative values of the binary-to-ternary fission ratio were obtained by taking, in each neutron group, the ratio of half the total number of fission counts above 45 MeV to the number of counts above 7.5 MeV in the corresponding LRA spectrum. This restriction on the ternary spectrum was imposed so that no correction would be necessary for the background present below 7 MeV. The only corrections made were therefore for the small fluctuations in the reactor-beam intensity. The results obtained are shown in Table 1. To look for a possible variation in the energy distribution of the LRA with neutron energy the ratio of the number of alpha particles above 7.5 MeV to those above 12.5 MeV (in order to separate the lower energies) was calculated for each of the distributions obtained in the three intervals measured. The results obtained from this analysis are shown in Table 2. The errors indicated in both these tables arise from the small uncertainties in the energy calibration of the LRA and the statistical error due to counting. As can be seen from these results no variation is observed in the binary-to-ternary fission ratio

or in the energy of the LRA for the energy intervals considered to within the precision of these measurements.

Lastly, as this experiment shows no variation in the relative values of the binary-to-ternary fission ratio in ^{239}Pu with neutron energy one can use a reactor beam to determine the value of this quantity. The problem in making such a measurement is in evaluating the hidden part of the LRA distribution (Fig. 1). In order to circumvent this problem the LRA distribution of both ^{239}Pu and ^{235}U were measured in the same geometry and the known value of the binary-to-ternary fission ratio of the second was used to normalize the first. The value thus formed was then compared with those obtained by analyzing the shape of the LRA distribution. The results of the measurement and subsequent analysis yields a value of 412 ± 11 for the binary-to-ternary fission ratio for the thermal neutron fission of ^{239}Pu .

Table 1. Relative values of the binary-to-ternary fission ratio in ^{239}Pu in the subthermal-, thermal- and resonance-neutron regions

Neutron energy region	Binary-to-ternary ratio (relative)
subthermal	509 ± 14
thermal	514 ± 10
resonance	503 ± 12

Table 2. Ratio of long-range α -particles above 7.5 MeV to those above 12.5 MeV in the subthermal-, thermal- and resonance-neutron fission of ^{239}Pu .

Neutron energy region	Ratio
subthermal	1.29 ± 0.05
thermal	1.32 ± 0.04
resonance	1.31 ± 0.06

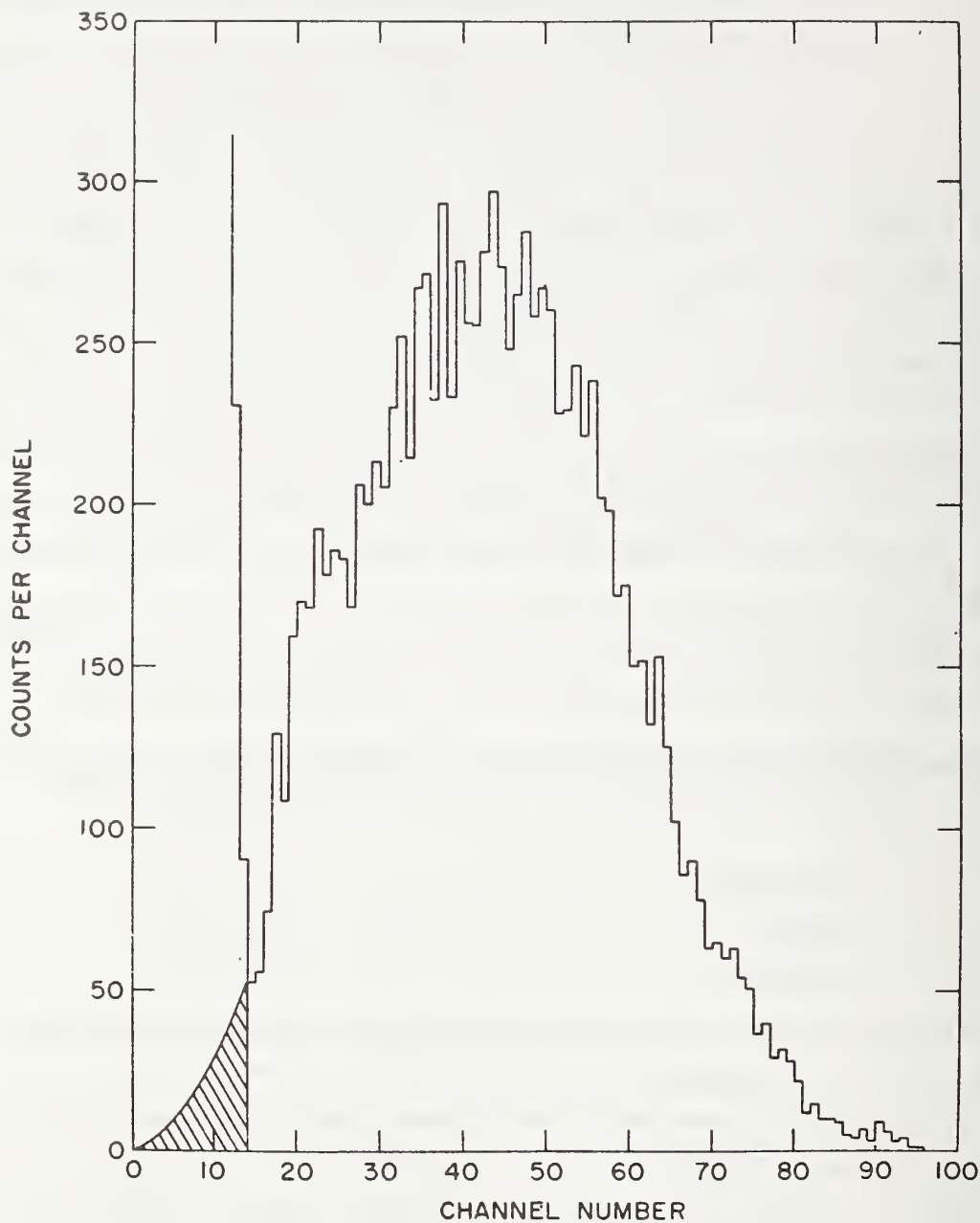


Fig. 1. Typical LRA spectrum. Shaded area represents estimated background.

EXTREME-ANGLE EMISSION OF LONG-RANGE ALPHA PARTICLES IN THE
THERMAL NEUTRON FISSION OF ^{235}U I. G. Schröder
(Nuclear Sciences Division)

An experiment has been performed in order to seek a correlation between the kinetic energy of long-range alpha particles emitted at extreme angles ($0^\circ < \theta < 150^\circ$) with respect to the line of emission of the light fission fragments and the kinetic energy of the fission fragments. An annular surface barrier detector (alpha detector) subtended an angle of $\pm 30^\circ$ at the target (^{235}U) with respect to a fission fragment detector placed behind the annular detector. An annular aluminum foil was introduced between the alpha detector and the source. This let through alpha particles ≥ 6 MeV but stopped all fission fragments. A coincidence circuit (15ns resolving time) demanded coincidence between the two detectors (Fig. 1). The coincident output from these two detectors were recorded on a 2-dimensional pulse-height-analyzer. The results obtained show that extreme-angle alpha particles have higher than average kinetic energies (Fig. 2A) and rate of emission. This energy distribution is in good agreement with the extrapolated angle vs. energy data of Carles et al at Bordeaux (Fig. 3). Furthermore these alpha particles are associated with fission fragments in the region of minimum kinetic energy (Fig. 2B) between the light and heavy fission fragments.

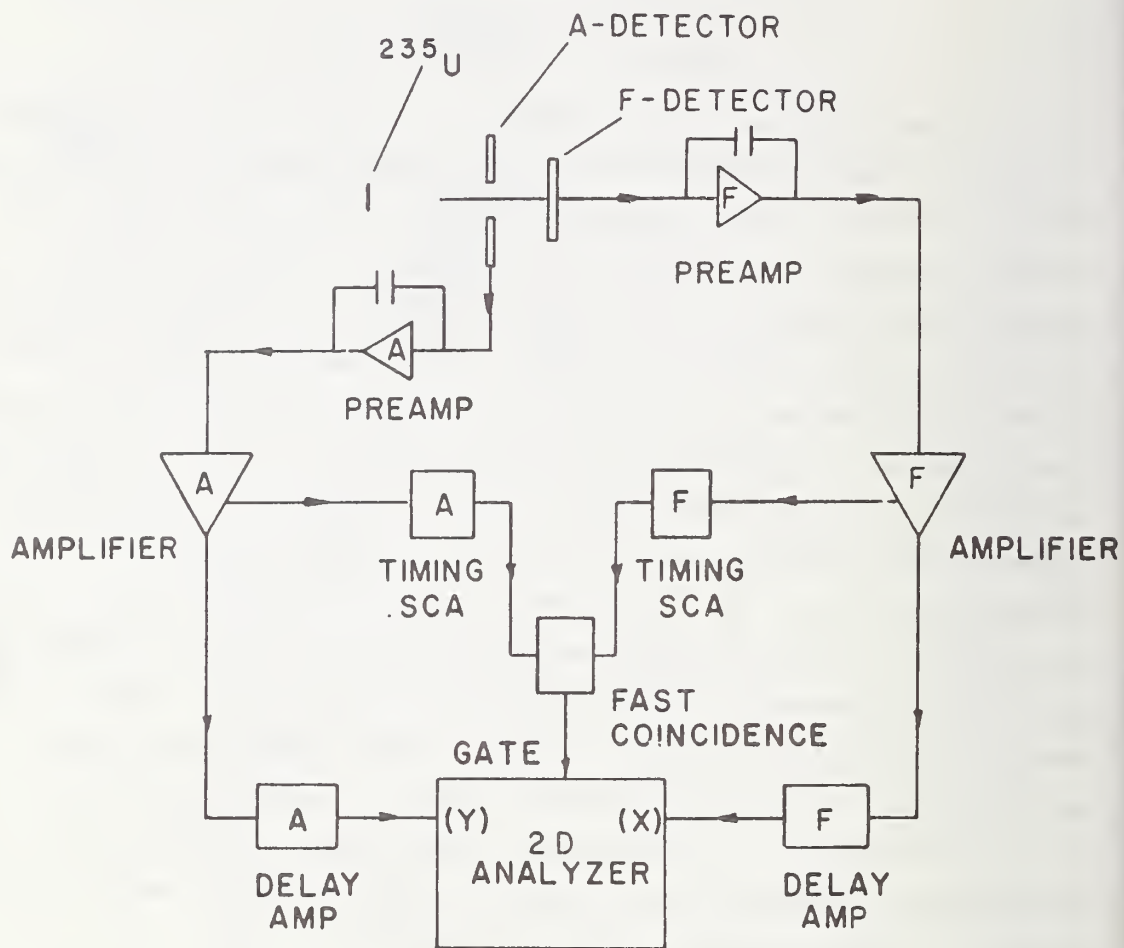


Fig. 1. Experimental arrangement and associated electronics.

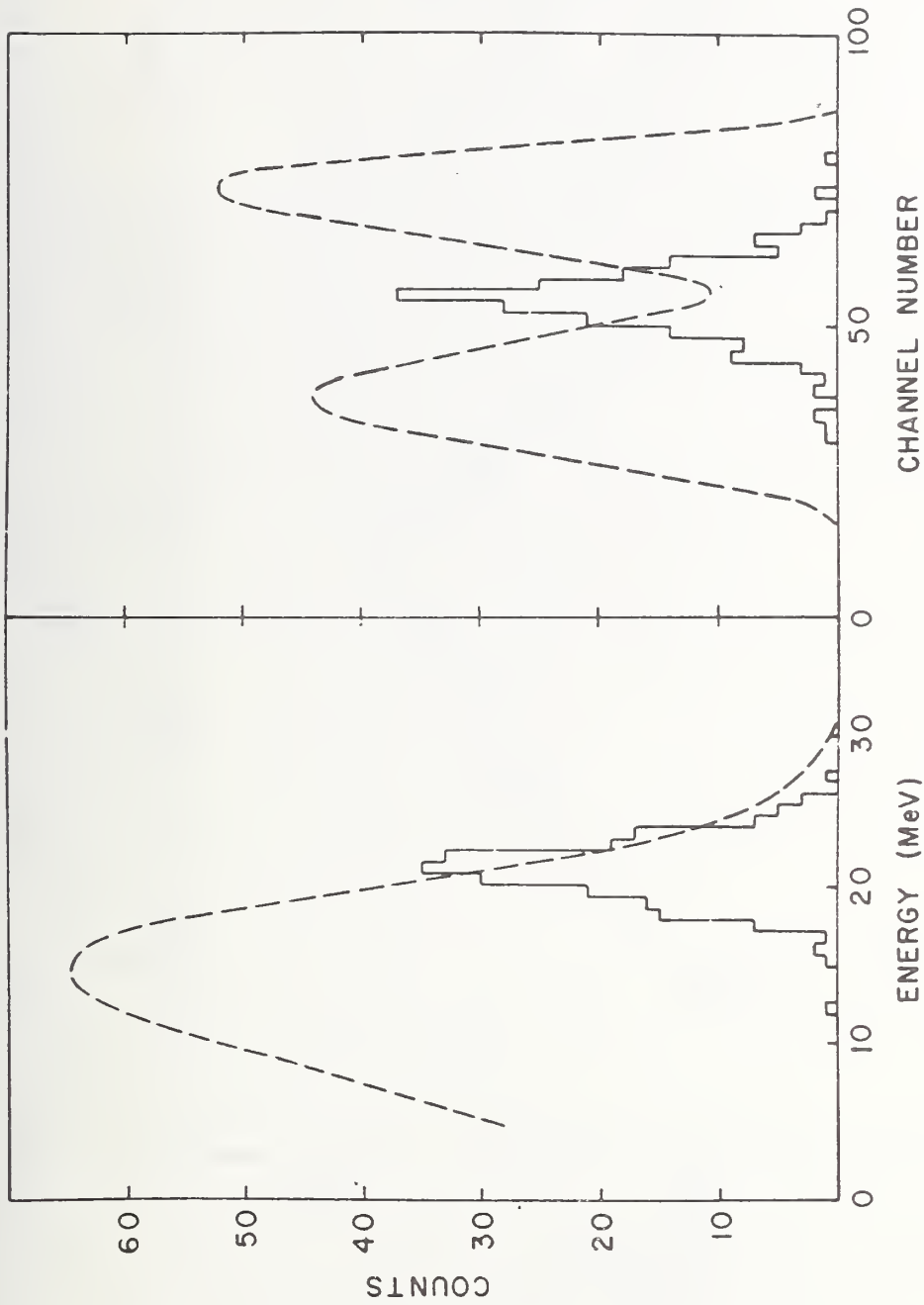


Fig. 2. Solid line represents A) Energy distribution of extreme-angle α -particles B) Energy distribution of fission fragments associated with the emission of extreme-angle α -particles. Broken lines represent corresponding distribution associated with normal emission of α -particles.

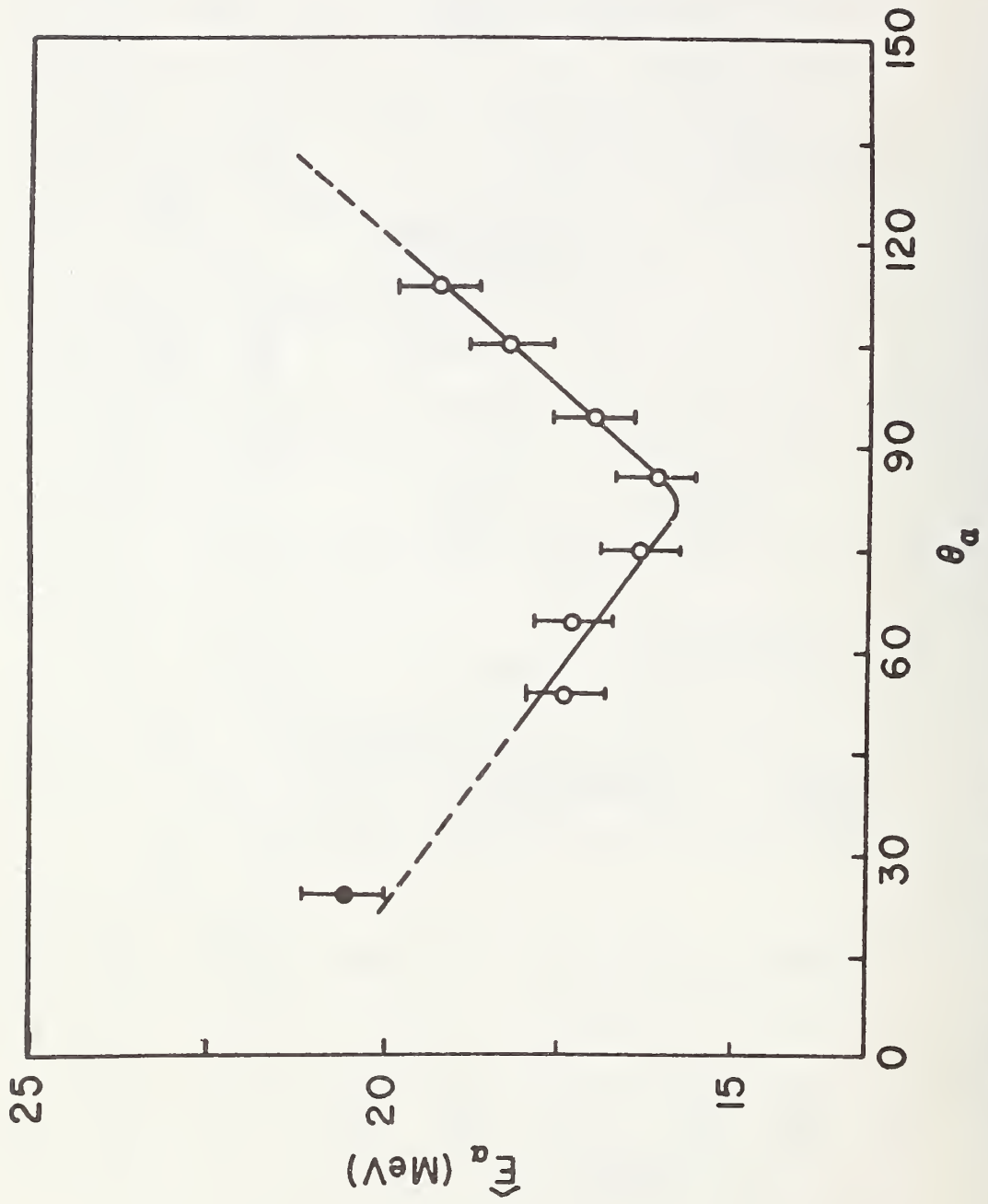


Fig. 3. Dependence on angle of emission on mean energy of long-range α -particles. Solid point represents present experiment.

DEVELOPMENT OF FAST-NEUTRON BEAMS

E. D. McGarry
(Harry Diamond Laboratories, Washington, D.C.)

and

I. G. Schröder
(Nuclear Sciences Division)

A cooperative research program between the Neutron Standards Section, NBS and Harry Diamond Laboratories (HDL) has been initiated to develop fast-neutron beams for the purposes of:

- (1) Developing better techniques to measure neutron-energy spectra in the vicinity of an operating reactor;
- (2) Providing beams with known spectra for in situ studies of damage to electronic components, with the possibility of incorporating controlled-temperature studies of damage annealing.

A principal feature of the program is to utilize the energy-resolution capability of certain neutron spectrometers to study fast spectra while circumventing the inherent inability of the spectrometers to operate in the high gamma backgrounds near reactors. The technique is to scatter high-flux spectra by selective filtering to obtain a variety of different energy distributions, collimate the beams, and measure their neutron-energy spectra with high-resolution spectrometers.

HDL is interested in the beams from the standpoint of radiation-damage to electronic materials. Such facilities provide the means to evaluate the significance of spectral changes to parameters frequently studied in radiation-damage experiments. Furthermore, it is possible to examine the capability of neutron dosimeters to monitor the fluence of interest to the damage studies. In particular, HDL plans to measure spectral indices (ratios of foil activities) and determine which of the indices are sensitive to differences among measured beam spectra. The foils can then be used by experimenters to evaluate spectra in or near pulsed reactors. The ultimate goal is to develop a more definitive method for quality control of fast-fluence measurements for those radiation-damage experiments that are plagued by perturbed and unknown

spectra.

Three features of the fast-neutron beams appear to be of greatest interest to users. These are: intensity; reproducibility; and credibility of the measured spectra. Only the second of these is easily obtainable. The credibility aspect necessarily dictates the early phases of the spectrum-development program, because one must be able to examine the effects of filtering and scattering to obtain known spectra of any intensity.

The tools for the study are fast-neutron spectrometers which use either proton-recoil proportional counters or helium-3 gas between semiconductors detectors. Present efforts involve instrumenting and calibrating the spectrometers for beam-geometry measurements and fabricating a collimator to extract beams from the immediate vicinity of the fuel of the NBS reactor during full-power operation. Of particular interest is the inclusion of an iron filter and titanium scatterer to provide a high-purity beam of 26-keV neutrons. Initially, this monoenergetic beam will provide a direct check on the energy calibration of the proton-recoil spectrometer.

PROTON-RECOIL SPECTROMETER RESEARCH

E. D. McGarry
(Harry Diamond Laboratories, Washington, D.C.)

and

I. G. Schröder
(Nuclear Sciences Division)

In preparation for measurements of fast-neutron spectra of beams from the NBS reactor, we are studying the voltage pulse-height response functions from cylindrical proton-recoil counters in well-collimated beams with known spectra. A natural starting point for this work is to examine pulse-height distributions from the $^{14}\text{N}(n,p)\text{C}^{14}$ reaction in a thermal-neutron beam. In particular, we wish to know the extent to which pulse-height distributions are distorted because of the truncation of proton-recoil tracks in the tube walls and because of space-charge saturation at high gas gains (high voltages).

Fig. 1 shows an experimental setup at the thermal column of the NBS reactor. A beam, 1/4-inch in diameter, is incident upon a proton-recoil counter positioned perpendicular to the beam. Use of beams smaller than three-quarters of the inside diameter of the tube minimizes pulse distortion because of wall effects and essentially eliminates distortions from the non-uniform electric field in the vicinity of the field tubes at either end of the anode. The photograph, Fig. 1A, shows a 5/8-inch proton-recoil tube connected to an aluminum housing for the high-voltage connection and the signal-coupling capacitor. All these components are mounted on an indexing way (from a lathe) to provide a means of repositioning the tube to within several mils.

To determine the extent of pulse distortion cause by the non-uniform electric field along the anode, the tube is moved perpendicular to the beam, in 1/8-inch increments, from one end of the tube to the other. This provides an exact determination of the center of the electrically-sensitive volume. Fig. 1B shows the central, next displaced, and final location of the beam for the experimental results presented in Fig. 2.

The data for Fig. 2 were collected with an applied voltage of

+2650 volts. The pressure and gas composition are 595 cm (Hg) of hydrogen, 26 cm (Hg) of methane, and 26 cm (Hg) of nitrogen for a total pressure of 647 cm (Hg) or nearly 8 atmospheres. The best resolution is 4.5 percent and is obtained with the beam positioned to within $\pm 1/16$ -inch of the center of the 1.25-inch anode. Fig. 2A and 2B compare the centered-beam configuration with and without a 0.030-inch thick cadmium filter. On the average, there are six counts/channel in the higher-energy channels of Fig. 2B (not visible on the two thousand counts-full-scale graphs of Fig. 2). Comparing Fig. 2B with the remaining five figures, we see that the pulse-height distribution in the channels between the main gamma background (to the left in each figure) and the principal proton peak is due to protons rather than gamma interactions. The decreased pulse-heights are because of truncation in the walls. Even in the case of Fig. 2A, the area under the distorted distribution is 15% to 20% of the area under the peak. Notice that there is a shift of the main peak toward lower energies as the beam nears the region of the field tubes. However, all the distortion in Fig. 2E and Fig. 2F is not due to the non-uniformity of the electric field. As the beam is moved toward the field tubes, there is an increased probability of protons reaching the insensitive region of gas beyond the ends of the field tubes. This leakage has the same effect on the pulse-height distribution as truncation of proton-recoil tracks in the walls of the counter.

Fig. 3 shows variation in the shape of the proton-recoil pulse-height distribution as a function of the applied voltage. In general, there is a range of 600 volts (from 2300 volts to 2900 volts) over which resolution of the $^{14}\text{N}(n,p)^{14}\text{C}$ proton peak is better than 6%. This range provides about a factor of 10 difference in the amount of gain available at the anode. By operating the tube at selected voltages, five or six overlapping energy ranges can be used to span the neutron-energy range from 10 keV to 100 keV without significant differences in resolution.

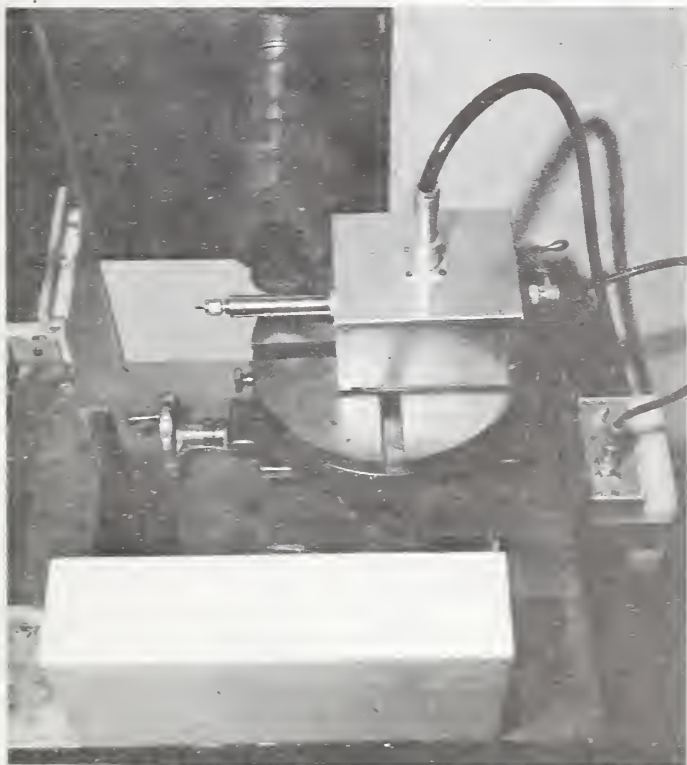


Fig. 1A. A 5/8-inch diameter proton-recoil tube positioned in front of a 1/4-inch diameter collimator in a port of the NBS thermal column.

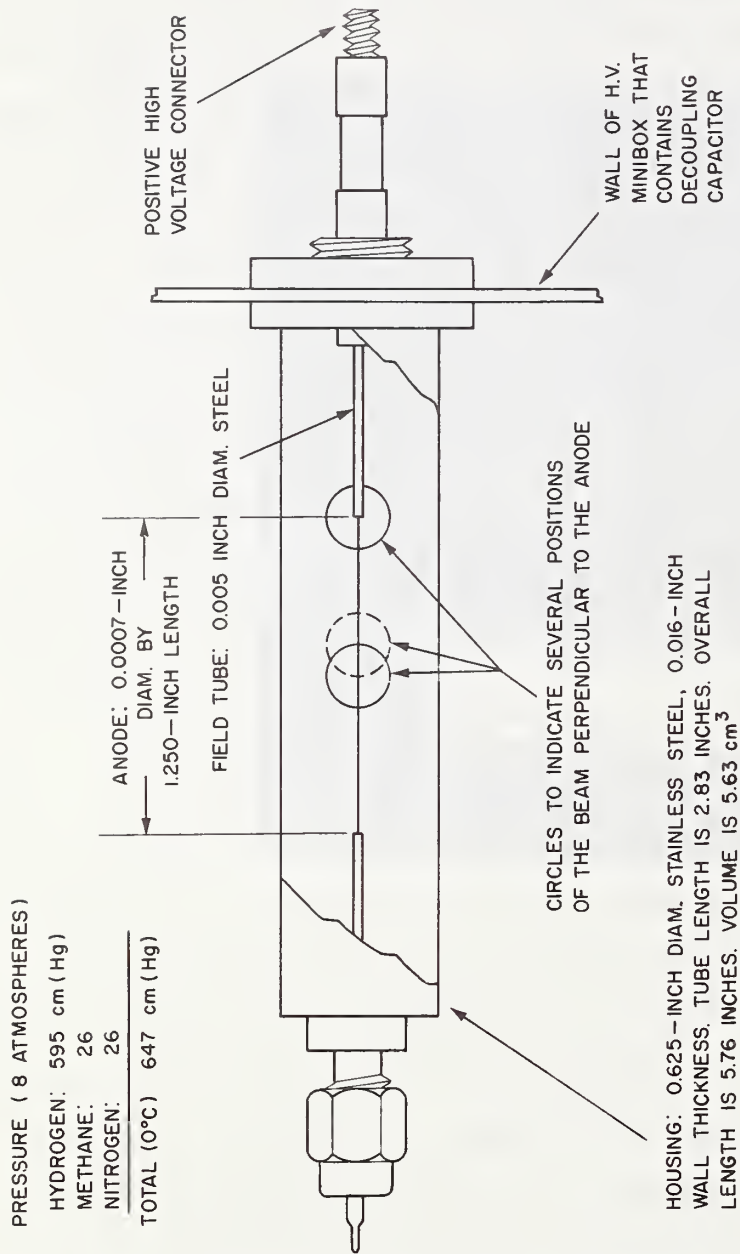


Fig. 1B. Schematic of the above-mentioned proton-recoil tube showing
 the locations of the beam, when centered and when displaced to
 the right. Only the central, first 1/8-inch displacement, and
 the final positions are shown.

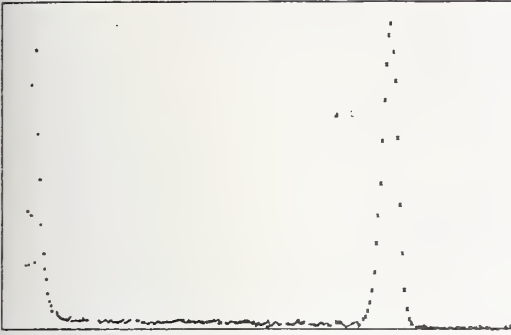


FIG 2A SPECTRUM WITH BEAM CENTERED ON THE 1.25-INCH LONG ANODE OF THE PROTON-RECOIL TUBE

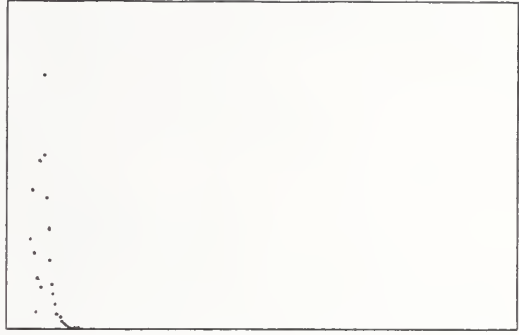


FIG 2B BACKGROUND SPECTRUM DUE TO GAMMA SPECTRUM OBTAINED WITH A CADMIUM PLATE BETWEEN BEAM AND PROTON-RECOIL COUNTER

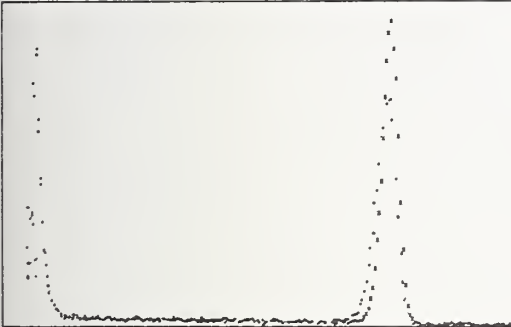


FIG 2C SPECTRA WITH BEAM AT CENTER AND WITH BEAM DISPLACED 1/8-INCH TO LEFT

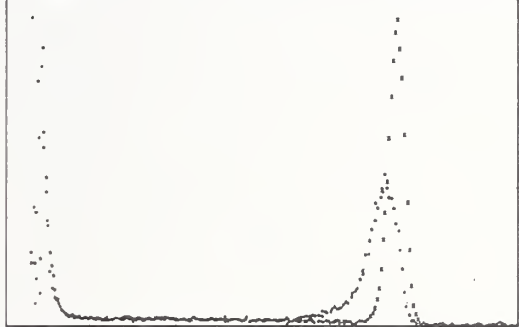


FIG 2D SPECTRA WITH BEAM AT CENTER AND WITH BEAM DISPLACED 1/4-INCH TO LEFT

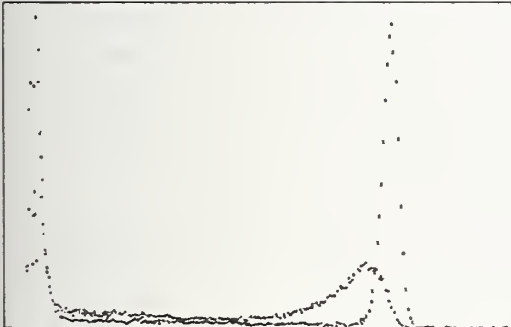


FIG 2E SPECTRA WITH BEAM AT CENTER AND WITH BEAM DISPLACED 3/8-INCH TO LEFT. HERE, EDGE OF DISPLACED BEAM SEES THE END OF THE FIELD TUBE

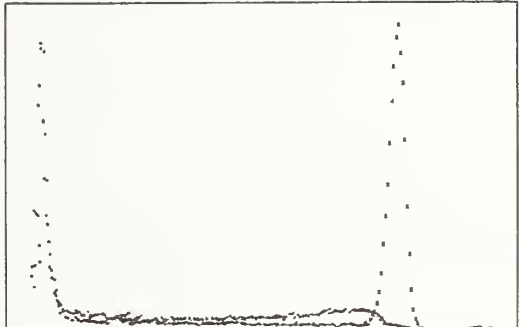


FIG 2F SPECTRA WITH BEAM AT CENTER AND WITH BEAM DISPLACED 1/2-INCH TO LEFT. HERE, DISPLACED BEAM IS CENTERED ON THE END OF THE FIELD TUBE.

Fig. 2. Pulse-height distribution of the $^{14}\text{N}(p,n)\text{C}^{14}$ reaction as a function of the location of the neutron beam along the 1.25-inch-long anode of a proton-recoil tube. Graphs 2c through 2f have graph 2a, the center anode distribution, as an overlay. The peak region of the central distribution is intensified in all cases for clarity. Graph 2b indicates the insignificance of the background in the vicinity of the peak.

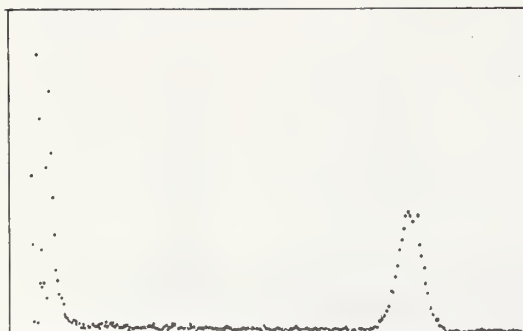
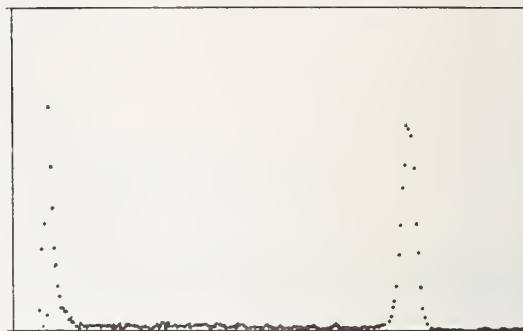
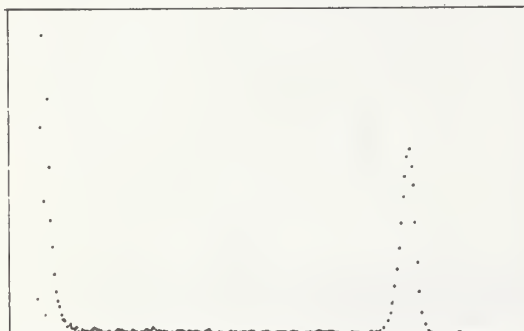
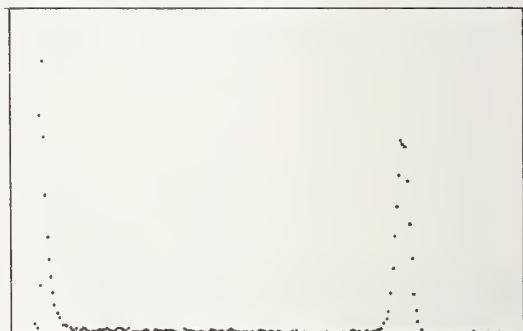
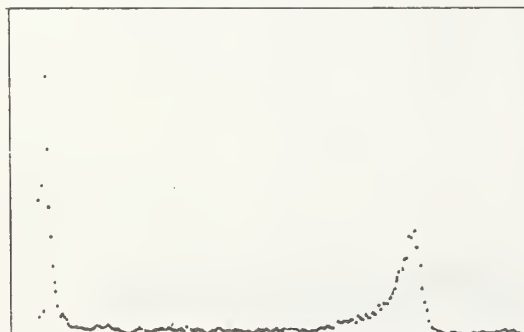
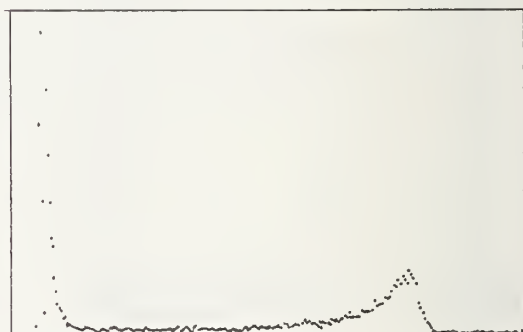
FIG 3A $^{14}\text{N}(n,p)\text{C}^{14}$ PULSE-HEIGHT DISTRIBUTION FOR 2000 VOLTS BIASFIG 3B $^{14}\text{N}(n,p)\text{C}^{14}$ PULSE-HEIGHT DISTRIBUTION FOR 2350 VOLTS BIASFIG 3C $^{14}\text{N}(n,p)\text{C}^{14}$ PULSE-HEIGHT DISTRIBUTION FOR 2650 VOLT BIASFIG 3D $^{14}\text{N}(n,p)\text{C}^{14}$ PULSE-HEIGHT DISTRIBUTION FOR 2800 VOLT BIASFIG 3E $^{14}\text{N}(n,p)\text{C}^{14}$ PULSE-HEIGHT DISTRIBUTION FOR 3100 VOLTS BIASFIG 3F $^{14}\text{N}(n,p)\text{C}^{14}$ PULSE-HEIGHT DISTRIBUTION FOR 3300 VOLTS BIAS

Fig. 3. Variation of the recoil proton pulse-height distribution as a function of the applied high voltage. The ionization pulses are due to protons from the $^{14}\text{N}(n,p)\text{C}^{14}$ reaction, induced by a 1/4-inch beam of thermal neutrons incident on the central region of the anode.

PARITY VIOLATION IN NEUTRON CAPTURE GAMMA-RAY EMISSION

J. L. Alberi and R. Wilson
(Harvard University, Cambridge, Mass.)

and

I. G. Schröder
(Nuclear Sciences Division)

Several theories of weak interactions suggest that parity non-conserving effects may be seen in the internucleon force. One such effect is parity mixing in nuclear states which is due to weak forces between hadrons which conserve strangeness but violate parity. The fact that parity violation in nuclei has been found to be of the order of 10^{-4} to 10^{-6} lends credence to the assumption that this effect arises from the self interaction of the strangeness conserving and strangeness changing parts of the hadronic current (current x current scheme). A manifestation of parity mixing in nuclear states is the circular polarization of neutron capture gamma-rays. As one knows a fully circularly polarized photon is a superposition of equal amounts of states of opposite parity. This follows from the fact that the states with opposite helicity transform into each other under the parity transformation. If one then has a nucleus decaying through an EL (or ML) transition the presence of circular polarization requires a small parity non-conserving admixture of ML (or EL) radiation of the same multipolarity. A search for such parity violating effects has been undertaken by studying the reaction $^{113}\text{Cd}(n,\gamma)^{114}\text{Cd}$.

Thermal neutron capture in ^{113}Cd populates a high-energy capture state that is 9.04 MeV above the ground state and has angular momentum and parity (1^+). The transition (9.04 MeV) direct to the ground state (0^+) and the transition (8.51 MeV) to the first excited state (2^+) are the gamma rays expected to exhibit parity-violating effects. In both of these electromagnetic transitions, the predominant parity-allowed transition is magnetic dipole (M1), while any parity-violating admixture to the capture-state wave function yields an electric dipole (E1) transition, which interferes with the magnetic dipole to produce circularly

polarized gamma rays. Allowed magnetic transition probabilities are less than allowed electric transition probabilities by $(v/c)^2$, where v is the velocity of the nucleons. The relative amplitudes of the weak and strong interactions (V_{wk}/V_{str}) is expected to be 10^{-7} . The parity-violating mixture to the capture-state wave function has been calculated to be $\approx 50(V_{wk}/V_{str})$, and with the enhancement $(c/v)^2$ noted above, the circular polarization is expected to be of the order of 10^{-4} .

An elemental Cd target, placed at the center of one of the tangential tubes of the NBS reactor provided the source of ^{113}Cd capture gamma rays which were collimated by a Bi-Pb collimator designed to view only the target at the detector. The gamma rays were analyzed by a Compton transmission polarimeter that converted the circular polarization of the gamma beam into a count rate change by reversing the polarization of the electrons in the Si-Fe polarimeter. Gammas were detected with a 4" x 5" NaI crystal adequately shielded magnetically to prevent any systematic errors arising from the leakage flux from the polarimeter. The photomultiplier-associated electronics were standard except for the provisions taken to deal with the high overall count rate (several megahertz). After clipping the signal (80 nsec) at the anode of the photomultiplier the pulses were processed through a dual (fast-slow) discriminator system which achieved a 5-kHz count rate above an 8 neV discriminator threshold.

A digital switching analyzer was designed and built to process the discriminator output. This analyzer scaled the output of the integral discriminator and at the same time, correlated the direction of analyzing magnet polarization. The input was counted by one 70-MHz scaler for the duration of each counting period, 1 sec, and then added to one of two registers, depending on the direction of the analyzing magnet polarization. This method was used to prevent systematic errors arising from the variation of the deadtime in the two separate scalers. During reversal of magnet spin polarization, the scaler was gated off to prevent any spurious inductive effects from the magnetic field. Figure 1 illustrates another feature of the switching analyzer. Rather than reversing the electron polarization in the analyzing magnet in a repetitive square-wave pattern as shown for $L=0$, the more complicated pattern shown for $L=4$ was used.

All the switching patterns shown in this figure have the ability to cancel systematic effects due to nonrandom drifts in count rate to the time dependence shown at the right of the figure. Such nonrandom drifts are caused by temperature fluctuations. However by using the L=4 pattern the effect of such drifts was less than 5×10^{-7} .

Various sources of systematic error were investigated and an upper limit measured or calculated for them. The possible sources of error arise from a) the internal bremsstrahlung from the core of the reactor which can be scattered by the target and which is circularly polarized b) from second order Compton scattering $\vec{\sigma}_e \cdot (\vec{k}_i \times \vec{k}_f)$ which can influence the count-rate asymmetry by changing the transmission if the apparatus is not totally spatially symmetric; c) stray magnetic fields which can induce gain changes in the photomultiplier and produce a spurious count-rate; d) magnetostriction and self-polarization. Table I gives the upper limits on these systematic errors.

Control runs were taken by replacing the Cd target with one of Ti which is expected to show no circular polarization. All experimental procedures were followed as with Cd. The energy threshold was set at 6.3 MeV, i.e., at the peak of the dominant gamma line. This procedure mimics the rising slope of the Cd energy spectrum. The Ti runs were also used to measure the amount of internal bremsstrahlung present as this target was 10 times more sensitive to this effect than Cd. Table II shows the results of the circular polarization experiment on ^{113}Cd for two values of discriminator threshold energy as well as the Ti control experiment; the errors quoted are purely statistical. These results are within the range of the estimates quoted above. As can be seen by comparing Tables I and II, the statistical errors are much larger than the systematic errors and hence the latter can be neglected.

The results of the present experiment on the circular polarization of gamma rays from capture of neutrons by ^{113}Cd agrees both in sign and magnitude with the asymmetry of gamma rays from the capture of polarized neutrons measured by Abov for the 9.1 MeV gamma ray. The relative sign of the asymmetry and circular polarization for the 8.6 MeV and 9.1 MeV

transitions are opposite. We seem to find that 8.6 MeV gamma rays have the same sign of circular polarization as the 9.1 MeV gamma rays. The asymmetries will be opposite; mixing these two gamma rays can result in no asymmetry when asymmetry experiments are done with a lower bias; this has been observed by Abov and others.

Table II. Results of main and control experiments.

	Bias	$\delta \cdot x 10^{-5}$	$P_{\gamma} \cdot x 10^{-4}$
$^{113}\text{Cd}(n,\gamma)^{114}\text{Cd}$	8.00 MeV	3.6 ± 0.90	-6.0 ± 1.5
$^{113}\text{Cd}(n,\gamma)^{114}\text{Cd}$	8.50 MeV	6.3 ± 2.6	-10 ± 4.2
$^{48}\text{Ti}(n,\gamma)^{49}\text{Ti}$	6.28 MeV	-0.4 ± 0.6	-

Table I. Upper limits on systematic errors.

1. Internal bremsstrahlung	$\delta = (4 \pm 6) \times 10^{-7}$
2. $\sigma_e \cdot (k_i \times k_f)$ Compton term	$< 10^{-7}$
3. Stray magnetic field	$< 7.5 \times 10^{-7}$
4. Magnetostriction and self-polarization	$< 10^{-8}$

PATTERN ORDER

TERMS CANCELLED

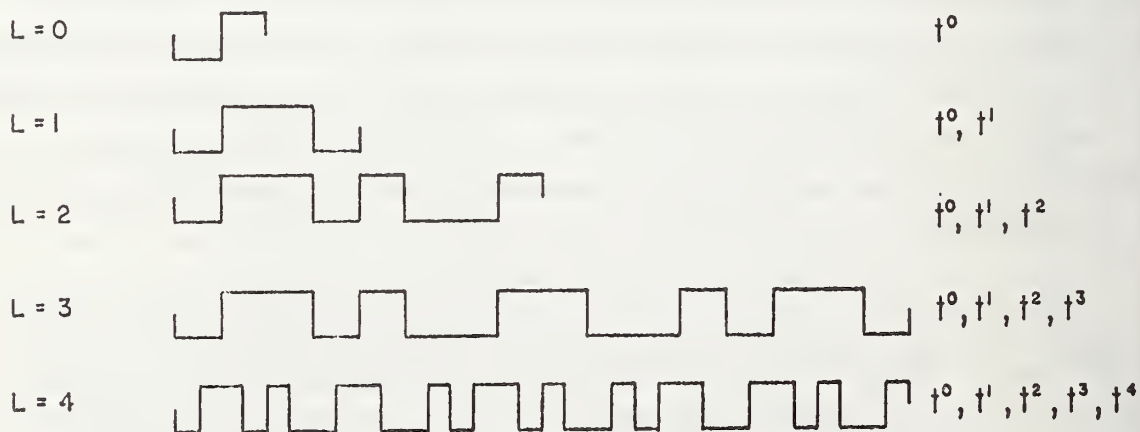


Fig. 1. Switching patterns from zeroeth to fourth order.

A SEARCH FOR DOUBLY RADIATIVE (N,P) CAPTURE

R. G. Arnold and B. T. Chertok
(American University, Washington, D.C.)

and

I. G. Schröder
(Nuclear Sciences Division)

and

J. L. Alberi
(Harvard University, Cambridge, Mass.)

Following a suggestion by R. J. Adler that the long standing discrepancy (9%) between the measured and the calculated thermal n-p capture cross sections might be ascribed to capture leading to emission of two photons, an experiment was performed to search for this mode of decay.

The method used was to look for two gamma-rays emitted in coincidence from an H₂O target in a beam of thermal neutrons. The spectrum of gamma-rays from two-photon events is continuous with $E_1 + E_2 = 2$ MeV and is expected to be peaked at $E_1 = E_2$. The phase space of the two-photon events is schematically represented in Fig. 1A. The experimental conditions were determined primarily by the requirement of detecting gamma-rays with a broad energy distribution that are in true coincidence amidst a large background of accidental events.

The cross section for doubly radiative (n,p) capture was determined relative to the cross section for single photon capture by comparing the singles coincidence counting rate (Fig. 1B) with the singles rate for 2.2 MeV capture gamma-rays (Fig. 1A) from the same target. Accidentals were obtained from the delayed coincidence spectrum (Fig. 1C), and the coincident oxygen background was determined by replacing the H₂O with an equivalent D₂O target. To reduce the accidental counting rate the targets used were surrounded by a large isotopically enriched (96%) ⁶Li₂CO₃ and a "fast-slow" coincidence configuration (Fig.2) was employed using two constant-fraction discriminators and a TAC in the "fast" leg (1.8 nsec fwhm) and cross-over discriminators in the "slow" leg (2t = 30 nsec). The energy resolution of the system [NaI] was 5% at 1.3 MeV.

Analysis of the data obtained in the experiment indicates that two-photon (n,p) capture events have not been observed. An upper limit at the three standard deviation confidence level of $\sigma_{2\gamma} < 1.0$ mb can be placed on the doubly radiative cross section. Therefore the two photon cross section does not explain the discrepancy between the experimental (n,p) capture cross section and the effective range theory prediction.

Since this measurement was completed several new calculations and predictions have appeared. Two of these new calculations include the catastrophic pion current which had been omitted in earlier works, and a rescattering current which is in qualitative agreement with the previously calculated 3-3 resonance contribution. Agreement with experiment is reported although the question of double counting of resonance and pion currents carried over from high energy duality leaves the good quantitative agreement in some doubt. A more complete treatment of the negative energy parts of the catastrophic pion current is a further question. This is being examined with two-nucleon negative-energy wave functions.

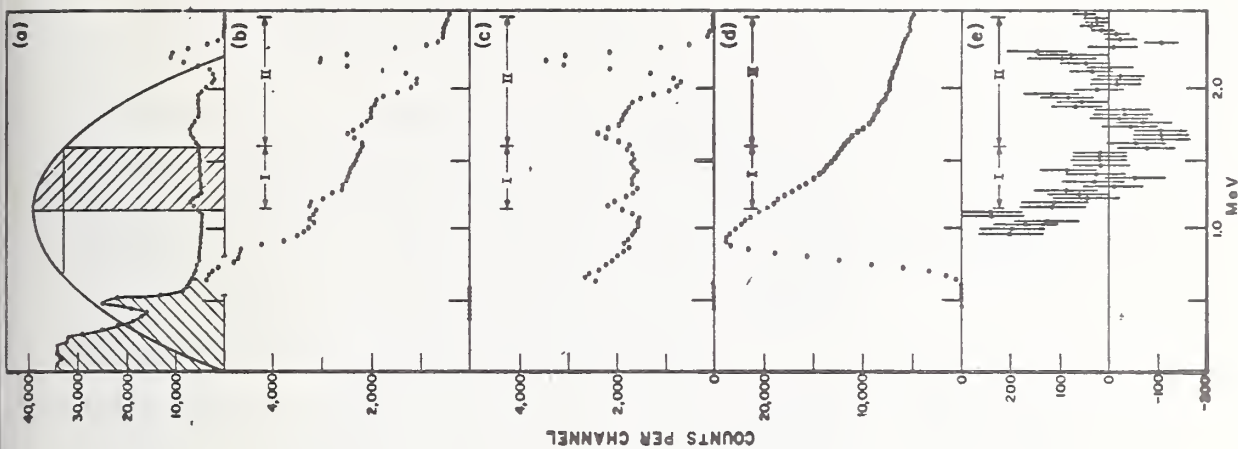


Fig. 1. (a) The two photon phase space and a singles spectrum with the H_2O target. The spectrum from one detector is plotted to indicate the response of the NaI detector to the large flux of 2.2 MeV gamma rays from single photon np capture. The phase space of the two photon events is schematically indicated by the curve peaked at 1.1 MeV. The shaded region below 0.6 MeV was biased out in both legs during the coincidence runs. The region marked I from 1.1 to 1.6 MeV represents the useful signal region. Region II was used for normalization in the background subtraction.

(b) The prompt coincidence spectrum F with the H_2O target.

(c) The delayed coincidence spectrum D with the H_2O target.

(d) The prompt coincidence spectrum B with the D_2O target.

(e) The residual spectrum $R_1 = F_1 - C_1D_1 - C_2B_1$ with normalization constants C_1 and C_2 determined by minimizing the residuals in region II.

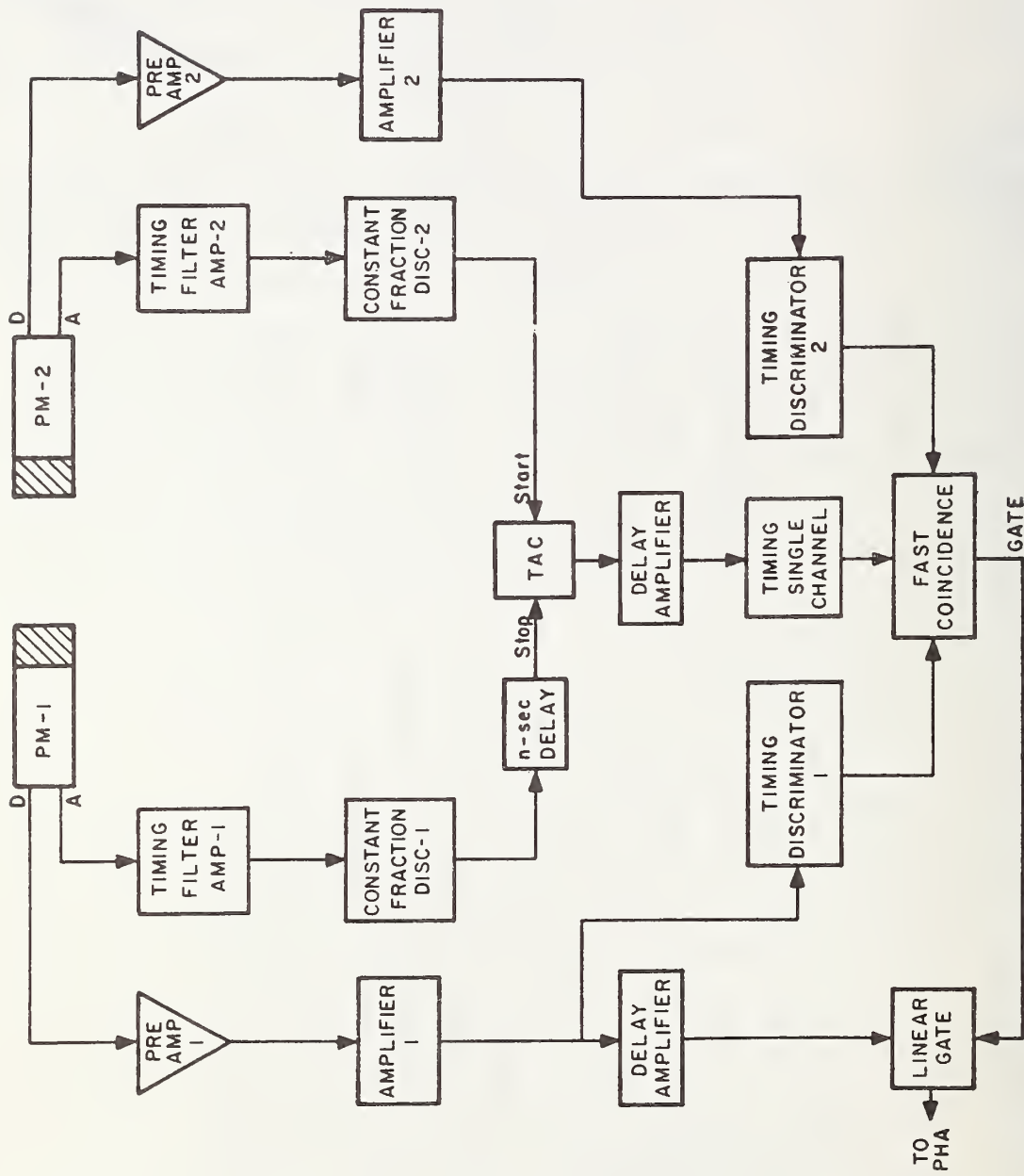


Fig. 2. Block diagram of electronics.

E, SUMMARY OF REACTOR OPERATIONS

July 1, 1972 to June 30, 1973 was the best year in the history of the facility. Performance statistics were also the best in the history of the facility. Significant among these are an on-line time at power of more than 80% equivalent to 77% at full power and a fuel burnup rate of more than 50%. These were accomplished in spite of eight main heat exchanger leaks, a 4-1/2 day per week summer schedule and a 10-20% reduction in power during the spring and summer months in order to preserve the heat exchanger. A summary of operating statistics for this and previous years are present in the following table.

NBSR Operating Summary

	Nov. 1969 to Nov. 1970	Oct. 1970 to Oct. 1971	Oct., 1971 to Oct. 1972	July 1972 to July 1973
Reactor Operations to date, MWh	78,000	124,000	175,000	229,000
Reactor Operations for year, MWh	59,000	51,000	51,000	67,000
Hours Reactor Critical	6,000	5,400	5,200	7,000
Number of Days at 10 MW	247	213	214	279
On-line time at 10 MW	67%	58%	58%	77%
Number of fuel elements used	44	24	26	28
Average U-235 Burnup	34%	48%	45%	52%
Number of Refueling Operations	11	6	6	7
Number of Unscheduled Shutdowns	3	10	11	14
Number of Irradiations	1,500	3,000	4,000	4,300
Number of Visitors	4,000	4,000	3,400	3,000

Aside from the eight heat exchanger leaks, there were no other significant operational difficulties. Seven of the leaks occurred in the first five months of the year. Subsequent reduction in secondary flow of about 20% and plugging of additional tubes that were suspect, reduced the number of leaks to only one in the remaining seven months. The new stain-

SUMMARY OF REACTOR OPERATIONS

less steel heat exchangers are scheduled to be delivered and installed in the spring of 1974.

Towards the end of the period there were indications of a possible small leak in one of the fuel elements in the core. This could result in a future reactor shutdown in order to locate and remove the faulty element.

F. SERVICE PROGRAMS

Service and irradiation programs again continued at a very high level. In all, approximately 4,300 irradiations involving 47,000 samples were performed this year. There was also a considerable increase in sample irradiation times. The irradiations again covered a wide range of programs. Highlights are presented in following sections.

ACTIVATION ANALYSIS PROGRAM OF THE FOOD AND DRUG ADMINISTRATION AT THE NBSR

J. T. Tanner and M. H. Friedman
(Food and Drug Administration, Washington, D.C.)

1. Multi-element Analysis of Foods

During the past few years work on mercury has progressed to the point where its occurrence and distribution in foods have been established. Interest has been directed lately to other elements which are either potential or known hazards. These include Se and As. The FDA NAA group has been working on methods to determine several elements routinely in food samples.

The first method involves a radiochemical separation by volatilization of Se, Hg, and As. Once these elements are separated from the food matrix their radioactivities may be determined to establish their levels in foods. By developing a rapid radiochemical separation and analysis method a large number of food samples may be surveyed routinely.

In addition to doing radiochemical analyses, an instrumental method is being developed to determine elements such as Na, Br, Zn, Co, Sc, Sb, and Fe. By using automated counting techniques and computer reduction of data a large number of samples may be surveyed.

2. MTELMT: A Computer Language For the Reduction of Neutron Activation Analysis Data

Neutron activation analysis (NAA) data reduction often employs a "custom built" computer program which takes into account the special requirements of the particular problem and equipment. Consequently there are many NAA programs written in high level languages such as FORTRAN and

ALGOL. However, the flexibility and power of these languages require the programmer to specify a large number of details, many of which are only of peripheral interest in solving the problem. If the specification of peripheral details could be avoided then a program could be written or changed with less effort. The MTELMT language (mnemonic for multi-element) was written to reduce NAA data while avoiding the need to specify unnecessary details. In this language the user "talks" to the computer in a language resembling English and tells it how to reduce the data.

MTELMT consists a number of interacting subroutines written in FORTRAN V and has been run on the UNIVAC 1108 computer at the National Bureau of Standards. It is used to reduce gamma or x-ray spectra for either a single element or combination of elements. It computes the micrograms or ppm of the element(s) present, the uncertainty of the measurement, and for those cases where the amount of the element is below the sensitivity of the measurements, calculates an upper limit. In addition, the language can be used to: (1) automatically search a spectrum, find the peaks and output the energies and areas of the peaks, (2) make linear or semi-logarithmic CALCOMP plots and (3) provide an accurate energy calibration.

The language consists of the set of commands given in Table 1. These commands can be given in any reasonable order. For example, the order in which FRZDRY and TIMEIN commands are given is not important. However, these commands must be given before the ANALYZM command. The language is set up so that information which is not necessary for data reduction need not be input. For example, if the sample was not freeze dried, then the FRZDRY command need not be given and the associated correction would not be made. The language is designed to be as automatic as possible. Accordingly, the simple command GRAPH1 causes a CALCOMP plot to be made regardless of how many channels the spectrum contains. Although the grammar of the language is simple, if a grammatical error is made, a diagnostic message is printed. For example, if the PRNTEC command is given but energy calibration information was not input then a diagnostic message would be printed out.

SERVICE PROGRAMS

In summary, with this language NAA data can be reduced easily, accurately, quickly and reliably while avoiding the need to specify unnecessary details for data reduction in special cases.

TABLE I. Commands used by MTELMT and their function.

Command	Mnemonic	Function
CDFRMT	card format	Specifies format of spectra punched on IBM cards.
KNTR0L	control	Controls options of other commands.
CDDATA	card data	Reads a spectrum with the format specified by CDFRMT from IBM cards.
TPDATA	tape data	Reads the next spectrum on the magnetic tape into the computer.
SRCHTP	search tape	Searches the magnetic tape for the identification number wanted and then reads spectrum into the computer.
FLSKIP	file skip	Moves the tape to the start of the next file.
REWIND	rewind	Rewinds the magnetic tape.
GRAPH1	graph	Causes a CAL COMP plot to be made of spectrum in computer with identification number label.
GTITLE	graph title	Words following GTITLE will appear on the CAL COMP plot made by GRAPH1.
ENCALI	energy calibration in	Enables energy calibration information for up to 20 peaks to be fed into computer.
ENCALO	energy calibration out	Prints out the energy for a specified channel number.
PRNTEC	print energy calibration	Prints a complete table of energy vs. channel number.
RABBIT	rabbit no.	Specifies rabbit number of samples being analyzed.
STNDRD	standard	Specified information characterizing the standard.

SERVICE PROGRAMS

SAMPLE	sample	Specified information characterizing the sample.
FRZDRY	freeze-dry	Specifies the ratio of dry to wet weight for materials which have been freeze dried.
TIMEIN	time in	Specified counting time and time of day for samples and standards.
INTPRM	integration parameters	Specifies location of peaks and how background is to be subtracted.
ANALYZM	analyze in manual mode	Causes a calculation of the centroid and ppm (or micrograms) to be executed based on parameters fed in by INTPRM, STNDRD, SAMPLE and TIMEIN.
CMPTAC	compute area and centroids	Computes areas of peaks and centroids based on the values of parameters fed in by ENCALI and INTPRM.
APKFND	auto peak find	Causes computer to search spectrum currently in memory for peaks and prints out their centroid, net area, background and estimate of error in net area.
FWHMIN	full-width-half-max in	Specifies estimate of fwhm characterizing spectra which helps APKFND find peaks more reliably.

3. An Automated Data Acquisition System For Neutron Activation Analysis

For the past few years the need to analyze large numbers of samples by neutron activation analysis for a variety of trace elements has increased to the point where it is no longer feasible to operate an analyzer and detector for 8 hour periods during the day. A much better approach would be to have a reliable, automated system which operates 24 hours a day, 7 days a week. This paper describes how such a system was constructed using commercially available equipment with only slight modification.

The heart of the system is a Nuclear Data 4410 programmable analyzer (minicomputer) with a 16 K memory. Instructions are given to the analyzer through a teletypewriter. Data may be received by either the teletype, magnetic tape, or an X-Y plotter. The magnetic tape system is a PEC 7 track tape which is computer-compatible. A small cassette unit may also be used but only for loading programs or for the temporary storage of data.

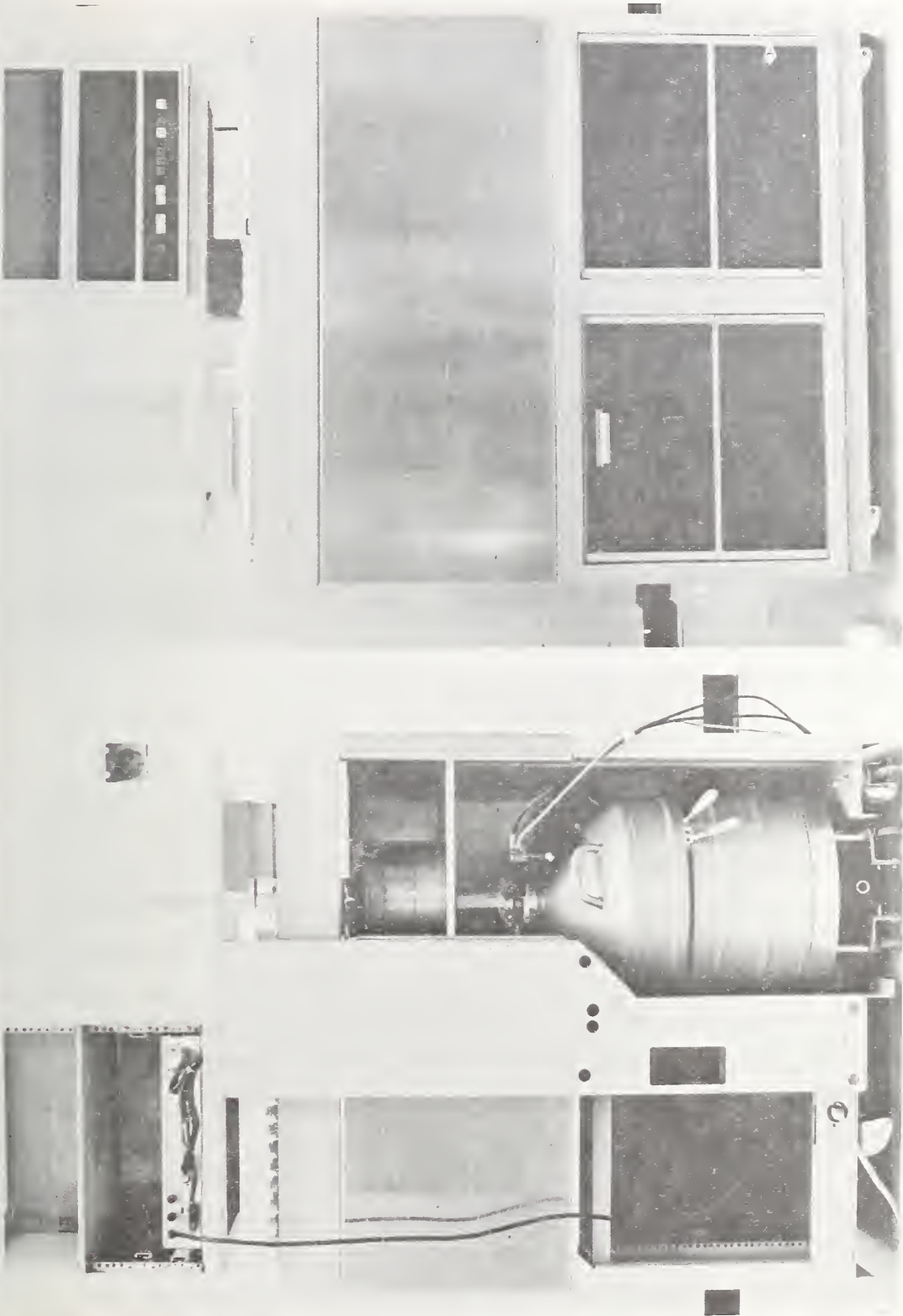


Fig. 1. Left: Rear view of sample changer with Ge(Li) detector in place.
Right: Front view of sample changer showing steel insert in cabinet.

SERVICE PROGRAMS

The sample changing is done using a Nuclear Chicago (Model 1185) automatic gamma sample changer which has been modified to accept a Ge(Li) detector. This was done by cutting the cabinet in two horizontally, just below the sample top, and inserting aluminum plate until the desired height was achieved. The internal supports were modified so that the lead shielding was retained around the top part of the changer but removed at the bottom to allow room for the detector's Dewar. The detector sits on a platform which can be rolled in and out of the changer and which can also be raised and lowered to any desired height to allow the detector geometry to be varied with respect to the sample. While the detector is in the changer it is retained by spring straps. The changer has a capacity of 200 samples, and solids or liquids may be counted individually or in a mixed sequence. A front and rear view of the sample changer with the Ge(Li) detector in position is shown in Figure 1.

A control program was developed which, when the proper instructions are given, will count the sample for a preset time, look at the spectrum, integrate four preselected peaks of interest and type these areas out on the teletype, identify the sample by a preselected code number, dump the entire spectrum onto magnetic tape, erase the memory, change the sample, and begin the sequence again. In addition, a print-out on the teletype of the elapsed time from the start of the routine in 0.1 minute units is given at the beginning and end of each operation to allow half-life corrections if necessary. The first peak area of interest to be integrated is checked at regular intervals to ensure that the memory does not overflow during the counting time. If the count rate is too high, the sample is rejected, the time counted is printed out, and the sequence is started on the next sample. If necessary, the data may be further reduced using a large computer since the complete spectrum is stored on the magnetic tape.

Using this system it has been possible to operate 24 hours a day for extended periods of time. The 200 sample capacity also makes weekend operation practical. The ease of sample handling and ability to recount samples easily have increased the capability and effectiveness of the operation without necessitating additional manpower.

THE USE OF NEUTRON ACTIVATION ANALYSIS ON BIOLOGICAL SAMPLES
BY THE VETERANS ADMINISTRATION HOSPITAL

J. C. Smith
(Veterans Administration Hospital, Washington, D. C.)

Human blood serum was analyzed for zinc in an effort to develop an internal reference standard for our laboratory; specifically, pooled serum was irradiated for one hour (RT-4). Analysis by the neutron activation technique was compared with four reported methods using atomic absorption spectrophotometry. The results are now being compiled for publication. A project entitled "Trace Element Profiles in Normal and Neoplastic Prostates", was submitted to the National Prostatic Cancer Project.

The main purpose of that study was to compare the trace element profile in cancerous, normal, and hyperplastic prostate tissue using neutron activation analysis. Unfortunately, this study has not been initiated due to lack of funding.

TRACE ELEMENTS IN THE ENVIRONMENT
AND RADIOACTIVE DECAY STUDIES

W. H. Zoller, G. E. Gordon and W. B. Walters
(University of Maryland, College Park, Md.)

During the past year we have been using instrumental neutron activation analysis (INAA) to determine concentrations of about 20 to 30 trace elements in atmospheric particulate material and pollution source materials. This represents a portion of a large project designed to determine the composition and characteristics of materials released to the atmosphere by several types of major pollution sources: coal- and oil-fired power plants, incinerators, motor vehicles, and airport activities. In connection with these studies we have irradiated and analyzed many of each of the following types of samples:

SERVICE PROGRAMS

- a. Atmospheric particulate samples collected in the Baltimore Harbor Tunnel, at Friendship and National airports, in College Park, and in rural areas near Washington, D.C.
- b. Many types of crude oil and various distillate and residual fractions from them.
- c. Automobile tires, lubricating oils and brake shoes.
- d. Municipal incinerator fly ash.

We are now analyzing and interpreting the results of these measurements to determine the amounts of various trace elements injected into the atmosphere by the major sources under study. Soon we will begin INAA of coal and fly ash from a coal-fired power plant and atmospheric samples collected nearby in the field. We will be also analyzing similar sets of samples from an oil-fired power plant and a municipal incinerator.

In order to check our INAA procedures for trace-element analyses, we participated in the NBS-EPA round-robin analyses of the new environmental standards that were conducted during the latter half of 1972. We turned in concentration values for about 20 elements in the coal, fly ash and residual oil standards.

We have continued the analysis and interpretation of atmospheric particulate samples collected at the South Pole in an effort to determine world-wide background levels and global transport of trace elements in the atmosphere. Despite the fact that the particulate loading in the polar atmosphere is orders of magnitude below that of typical urban areas, meaningful values for the concentrations of about 15 elements can be measured by INAA. This is accomplished by using filter materials that have reproducible blank values, collecting particles from enormous volumes of air (several thousand m^3), taking extreme care in the handling of samples to prevent contamination, and observing γ rays from irradiated samples with Ge(Li) detectors of high resolution and efficiency. The lowest measurable atmospheric concentrations were those obtained for Eu, which went as low as $15 \text{ fg}/m^3$ ($\text{fg} = \text{femtogram} = 10^{-15} \text{ g}$), corresponding to about $60 \text{ atoms}/\text{cm}^3$! Mr. John Ondov collected additional samples at Pole Station during January 1973 and we expect to send about two people from the group

there during the coming summer season at the Pole. In order to seek possible natural sources of elements observed at the Pole, we are analyzing filter samples and lava collected near the Icelandic volcano in June, 1973.

Work is currently in progress on the study of the radioactive decay of ^{107}Cd , ^{117}Cd isomers, ^{105}Ru , $^{131\text{m}}\text{Te}$, and ^{161}Gd . In these studies, the energies, intensities, and coincidence relationships are measured with high accuracy for the γ rays emitted by each radionuclide. The resulting data are combined to deduce the level structure for the daughter nuclides.

THE USE OF ACTIVATION ANALYSIS IN SCIENTIFIC CRIME DETECTION BY THE FEDERAL BUREAU OF INVESTIGATION

J. F. Gallagher

(Federal Bureau of Investigation, Washington, D. C.)

The FBI Laboratory has continued to use neutron activation analysis (NAA) as a method of elemental analysis for major, minor and trace constituents in materials such as metals, biologicals and plastics. The qualitative and quantitative measurement of antimony and barium on lifting mechanisms such as paraffin or cotton removed from the hands of a suspected shooter is accomplished by NAA.

Research into the effects of various activities on the retention of antimony and barium is under way. When a firearm is discharged, antimony and barium, which are components of most primer mixtures, can be deposited on the hand. Test firings are made and then the subject involves himself in controlled activities such as being handcuffed, washing and wiping his hands and placing his hands in his pockets. Another phase of the research project concerns itself with measuring the concentrations of antimony and barium on the hand holding the weapon after the passage of time regardless of the activities the subject is engaged in. Antimony and barium determinations by NAA are well-known by law enforcement agencies and they comprise a significant portion of the cases in which NAA is employed.

SERVICE PROGRAMS

Plans are being made to purchase a new multichannel analyzer with data reduction capabilities. This will permit single element analysis to be conducted more efficiently.

U. S. POSTAL SERVICE ACTIVATION ANALYSIS PROGRAM

J. B. Upton
(U. S. Postal Service, Washington, D. C.)

The U. S. Postal Service is continuing to use neutron activation analysis as one of its most important and convenient methods of the elemental analysis. Because it is non-destructive and possesses extremely sensitive quantitative and qualitative analytical capabilities, NAA is presently unsurpassed in obtaining trace elemental compositions of evidentiary samples. Items of evidence routinely examined by the U. S. Postal Service Crime Laboratory, utilizing NAA, include paint, metals, safe insulation and glass.

Presently, the Laboratory is expanding its NAA capabilities and has acquired a Lithium Drifted - Germanium Detector. Analytical data obtained from using the new detector has been most helpful in identifying isotopes that are either short lived or have gamma ray energies that are very close together.

In one important case involving a mail shipment and loss of a ring of great value, it became necessary to establish whether or not the sender had actually shipped the ring in the package mailed. Unused ring boxes identical to the one the ring was allegedly shipped in were sampled and analyzed by NAA for their elemental composition. Through Laboratory testing and comparison of data obtained from the standard boxes with the analytical results obtained from the questioned ring box, it was clearly demonstrated that a ring had previously been placed in the box in question.

THE USE OF NEUTRON ACTIVATION ANALYSIS IN
SCIENTIFIC CRIME DETECTION

K. B. Snow
(U. S. Treasury Department, Washington, D. C.)

During FY 73 the Bureau of Alcohol, Tobacco and Firearms used the NBS reactor facility to perform 406 separate irradiations. These irradiations involved some 1200 separate criminal cases and over 9100 individual samples.

While the majority of the samples were cotton swabs connected with gunshot residue detection, other types of materials irradiated included paint, metal, soil, hair, and narcotics. This wide range of materials is indicative of the Bureau's continuing interest in the development and application of neutron activation analysis in the field of criminalists.

ACTIVATION ANALYSIS PROGRAM OF THE U.S. GEOLOGICAL SURVEY

J. J. Rowe
(U. S. Geological Survey, Washington, D.C.)

Using the National Bureau of Standards Reactor, the U.S. Geological Survey has applied neutron activation analysis and isotope dilution to the analysis of rocks and minerals for trace constituents in relation to various geochemical studies.

During the last fiscal year, more than 1,000 samples of soils were analyzed for arsenic by an isotope dilution method (Brown, Simon and Greenland, in preparation) to determine background levels of arsenic.

Gold at trace levels is routinely determined using a fire assay radiochemical method (Rowe and Simon, 1968). These analyses are part of an ongoing study of the geochemistry of gold related to gold mineralization. Analyses are made of continental, Hawaiian, Pacific Island arc, Atlantic Ridge and Icelandic samples. These studies are serving to identify magnetic sources involved in the formation of geologic features. Extensive analyses (more than 1,000) have indicated that gold mineralization is

largely determined by geologic, geochemical and geophysical factors other than the concentration of gold at various places in the mineralizing system, (Tilling, Gottfried and Rowe, 1973).

Instrumental neutron activation, using a synthetic multielement standard has been applied to the determination of antimony, tantalum and hafnium in the U.S. Geological Survey standard rocks (SRG-1, SDC-1, MAG-1, BHVO-1, QLO-1, RGM-1, STM-1, SCO-1, G-2, GSP-1, AGV-1 and BCR-1). The standard samples are homogeneous for the three elements determined at $F_{.95}$ except for MAG-1 which is homogeneous with respect to antimony and hafnium at $F_{.975}$, (Schwarz and Rowe, in press).

Using fire assay radiochemistry, gold was determined in the U.S.G.S. standard rocks which ranged from 0.4 to 10 ppb. The standards were homogeneous for gold, except for SDC-1.

Numerous analyses were performed on samples submitted by geologists. Some of these were the instrumental neutron activation analysis of samples of shalerites, galenas, pyrite and chalcopyrite for Mn, Sb, As, Se, Ag, Au and Hg. Instrumental methods were also applied to the determination of Th, Ta, Hf, Sc, Cs, Eu and Sb in samples from Hawaii, Montana, Iceland, and Wyoming. A procedure using post irradiation radiochemistry was applied to the determination of tungsten in various rocks and minerals.

¹F. W. Brown, F. O. Simon and L. P. Greenland, "The Isotope-dilution determination of arsenic in soils (in preparation).

²J. J. Rowe and F. O. Simon, "The Determination of Gold in Geologic Materials by Neutron Activation Analysis Using Fire Assay for the Radiochemical Separations", *U.S. Geological Survey Circular 599*.

³L. J. Schwarz and J. L. Baker, "Gold Content of U.S.G.S. Standard Rocks, *U.S. Geological Survey Prof. Paper 840*, edited by F. J. Flanagan (in press).

⁴L. J. Schwarz and J. J. Rowe, "Determination of Antimony, Hafnium, and Tantalum in the U.S.G.S. Standard Rocks, *U.S. Geological Survey Prof. Paper 840*, edited by F. J. Flanagan (in press).

⁵R. I. Tilling, D. Gottfried and J. J. Rowe, "Gold Abundance in Igneous Rocks: Bearing on Gold Mineralization, *Econ. Geol.* 68, 168-186 (1973).

COMBINED EFFECTS OF RADIATION AND SHOCK WAVES IN MATERIALS

C. M. Cialella

(Ballistic Research Laboratories, Aberdeen Proving Ground, Md.)

The objective of this study is to determine the influence of lattice vacancies, formed by neutron irradiation of a solid specimen, on the subsequent fracture of the solid by shock loading. The purpose of this study is to harden ABM materials by developing "vacancy getters" which would quench the vacancies created by the neutron irradiation.

The samples consisted of three single crystals of copper and four aluminum cylinders with the following dimensions and weights:

- a. Cu, 1.137 cm dia., 2.535 cm long, 22.99 g
- b. Cu, 1.103 cm dia., 2.541 cm long, 21.74 g
- c. Cu, 0.635 cm dia., 2.545 cm long, 7.22 g
- d. 1100Al, 1.27 cm dia., 2.54 cm long, ~ 8.7 g
- e. 1100Al, 2.53 cm dia., 2.54 cm long, ~ 34.6 g
- f. 2024Al, 1.27 cm dia., 2.54 cm long, ~ 9.0 g
- g. 2024Al, 2.54 cm dia., 2.54 cm long, ~ 35.8 g

To insure a sufficient number of vacancies to observe their effects a total of 10^{20} n/cm² was requested.

The samples will be characterized before irradiation, after irradiation and then following shock loading. A combination of techniques including optical and electron microscopy, x-ray topography, and stored energy measurements will be employed to characterize the defect state at each stage.

The samples have been irradiated and are being prepared for shock loading and analysis. The results will be reported in next year's publication.

NEUTRON IRRADIATION OF LPE BUBBLE DOMAIN GARNETS

R. S. Sery and H. R. Irons
(Naval Ordnance Laboratory, Silver Spring, Md.)

Five LPE iron garnets (IG) were irradiated in the NBS reactor to 0.4×10^{15} n/cm² initially, and finally to a total of 2×10^{15} n/cm² ($\gamma \sim 10^8$ R), where $E_f > 10$ keV. Samples included GdEr-, GdY-, GdYtm-, GdYYb- and GdYLa- IG's (e.g., $Gd_{0.44}La_{0.04}Y_{2.52}Fe_{4.01}Ga_{0.99}O_{12}$). Only pre- and post irradiation measurements were made for both doses. Properties measured, percentage errors and ranges of properties were: characteristic length, l ($\pm 10\%$, 0.5 to 0.9 μ m); saturation moment, $4\pi M_s$ ($\pm 7\%$, 120 to 170 G); collapse field, H_o ($\pm 5\%$, 43 to 130 G); mobility, μ_w ($\pm 25\%$, 120 to 540 cm/Oe sec); anisotropy field, H_K ($\pm 10\%$, 220 to 1470 G).

A pre-irradiation pressure vessel test of the samples - carried out at 11 psi and 75°C - showed that the properties were not affected by this simulation of reactor ambient conditions. The subsequent irradiations indicated that neutron plus gamma irradiation, to the dose levels reached, had negligible effects on these properties. The fractional number of vacancies, interstitials and combinations of either is estimated to be $\sim 5 \times 10^{-7}$. This fraction of defects is considered to be too small to cause significant changes in characteristic properties. Moreover, the sizes of the radiation induced defects are smaller by orders of magnitude than the voids, inclusions and other defects - normally occurring during fabrication - which interfere with bubble generation and propagation.

CHEMICAL STUDIES ON LUNAR MATERIALS AND METEORITES

E. Anders, R. Ganapathy and J. Morgan
(University of Chicago, Chicago, Ill.)

Neutron activation methods were used to determine the abundances of 20 rare elements that occur on the moon and meteorites in the range of 10^{-9} and 10^{-12} gram per gram sample. On the basis of this study the amount of meteoritic materials on the moon was calculated.

SERVICE PROGRAMS

In addition it was possible to characterize the chemical composition of the projectiles that produced major impacts on the moon.

The study of meteorites is being expanded in order to understand the chemical fractionations which occurred on chondrites. Recent results indicated that the observed fractionations took place in the solar nebula rather than on meteoritic parent bodies.

G. STAFF ROSTER

ORGANIZATION CHART

314.00

REACTOR RADIATION DIVISION

R. S. Carter, Chief
T. M. Raby, Deputy Chief
 E. Maxwell, Admin. Officer*
 E. Simms, Receptionist

Technical Support

R. Casella
 M. Ganoczy
 V. Myers
 F. Shorten

314.01

Reactor Operations

T. M. Raby, Chief
J. F. Torrence, Deputy
 D. Ahalt, Sec'y
 J. Bowers, Admin. &
 Tech. Ass't.
 R. Beasley
 M. Bell
 N. Bickford
 H. Brake
 D. Cea
 A. Chapman
 H. Dilks
 D. Nelson
 J. Ring
 R. Scheide
 R. Stiber
 D. Wilkison
 B. Young

314.02

Engineering Services

J. H. Nicklas, Chief
 D. Davitt, Sec'y*
 P. Beachley
 R. Conway
 J. Darr
 O. Frizzell
 E. Guglielmo
 R. Hayes
 H. Jackson
 J. Sturrock

314.03

Neutron S-S Physics

J. J. Rush, Chief
 L. Clutter, Sec'y
 A. Cinquepalma
 D. Fravel
 R. Livingston
 E. Prince
 J. Rowe
 W. Rymes
 A. Santoro
 A. Tudgay

STAFF ROSTER

NON-RRD NBS STAFF LOCATED AT REACTOR

Division 240.01

P. R. Cassidy
H. E. DeSpain
E. J. Embree
J. J. Shubiak
F. Moore

Division 241.05

R. A. Dallatore
J. A. Grundl
I. G. Schröder
A. Fabry (Cen-Sek, Belgium)

Division 313.00

B. Mozer

Division 310.08

D. A. Becker
B. S. Carpenter
L. A. Currie
T. E. Gills
E. S. Gladney
S. H. Harrison
P. D. LaFleur
S. R. Lantz
R. M. Lindstrom
G. J. Lutz
L. T. McClendon
G. M. Reimer
H. L. Rook
R. W. Shideler
J. E. Suddueth

GUEST WORKERS AND COLLABORATORS

Division 221.03

H. Marshak
R. J. Soulen, Jr.
D. B. Utton

Division 221.05

R. D. Mountain
H. J. Raveche

Division 232.06

R. D. Deslattes
W. C. Sauder
E. G. Kessler

Division 242.02

L. D. Miller
F. J. Schima

Division 311.03

J. D. Barnes

Division 311.05

B. Dickens
L. W. Schroeder

Division 313.01

C. W. Reimann

Division 313.06

A. D. Mighell
C. S. Brickencamp

Aberdeen Proving Grounds

C. M. Cialella

Argonne National Laboratory

H. Flotow
D. L. Price

Brookhaven National Laboratory

J. L. Alberi

STAFF ROSTER

Federal Bureau of Investigation

D. B. Davies
J. W. Kilty
J. M. Little
G. P. Mahoney
J. P. Riley

Food and Drug Administration

M. Friedman*
R. E. Simpson
J. T. Tanner*

Harry Diamond Laboratory

D. McGarry

Naval Ordnance Laboratory

H. Alperin*
D. I. Gordon
D. A. Kubose
S. J. Pickart*
J. J. Rhyne*
R. S. Sery
R. H. Williams

Naval Research Laboratory

D. J. Bresson
A. C. Ehrlich
G. A. Ferguson
J. Karle
J. H. Konnert
L. F. Paolella*
P. E. Wilkniss

Picatinny Arsenal

C. S. Choi*
H. J. Prask*
R. S. Singh*
S. F. Trevino*

U. S. Atomic Energy Commission

J. C. Glynn

U. S. Geological Survey

F. W. Brown
R. Finkelman
L. P. Greenland
J. J. Rowe
G. Sellers
F. O. Simon

U. S. Postal Service

M. Beckman
G. R. Stangoehr
J. Upton

U. S. Treasury Department

R. L. Brunelle
P. C. Buscemi
C. M. Hoffman
F. A. Lundgren
M. J. Pro

V. A. Hospital

J. Smith

The Ford Motor Company

W. G. Rothschild

American University

R. G. Arnold
B. T. Chertok
R. A. Segnan
R. Simon
D M. Sweger

Carnegie Institute of Washington

L. W. Finger

McGill University

G. Donnay
J. D. H. Donnay
R. F. Martin

Temple University

M. Green
V. P. Warkulwiz*

STAFF ROSTER

University of Chicago

E. Anders
R. Ganapathy

University of Maryland

J. Barker
P. Buhl
R. A. Cahill
T. J. Conry
E. Gladney
C. Glinka
G. E. Gordon
J. Graber
S. Harrison
A. Jones
R. Khanna
V. J. Minkiewicz
F. J. Munno
J. Ondov
L. Raber
J. Reednick
W. B. Walters
W. H. Zoller

U. S. Naval Academy

C. S. Schneider

*Located full time at Reactor

H. PUBLICATIONS

COLLABORATIVE PROGRAMS

- BARNES, J. D., "Inelastic Neutron Scattering Study of the "Rotator" Phase Transition in n-Nonadecane", *J. Chem. Phys.* 58, 5193 (1973).
- CASELLA, R. C. and TREVINO, S. F., "Group-Theoretical Selection Rules in Inelastic Neutron Scattering within the Rigid Molecule Model", *Phys. Rev.* B6, 4533 (1972).
- CASELLA, R. C. and ROBERTSON, B., "Direct Tests for Violation of CP Invariance" (*Phys. Rev. Lett.*, in press).
- CHOI, C.S. and ABEL, J.E., "The Crystal Structure of 1,3,5,7-tetraceto-1,3,5,7,-tetrazacyclo-octaine", *Acta Cryst.* B29, 651 (1973).
- DEGRAAF, L. A., RUSH, J. J. and LIVINGSTON, R. C., "Inelastic Neutron Scattering", *Proc. Symp. 5th*, Grenoble (I.A.E.A. Vienna, 1972), p. 247.
- KONNERT, J., KARLE, J. and FERGUSON, G. A., "Crystalline Ordering in Silicon and Germanum Glasses", *Science* 179, 177 (1973).
- LEUNG, P. A., RUSH, J. J. and TAYLOR, T. I., "Study of Hindered Rotation in Crystals by Neutron Transmission Measurements: Comparison of Calculated and Measured Scattering Cross Sections", *J. Chem. Phys.* 57, 175 (1972).
- LIVINGSTON, R. C., ROTHSCHILD, W. G. and RUSH, J. J., "Molecular Reorientation in Plastic Crystals: Infrared and Raman Band Shape Analysis of Neopentane" (*J. Chem. Phys.*, in press).
- MAREZIO, M., DERNIER, P. D. and SANTORO, A., "Twinning in Cr-Doped Vo_2 ", *Acta Cryst.* (to be published).
- MOZER, B. and LENEINDRE, B. L., "Neutron Diffraction Studies of the λ Transition of Liquid ^4He at Constant Density", *Phys. Rev. A.* (to be published).
- MOZER, B., DEGRAAF, L. A., and LENEINDRE, B., "Neutron Diffraction Studies of Liquid ^4He ", *Phys. Rev. A.* (to be published).
- MYERS, V. W., "Klein-Gordon Equation for a Charged Particle Interacting with an Electromagnetic Wave", *J. Franklin Inst.* 295, 497 (1973).
- PICKART, S. J., ALPERIN, H. A., HOLTZBERG, F. and MCGUIRE, T. R., "Magnetic Structures of $\text{Eu}_{1-x}\text{Gd}_x\text{S}$ ", *AIP Conf. Proc.*, No. 10, 1569 (AIP, 1973).

PUBLICATIONS

- PRINCE, E. and FINGER, L. W., "Use of Constraints on Thermal Motion in Structure Refinement of Molecules with Librating Side Groups", *Acta Cryst.* B29, 179 (1973).
- PRINCE, E., SCHROEDER, L. W. and RUSH, J. J., "A Constrained Refinement of the Structure of Durene", *Acta Cryst.* B29, 184 (1973).
- PRINCE, E., DONNAY, G. and MARTIN, R. F., "Neutron Diffraction Refinement of an Ordered Orthoclase Structure", *Am. Mineralogist* 58, 500 (1973).
- PRINCE, E., MIGHELL, A. D., REIMANN, C. W. and SANTORO, A., "Hexakis (Imidazole) Cobalt(II) Nitrate $[\text{Co}(\text{C}_3\text{H}_4\text{N}_2)_6^2(\text{NO}_3)_2$ ", *Cryst. Struct. Comm.* 1, 247 (1972).
- RHYNE, J. J., PICKART, S. J. and ALPERIN, H. A., "Direct Observation of an Amorphous Spin Polarization Distribution", *Phys. Rev. Lett.* 29, 1562 (1972).
- RHYNE, J. J., PICKART, S. J. and ALPERIN, H. A., "Amorphous Spin Polarization in a Tb-Fe Compound", *Amorphous Magnetism* (Plenum Press, New York, 1973), p. 373.
- ROWE, J. M., RUSH, J. J., DEGRAAF, L. A. and FERGUSON, G. A., "Neutron Quasielastic Scattering Study of Hydrogen Diffusion in a Single Crystal of Palladium", *Phys. Rev. Lett.* 29, 1250 (1972).
- ROWE, J. M., HINKS, D. G., PRICE, D. L., SUSSMAN, S. and RUSH, J. J., "Single Crystal Neutron Diffraction Study of Sodium Cyanide", *J. Chem. Phys.* 58, 2039 (1973).
- ROWE, J. M., LIVINGSTON, R. C. and RUSH, J. J., "Neutron Quasielastic Scattering Study of SH^- Reorientation in the Cubic Phases of Cesium and Rubidium Hydrosulfide", *J. Chem. Phys.* 58, 5469 (1973).
- ROWE, J. M., RUSH, J. J. and SMITH, H. E., "The 'In-Band' Modes of Vibration of PH_{03} " (*Phys. Rev.*, in press).
- RUSH, J. J., DEGRAAF, L. A. and LIVINGSTON, R. C., "Neutron Scattering Investigation of the Rotational Dynamics and Phase Transitions in Sodium and Cesium Hydrosulfides", *J. Chem. Phys.* 58, 3439 (1973).
- RUSH, J. J., "Study of Large-Amplitude Vibrations in Molecules by Inelastic Neutron Scattering", *Advances in Chem.* (to be published).
- RUSH, J. J., LIVINGSTON, R. C. and ROSASCO, G. J., "Raman Scattering Study of Crystal Dynamics and Order-Disorder Transitions in Alkali Hydrosulfides" (*Solid-State Comm.*, in press).
- SANTORO, A. and MIGHELL, A. D., "Coincidence-site Lattices", *Acta Cryst.*

PUBLICATIONS

A29, 171 (1973).

- SANTORO, A., "Characterization of Twinning", *Acta Cryst.* (to be published).
- SCHNEIDER, C. S., "Forward Scattering Amplitude of Silicon for Thermal Neutrons", *Rev. Sci. Inst.* (to be published).
- SINGH, R. S., TREVINO, S. F., and PRASK, H. J., "Long-Wavelength ($K\sim 0$) IR Active Phonons of NaHF_2 and KHF_2 ", *J. Chem. Phys.* 58, 4703 (1973).
- TREVINO, S. F. and PRASK, H. J., "Neutron Spectroscopy", *Progress in Nuclear Energy*, Chapter 2, Series IX, II, (Pergamon Press, Oxford, 1972).

INDEPENDENT PROGRAMS

- ARAS, N. K., ZOLLER, W. M., GORDON, G. E., LUTZ, G. J., "Instrumental Photon Activation Analysis of Atmospheric Particulate Mineral", *Anal. Chem.*, 45, 8, 1481 (1973).
- ARNOLD, R. G., CHERTOK, B. T., SCHRODER, I. G., and ALBERI, J. L., "Search for Doubly Radiative np Capture", *Phys. Rev. C.* (to be published).
- BECKER, D. A. and LAFLEUR, P. D., "Characterization of a Neutron Reactor for Neutron Activation Analysis" (*J. Radioanal. Chem.*, in press).
- CARPENTER, B. S., "Lithium Determination by the Nuclear Track Technique" (*J. Radioanal. Chem.*, in press).
- FRIEDMAN, M. H., MILLER, E. and TANNER, J. T., "Instrumental Neutron Activation Analysis for Mercury in Dogs Administered Methyl Mercury Chloride: Use of a Low Energy Photon Detector" (*Anal. Chem.*, in press).
- FRIEDMAN, M. H., FARBER, M., and TANNER, J. T., "Instrumental Neutron Activation Analysis of Bromine in Pig Tissue" (*Analytica Chimica Acta*, in press).
- GILLS, T. E., and LAFLEUR, P. D., "The Determination of Hafnium in Standard Reference Materials Using Bis(2-ethylhexyl) phosphate (HDEHP) with Neutron Activation Analysis" (*J. Radioanal. Chem.*, in press).
- LAFLEUR, P. D., and THOMPSON, B. A., *The Encyclopedia of Chemistry*, 3rd edition, C. Pampel and G. C. Hawley, Editors, Van Nostrand Reinhold, N. Y., Chapter on Spectroscopy, p. 1030 (1973).
- LEFLEUR, P. D., "Biological Matrix Standard Reference Materials for Trace Element Determinations" (*J. Radionanal. Chem.*, in press).

PUBLICATIONS

- LAFLEUR, P. D., "Biological Matrix Standard Reference Materials for trace Element Determinations" (J. Radioanal. Chem., in press).
- LUTZ, G. J., "The Analysis of Biological and Environmental Samples for Lead by Photon Activation" (J. Radioanal. Chem., in press).
- MARGOSIS, M., and TANNER, J., "Determination of Mercury in Pharmaceutical Products by Neutron Activation Analysis", *J. Pharmaceutical Science* 61, 936 (1972).
- MCCLENDON, L. T., and LAFLEUR, P. D., "Determination of Rare Earths in Standard Reference Material Glass Using Neutron Activation Analysis and Reversed-Phase Chromatography" (J. Radioanal. Chem., in press).
- REIMER, G. M., WAGNER, G. A. and CARPENTER, B. S., "The Thermal Stability of Fission Tracks in the Standard Reference Materials Glass Standard (National Bureau of Standards)" *Rad. Effects* 15, p. 272 (1972).
- ROOK, H. L., LUTZ, G. J., and LAFLEUR, P. D., "The Use of a High Efficiency Mass Separator in Activation Analysis" (J. Radioanal. Chem., in press).
- TANNER, J. T., and FRIEDMAN, M. H., "Arsenic and Antimony in Laundry Aids by Instrumental Neutron Activation Analysis" (*Analytica Chimica Acta*, in press).



U.S. DEPT. OF COMM. BIBLIOGRAPHIC DATA SHEET	1. PUBLICATION OR REPORT NO. NBS TN-813	2. Gov't Accession No.	3. Recipient's Accession No.
4. TITLE AND SUBTITLE NBS Reactor: Summary of Activities July 1972 to June 1973		5. Publication Date February 1974	6. Performing Organization Code
7. AUTHOR(S) Robert S. Carter		8. Performing Organ. Report No.	
9. PERFORMING ORGANIZATION NAME AND ADDRESS NATIONAL BUREAU OF STANDARDS DEPARTMENT OF COMMERCE WASHINGTON, D.C. 20234		10. Project/Task/Work Unit No.	11. Contract/Grant No.
12. Sponsoring Organization Name and Complete Address (Street, City, State, ZIP) Same as No. 9.		13. Type of Report & Period Covered Interim 7/1/72 to 6/30/73	14. Sponsoring Agency Code
15. SUPPLEMENTARY NOTES			
16. ABSTRACT (A 200-word or less factual summary of most significant information. If document includes a significant bibliography or literature survey, mention it here.) This report summarizes all those programs which depend on the NBS reactor. It covers the period from July 1972 through June 1973. The programs range from the use of neutron beams to study the structure and dynamics of materials through nuclear physics and neutron standards to sample irradiations for activation analysis, isotope production and radiation effects studies.			
17. KEY WORDS (six to twelve entries; alphabetical order; capitalize only the first letter of the first key word unless a proper name; separated by semicolons) Activation analysis; crystal structure; diffraction; isotopes; molecular dynamics; neutron; nuclear reactor; radiation.			
18. AVAILABILITY <input checked="" type="checkbox"/> Unlimited <input type="checkbox"/> For Official Distribution. Do Not Release to NTIS <input type="checkbox"/> Order From Sup. of Doc., U.S. Government Printing Office Washington, D.C. 20402, SD Cat. No. C13 <input type="checkbox"/> Order From National Technical Information Service (NTIS) Springfield, Virginia 22151	19. SECURITY CLASS (THIS REPORT) UNCLASSIFIED	21. NO. OF PAGES 135	
		20. SECURITY CLASS (THIS PAGE) UNCLASSIFIED	22. Price \$1.55



NBS TECHNICAL PUBLICATIONS

PERIODICALS

JOURNAL OF RESEARCH reports National Bureau of Standards research and development in physics, mathematics, and chemistry. Comprehensive scientific papers give complete details of the work, including laboratory data, experimental procedures, and theoretical and mathematical analyses. Illustrated with photographs, drawings, and charts. Includes listings of other NBS papers as issued.

Published in two sections, available separately:

• Physics and Chemistry (Section A)

Papers of interest primarily to scientists working in these fields. This section covers a broad range of physical and chemical research, with major emphasis on standards of physical measurement, fundamental constants, and properties of matter. Issued six times a year. Annual subscription: Domestic, \$17.00; Foreign, \$21.25.

• Mathematical Sciences (Section B)

Studies and compilations designed mainly for the mathematician and theoretical physicist. Topics in mathematical statistics, theory of experiment design, numerical analysis, theoretical physics and chemistry, logical design and programming of computers and computer systems. Short numerical tables. Issued quarterly. Annual subscription: Domestic, \$9.00; Foreign, \$11.25.

DIMENSIONS, NBS

The best single source of information concerning the Bureau's measurement, research, developmental, cooperative, and publication activities, this monthly publication is designed for the layman and also for the industry-oriented individual whose daily work involves intimate contact with science and technology—for engineers, chemists, physicists, research managers, product-development managers, and company executives. Annual subscription: Domestic, \$6.50; Foreign, \$8.25.

NONPERIODICALS

Applied Mathematics Series. Mathematical tables, manuals, and studies.

Building Science Series. Research results, test methods, and performance criteria of building materials, components, systems, and structures.

Handbooks. Recommended codes of engineering and industrial practice (including safety codes) developed in cooperation with interested industries, professional organizations, and regulatory bodies.

Special Publications. Proceedings of NBS conferences, bibliographies, annual reports, wall charts, pamphlets, etc.

Monographs. Major contributions to the technical literature on various subjects related to the Bureau's scientific and technical activities.

National Standard Reference Data Series. NSRDS provides quantitative data on the physical and chemical properties of materials, compiled from the world's literature and critically evaluated.

Product Standards. Provide requirements for sizes, types, quality, and methods for testing various industrial products. These standards are developed cooperatively with interested Government and industry groups and provide the basis for common understanding of product characteristics for both buyers and sellers. Their use is voluntary.

Technical Notes. This series consists of communications and reports (covering both other-agency and NBS-sponsored work) of limited or transitory interest.

Federal Information Processing Standards Publications. This series is the official publication within the Federal Government for information on standards adopted and promulgated under the Public Law 89-306, and Bureau of the Budget Circular A-86 entitled, Standardization of Data Elements and Codes in Data Systems.

Consumer Information Series. Practical information, based on NBS research and experience, covering areas of interest to the consumer. Easily understandable language and illustrations provide useful background knowledge for shopping in today's technological marketplace.

BIBLIOGRAPHIC SUBSCRIPTION SERVICES

The following current-awareness and literature-survey bibliographies are issued periodically by the Bureau:

Cryogenic Data Center Current Awareness Service (Publications and Reports of Interest in Cryogenics).

A literature survey issued weekly. Annual subscription: Domestic, \$20.00; foreign, \$25.00.

Liquefied Natural Gas. A literature survey issued quarterly. Annual subscription: \$20.00.

Superconducting Devices and Materials. A literature survey issued quarterly. Annual subscription: \$20.00.

Send subscription orders and remittances for the preceding bibliographic services to the U.S. Department of Commerce, National Technical Information Service, Springfield, Va. 22151.

Electromagnetic Metrology Current Awareness Service (Abstracts of Selected Articles on Measurement Techniques and Standards of Electromagnetic Quantities from D-C to Millimeter-Wave Frequencies). Issued monthly. Annual subscription: \$100.00 (Special rates for multi-subscriptions). Send subscription order and remittance to the Electromagnetic Metrology Information Center, Electromagnetics Division, National Bureau of Standards, Boulder, Colo. 80302.

Order NBS publications (except Bibliographic Subscription Services) from: Superintendent of Documents, Government Printing Office, Washington, D.C. 20402.

U.S. DEPARTMENT OF COMMERCE
National Bureau of Standards
Washington, D.C. 20234

OFFICIAL BUSINESS

Penalty for Private Use, \$300

POSTAGE AND FEES PAID
U.S. DEPARTMENT OF COMMERCE
COM-215

